Escola de Camins
Escola Tècnica Superior d'Enginyeria de Camins, Canals i Ports
UPC BARCELONATECH

Study of the stability of the structure of the Cathedral of Seu d'Urgell by means of graphic statics

TREBALL FINAL DE MÀSTER

Treball realitzat per:

Luca Melcore

Dirigit per:

Dr. Pere Roca Fabregat

Màster en:

Enginyeria de Camins, Canals i Ports

Barcelona, 25/01/2019

Departament:

DECA - Departament d'Enginyeria Civil i Ambiental

DECLARATION

Name: Luca Melcore

Email: luca.melcore@virgilio.it

Title of the MSc Dissertation: Study of the stability of the structure of the Cathedral of Seu d'Urgell by means of graphic statics

Supervisor: Dr. Pere Roca Fabregat

Year: 2019

I hereby declare that all information in this document has been obtained and presented in accordance with academic rules and ethical conduct. I also declare that, as required by these rules and conduct, I have fully cited and referenced all material and results that are not original to this work.

University: Universitat Politécnica de Catalunya

Date: 25th of January, 2019

Signature: 

ACKNOWLEDGEMENTS

I would like to express my gratitude to the European Commission for the Erasmus Mundus scholarship that allowed me to have this experience, it’s something that I will hold dear to my heart for as long as I live.

I owe my deepest gratitude to professor Pere Roca for accepting my application but especially for his helpfulness during all the work.

Special thanks to all my friends in Barcelona, Manuela, Luca, Aldo, Sampa, Bole and Teresa with whom I passed my best nights.

I am grateful to Rita, Matteo, Niccolò and the little Adele who always help me with their love.

I would particularly like to thank my roommate Julia for permanent support.

Finally, I would like to offer my special thanks to all the people who I love, my mum, my sister, my dad, my aunts, my grandma and Giulia for their support and encouragement.

ABSTRACT

The majority of the heritage buildings that remain until today is represented by masonry structures. Because of their historical-cultural importance, one of the aims of the civil engineer's job is to preserve them for the future.

The analysis of the masonry structures is very complex due to the heterogeneity of the material and the lack of information regarding the structures themselves. Limit analysis represents a simplified method for the assessment of masonry historical constructions.

In particular, the main purpose of this work is to study the stability of the Cathedral of Seu d'Urgell. The structure is studied in different cases which include the structure in its original state, in the current state (with flying arches), with deformations subjected to dead load and finally, the structure subjected to seismic action. The structure is analyzed by means of graphic statics in order to apply the static approach of the limit analysis, so for each case a thrust line is found inside the structure.

RESUMEN

La mayoría de los edificios patrimoniales que permanecen hasta hoy están representados por estructuras de mampostería. Debido a su importancia histórico-cultural, uno de los objetivos del trabajo del ingeniero civil es preservarlos para el futuro.

El análisis de las estructuras de mampostería es muy complejo por la heterogeneidad del conjunto y la falta de información sobre las estructuras. El análisis límite representa un método simplificado para la evaluación de construcciones históricas de mampostería.

El objetivo principal de este trabajo es estudiar la estabilidad de la Catedral de La Seu d'Urgell. La estructura se estudia en diferentes casos que incluyen en su estado original, en el estado actual (con arbotantes) y la estructura con deformaciones, sometidas a su peso propio, y finalmente, la estructura sometida a acción sísmica. La estructura se analiza mediante estática gráfica para aplicar el enfoque estático del análisis límite, por lo que para cada caso se encuentra una línea de empuje dentro de la estructura.

TABLE OF CONTENTS

LIST OF FIGURES

LIST OF TABLES

1. INTRODUCTION

This work concerns the study of stability of the Cathedral of Seu d'Urgell by means of graphic statics in order to apply the static approach of the limit analysis. Limit analysis allows to calculate the collapse and capacity of masonry arches in a simple and effective way.

First of all, the work focuses on the characteristics of masonry structures and the calculation rules that have followed over time, up to the modern limit analysis. Initially, a reference is made to the ancient rules of calculation of masonry constructions which are purely empirical based on past experience, up to the first rational approaches. However, the attention focused mainly on the graphic statics in order to provide a clear and detailed explanation of all the steps to the reader.

Furthermore, a historical investigation is carried out concerning the development of the Cathedral over time. Besides, thanks to an inspection, it was possible to evaluate closely the current state of the cathedral, focusing attention in particular on the significant deformations and damage of the nave, in particular of the barrel vault.

Then, the Cathedral is analyzed under gravity loads and under earthquake by means of static graphic in different cases, starting from its original state until to considerate the real deformations which presently present.

Finally, discussing the results obtained, possible strengthening interventions are proposed in order to improve the conditions of the structure.

1.1. OBJECTIVES

The main purpose of this work is to evaluate the equilibrium and the stability of the structure. The method used is based on the static approach of limit analysis, so it’s necessary to find at least one thrust line that is within the structure.

Firstly, this work wants to carry out a state of knowledge about classical calculation methods applicable to masonry structures.

Then, it provides a knowledge about the current state of the Cathedral, including its deformations and damages. In this way it was possible to analyze the structure subjected to dead load, considering its real configuration deformed by means of graphic static.

Besides, the study concerns about the seismic behavior of the structure, analyzed by means of graphic static.

Finally, the study proposes conclusions about the safety and the behavior of the structure and possible reinforcement needs.

2. STATE OF ART

2.1. MASONRY

The term masonry refers to a heterogeneous material composed of several solid phases. Masonry is the building of structures from the individual units, which are often laid in and bound together by mortar, and represents the oldest construction technique together with that of wooden constructions.

Masonry is generally a highly durable form of construction and in fact these structures represent the majority of the heritage buildings which still exist. The resistance of the masonry structures is attributed to several factors, in particular the characteristics of the materials used (both blocks and mortar), workmanship and the pattern in which the units are assembled (Asteris et al., 2015).

With regard to masonry structures various techniques have followed over time. In the following figure there are some examples like cyclopean walls, megalithic walls, Romans technique, Opus mixtum, until particular examples with the Cathedrals of Florence and Milan (Magenes G., 2013).

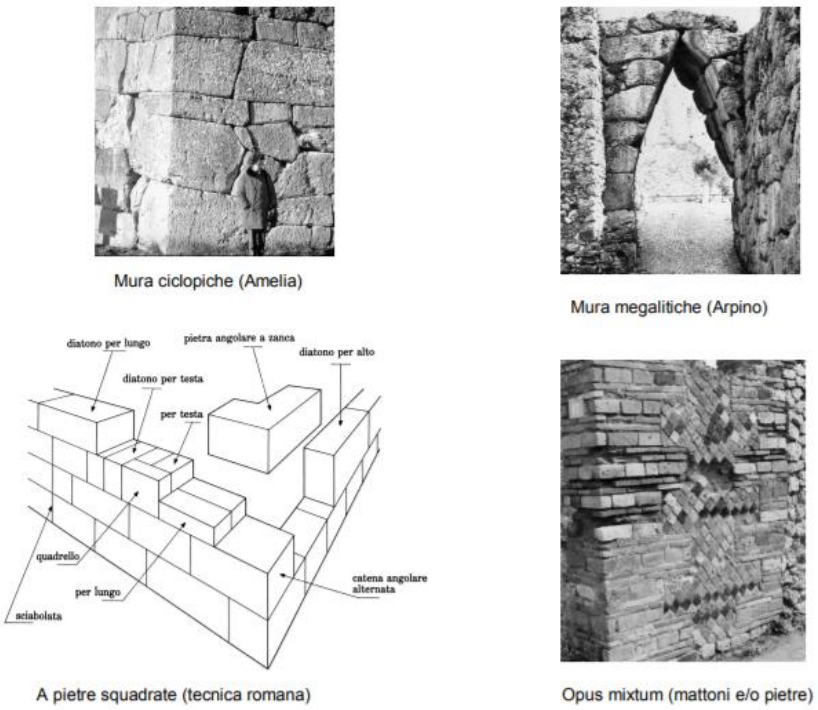

Fig. 1- Different types of masonry arrangements (1) (Magenes G., 2013)

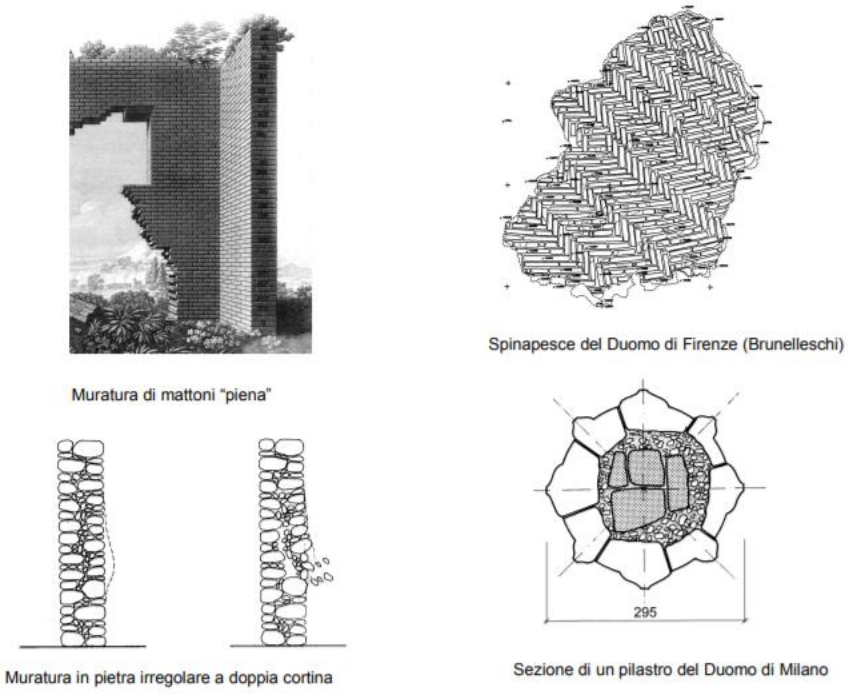

Fig. 2- Different types of masonry arrangements (2) (Magenes G., 2013).

The masonry is a composite material whose main characteristics are (Sabia, 2018):

- Heterogeneity;
- Anisotropy;
- Asymmetry of compression-traction behavior;
- Non-linearity of the tension-strain bond.

The mechanical behavior is the result of the interaction between the elements and the mortar, through their interface. For this reason, the modelling of the masonry structures requires more care than other constructions. Masonry structures can be generally modelled as homogeneous models with "macro-modelling" technique and as heterogeneous models with "micro-modelling" technique (Kömürcü et al., 2017).

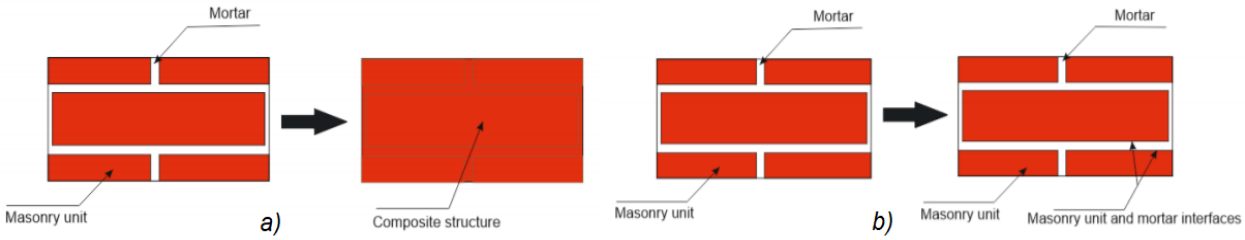

Fig. 3- a) Macro-modelling and b) micro-modelling procedure (Kömürcü et al., 2017)

In macro modelling technique, masonry units and the mortar are modelled as a single material. It is beneficial to use elementary masonry wall parts which periodically repeat themselves on the wall in order to model the masonry walls by homogenization.

In micro technique, masonry units and the mortar are modelled separately. Interfaces in the joining areas of these elements can be also included in the model. Although modelling of structures with micro modelling technique is a detailed process, local behavior of the structures can be investigated with this technique (Kömürcü et al., 2017).

The main mechanical characteristics of masonry structures are the following (Sabia, 2018):

- The compressive strength is good but very varied like the elastic modulus;
- The tensile strength is low; in particular that of a mortar-block joint is of the order of 1/30 of the compressive strength of the masonry;
- Ductility is low.

In the historical buildings the horizontal structures were wooden or constituted by arched structures or vaulted structures. The strength of masonry arches and vaults is highly dependent on their geometry and support conditions while the material has normally a secondary influence. In fact, the design criteria of arches and vaults were founded on geometrical rules for many years based on their shape and dimensions. These rules were sanctioned by the experience and the observation of past successful structures (Roca, 2018).

2.2. CONSTRUCTION RULES OVER TIME

Currently there is a rational and general theory for masonry arches but the ancient and early empirical criteria are still worth and can be successfully used to verify historical masonry structures.

The most ancient construction treatise is “The ten books of architecture” written by Marcus Vitruvius Pollio (80/70 bC., ca. 25 bC.) in Latin and Greek and talk about the architecture and construction from classical antiquity (Roca, 2018). It provides precious information on Roman construction technology, landscape architecture, construction

materials, design of temples, theatres, harbors, private dwellings, finishes, mechanical engineering but it doesn't supply any hint on rules for structural design.

Another important document is a portfolio of 33 parchment leaves with 250 drawings including architectural details of contemporary important buildings (c. 1230) written by Villard de Honnecourt (13th c.). Even if it was unique in the Middle Ages it doesn't provide any construction technique (Roca, 2018).

Alberti compiled all the construction technique known until the 15th in "De Re Aedificatoria" (1435-1440, 1452) including the rules for the design of arches, bridges, domes and towers. This treatise remained the official document on construction up to mid-18th c.

A set of treatises written from 15th to 19th provided some geometrical rules for the design of gothic structure that are still valid. One of these is the Blondel's rule worth to calculate the buttress depth that consists in dividing the arch in three parts, then mark the intersection of line BC with the circumference of radius BC and center in C that represent the buttress depth.

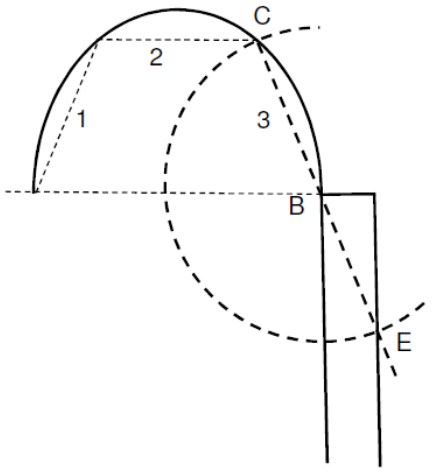

Fig. 4- Blondel's rule (Roca, 2018)

Also Derand (1643) and Viollet-le-Duc (1874) presented this ancient rule in their treateases.

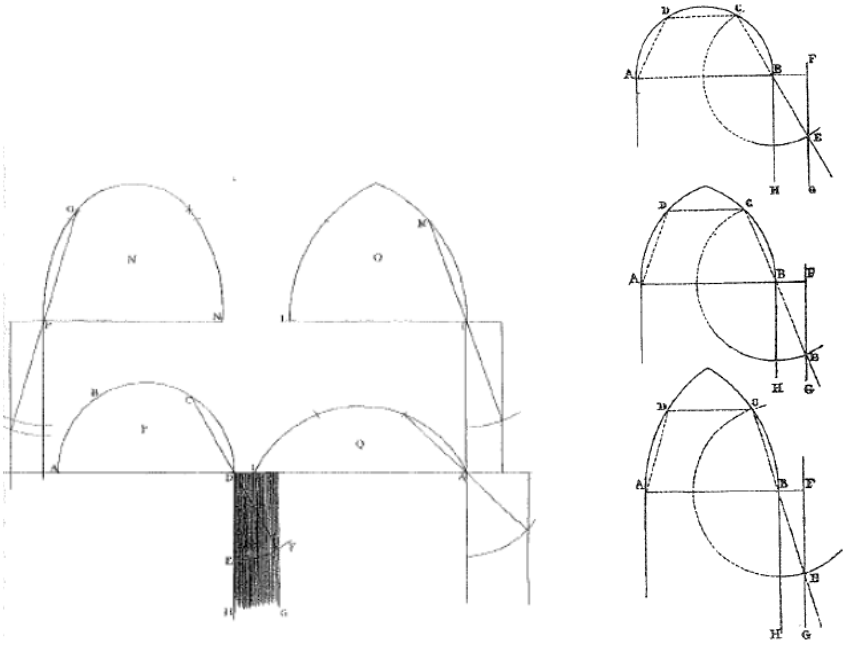

Fig. 5- Blondel's rule described in Derand's (left) and Viollet-le-Duc books (right) (Roca, 2018)

Also Rodriguez de Aranda (Spain, 16th) utilized a similar procedure to this one that gives the same result.

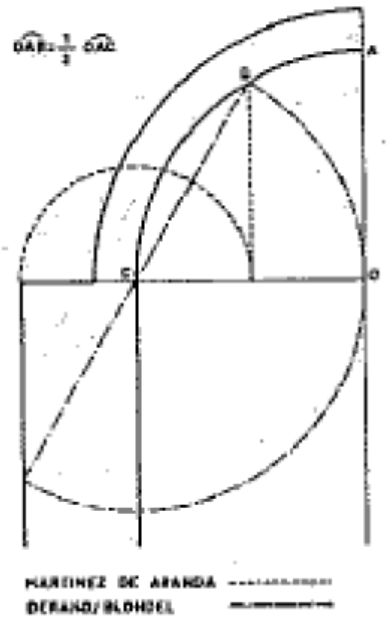

Fig. 6- Alternative procedure of Rodriguez de Aranda (Roca, 2018)

Today the Blodel's rule can be used as shown by Huerta in 1990 when he used it in the Girona Cathedral and in the Sainte Chapelle in Paris in order to show that they were in fact originally designed using this rule (Roca, 2018).

In addition to these geometrical rules there were other empirical rules during 15th to 18th formulated by different authors like Alberti, Palladio, Fray Lorenzo, Fontana to design different structural members. These rules were exclusively based on observation of existing structures and basically consisted on proportions between different structural parts. As said previously all these rules didn't have scientific base.

2.3. THE ADVENT OF GRAPHIC STATICS

The first rational concept was given by Robert Hooke (1635 – 1703) in fact the principle of the inverted catenary is attributed to him with the following anagram *"Ut pendet continuum flexile, sic stabit contiguum rigidum inversum"* that means as hangs the flexible line, so but inverted will stand the rigid arch (Heyman, 1998).

In 1690 David Gregory wrote a treatise on the catenary curve which is worth to describe the equilibrium of an arch with uniform depth subject to dead load and later he provides the stability of an arch when it's possible to fit a catenary within its thickness. Other arch shapes that have depth variations or different load conditions require different curves called anti funicular shapes. The curve determined is called equilibrium line.

The principle of the catenary stated the advent of Graphic Statics which is a graphically procedure born with La Hire (18th c.) and Rankine (19th) and later developed by Mery and Moseley. This procedure is useful for determining the equilibrium of structures, resolving problems of the statics of two-dimensional systems and it was utilized until the beginning of 20th c. before the introduction of elastic theory.

It consists in decomposing the arch in a series of real or fictitious voussoirs separated by a series of plane so it's possible to calculate the thrust line of the arch, which is the the geometrical locus of the points of application of the sectional forces across the arch. The limit of this technique is that represents an indetermination problem. In fact it's necessary to suppose a thrust force value, its position and its direction at one of the ends so there are three variables and for each combination it gets a different thrust line so there are infinitive thrust lines.

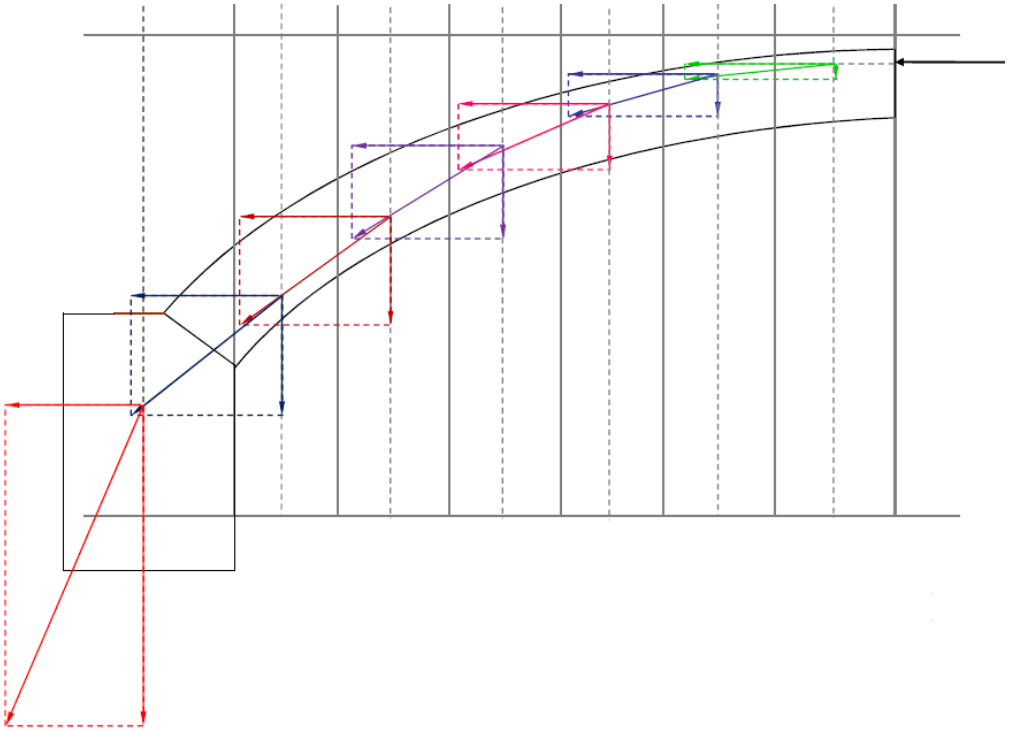

Fig. 7- Procedure of Graphic Statics (Roca, 2018)

In according to Gregory's treatise it's necessary to find at least one thrust line contained within limits of the arch. However, the arch does not necessarily work according to the solution found.

Explanation of the method:

- Divide the arch into some voussoirs and calculate the force vector of each ones;
- Draw the force polygon and the funicular polygon, which is a graphical method of finding the reactive forces and resultants of a system of forces;

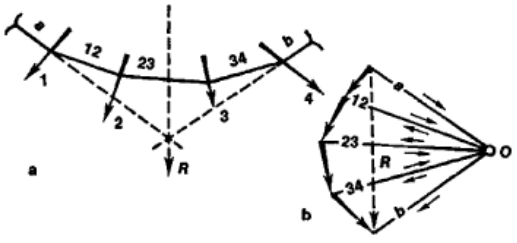

Fig. 8- Force polygon and funicular polygon construction

- Find a thrust line hypothesizing the passage of the thrust line by three points or assuming position, value, direction of a thrust in the arch.

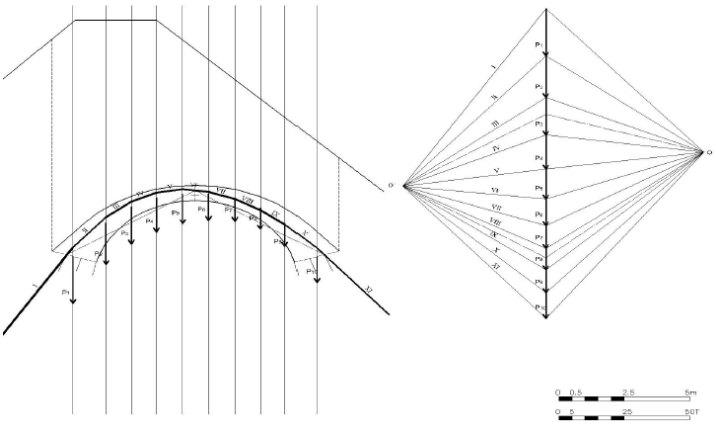

Fig. 9- Example of Graphic Statics to an arch (Roca, 2018)

Here is an example of graphic statics applying to Mallorca Cathedral (Roca, 2018).

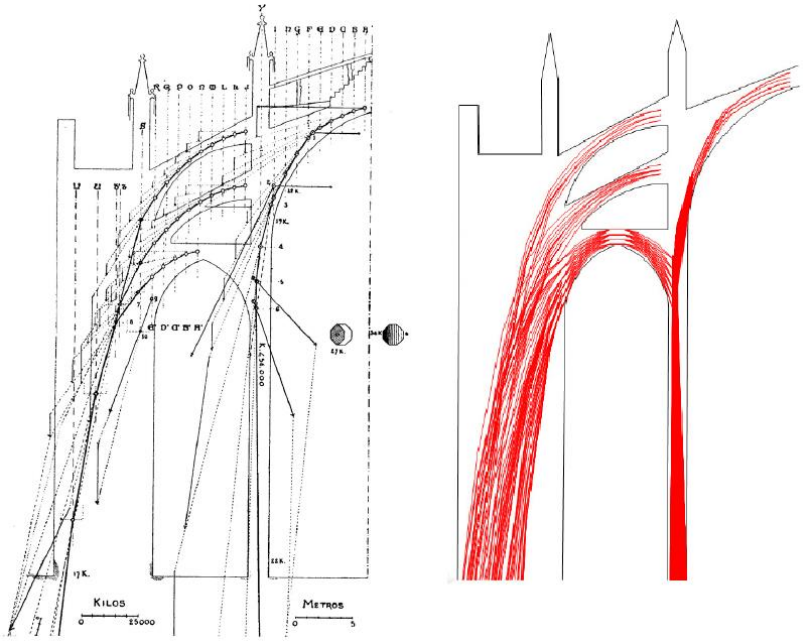

Fig. 10- Application to Mallorca Cathedral (Roca, 2018)

2.4. FAILURE OF ARCHES

In 1730 Couplet showed in his theorem the two ways of approaching any structural problem in the arch, through equilibrium (statics) in which thrust lines are considered and through deformation (mechanisms) in which patterns of hinges are constructed. So he proposed that an arch would collapse due to the development of a number of hinges required to cause the arch become a mechanism.

Beside in his work Couplet stated precise assumptions about material behavior, indeed he noted that friction locks the voussoirs together against sliding and didn't remark the strength of the stone of which the voussoirs are made and by implication he assumed that crushing strength is of little importance (Heyman, 1998).

He showed his theorem in a simplified application in which the hinges appear at the base of the buttresses, in the center and at 45°. This approach was experimentally demonstrated by Danizy in 1732 applying it on the Dome of Saint Peter.

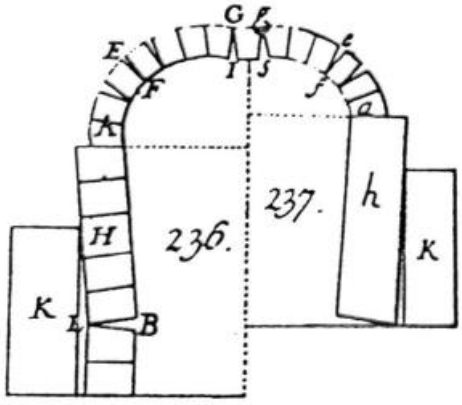

Fig. 11- Application to the Dome of Saint Peter by Danizy (Heyman, 1998)

In 1773 Coulomb proposed the first general and accurate theory on the stability of masonry arches considering that sliding between voussoirs is prevented by frictional forces and collapse will be caused by the rotation between parts due to the appearance of a number of hinges. Beside he showed how determine the location of the hinges which cause the collapse with the method of "maxima and minima". He studied and half arch that is maintained in equilibrium by a horizonal thrust H at the crown (supplied by the other half arch) acting through the point f (Heyman, 1998).

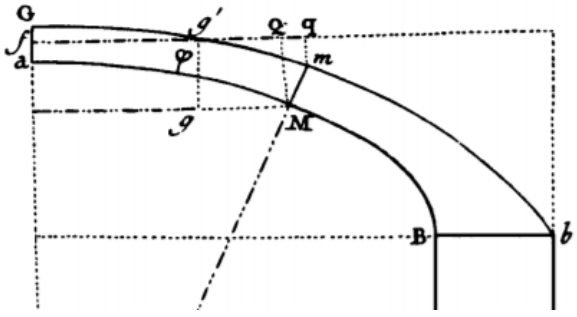

Fig. 12- The equilibrium of the arch as considered by Coulomb (1773) (Heyman, 1998)

So he supposed that hinging can occur about the point M in the intrados or can occur about the point m.

There is a correspondence of this idea with thrust line theory. In fact, a hinge will develop each time the equilibrium line becomes tangent to an alternate boundary (Roca, 2018).

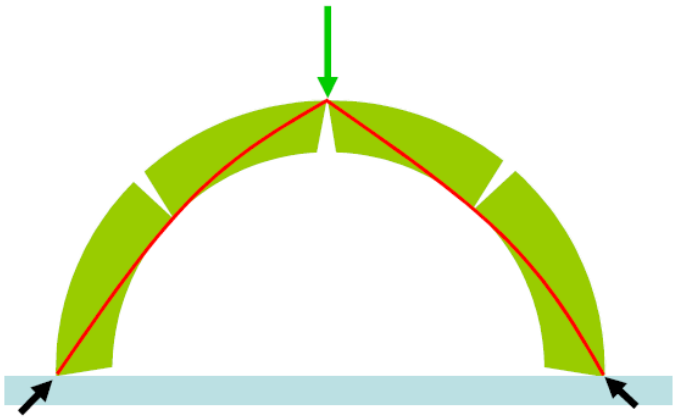

Fig. 13- Formation of hinges linked to thrust line theory (Roca, 2018)

Here there is a situation of failure, so the determined thrust line is unique.

This approach was demonstrated at the Institution of Civil Engineers by Barlow in 1846. In this figure Barlow demonstrated alternative positions of the thrust line.

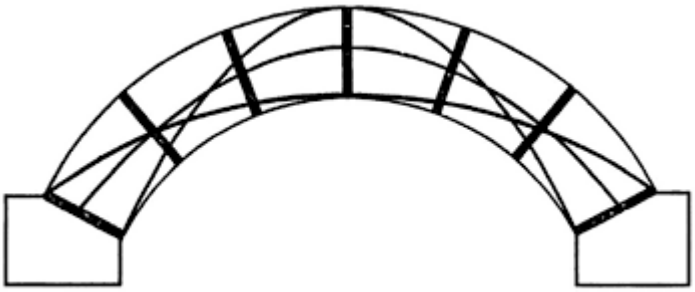

Fig. 14- Alternative positions of the thrust line by Barlow (Heyman, 1998)

In 1879 Castigliano applied his elastic energy theorems to masonry bridges, so he considered elastic properties of the stone and mortar and showed that cracking occurs when the thrust line fall outside the middle-third of the cross-section. Similarly, in the 1930s Pippard showed that the slightest imperfection of fit in steel arches converted an apparently hyperstatic into a statically determinate three-pin arch. The justification for the equilibrium approach of Coulomb and Barlow is provided by the plastic theorems.

2.5. THE MODERN FORMULATION OF LIMIT ANALYSIS.

Limit Analysis developed within the modern theory of plasticity during the 20th century when Jacques Heyman, in 1966, applied this approach to evaluate the load capacity and failure mechanisms of masonry arches. Limit analysis consists in determining the safety and collapse load of a structure. This is achieved when a number of hinges is formed to make the structure a mechanism.

Kooharian showed in 1953 that the limit theorems of limit analysis, based on plasticity theory, are applicable to masonry structures considering the following hypothesis:

- Masonry has no tensile strength;
- Masonry has infinite compressive strength;
- Sliding does not occur.

Plasticity theory is based on the following theorems (Roca, 2018):

- Lower-bound theorem: “The structure is safe, meaning that the collapse will not occur, if a statically admissible state of equilibrium can be found”.

A statically admissible state of equilibrium occurs when a thrust line can be determined, in equilibrium with the external loads, which falls within the boundaries of the structure. In this case the load applied is a lower-bound of the actual ultimate load which causes failure.

- Upper bound theorem: “If a kinematically admissible mechanism can be found, for which the work developed by external forces is positive or zero, then the arch will collapse”.

In this case the load applied is an upper-bound of the actual ultimate load. In order to obtain a mechanism, the structure is formed by a series of rigid block identified by the introduction of hinges.

- Uniqueness theorem: “A limit condition (meaning that the structure will be about to collapse) will be reached if a both statically and cinematically admissible collapsing mechanism can be found”.

The limit condition will be reached if a thrust line can be found causing as many hinges as needed to develop a mechanism. When this occurs, the load is the true ultimate load, the mechanism is the true ultimate mechanism, and the thrust line is the only possible one.

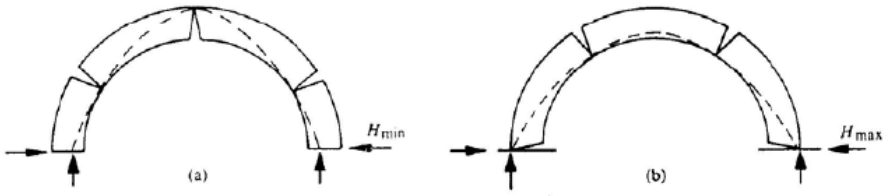

Fig. 15- (a) Minimum thrust and (b) maximum thrust by applying uniqueness theorem (Heyman 1995)

In the following figures, there are some examples of mechanisms for an arch and for multiple arch system.

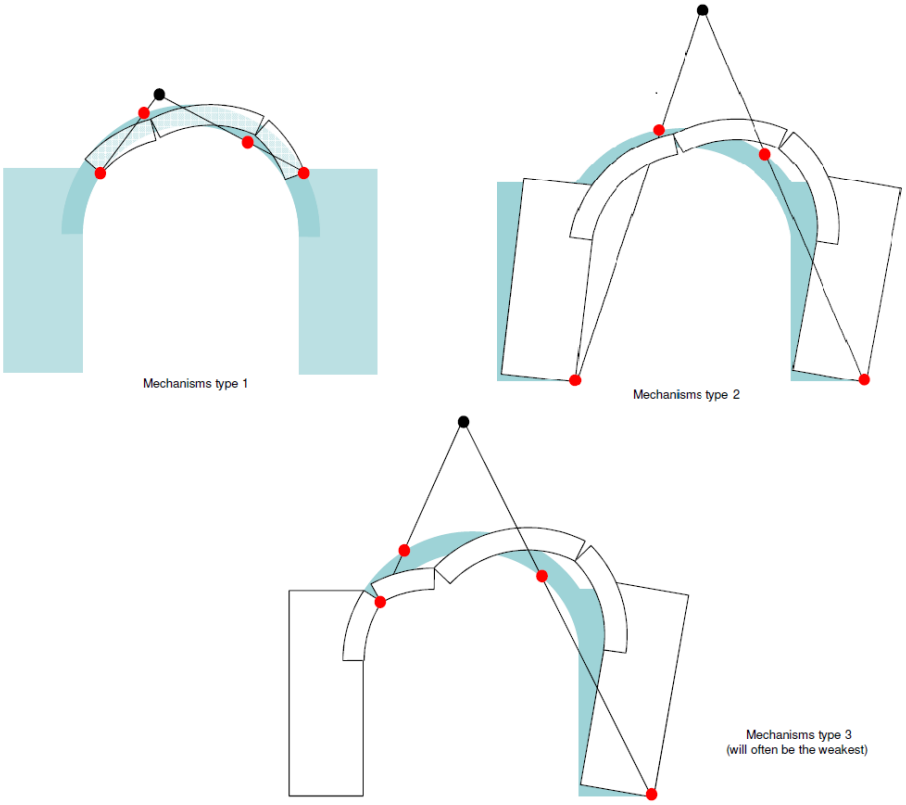

Fig. 16- Alternative mechanisms (Roca, 2018)

-

Instead, in the case of multiple arch system, each individual arch must include at least 3 blocks and 4 hinges and each additional arch should add at least 2 additional moving blocks and 3 additional hinges.

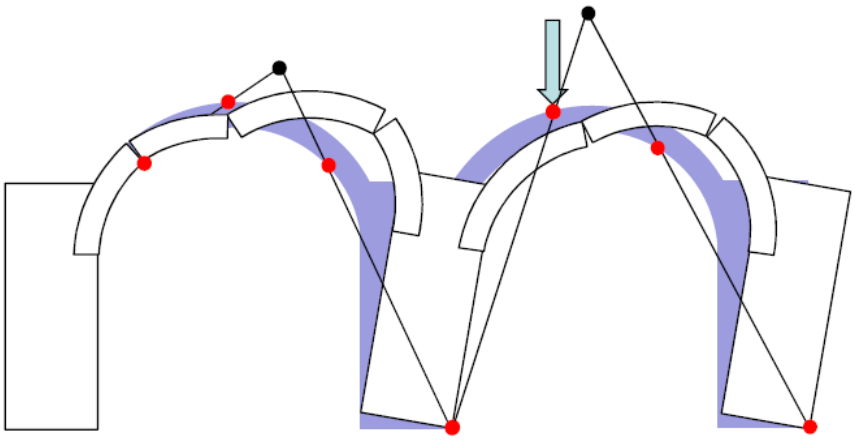

Fig. 17- Example of multiple arch system (Roca, 2018)

2.6. APPLICATION TO VAULTS AND DOMES

Domes and vaults can crack if they are subjected to tensile stress and become a system of compatible arches. So for calculation purposes they can be studied like a system of one-dimensional arches, each of them in equilibrium with limit analysis.

There isn't only one decomposition of a cross vault into arches and it doesn't mean that one decomposition is more realistic or safer than others. There are two possibilities: in the first, all the weight of the vault is transmitted to the diagonal arches, in the second the membrane works while the diagonal arches don't work (Roca, 2018).

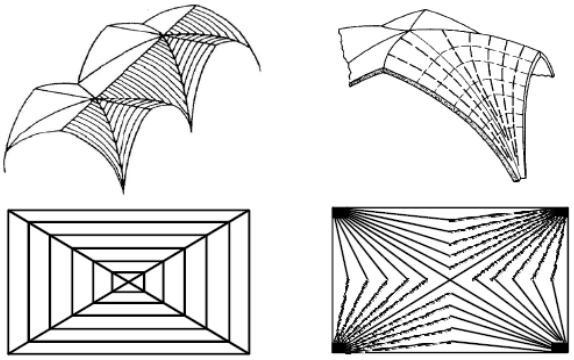

Fig. 18- Cross-vault resisting mechanism (Roca, 2018)

In reality as a consequence of Sabouret cracks another resisting mechanism has been hypothesized in which cross vaults might behave as a one-dimensional arch, shaped by membranes 1 and 2, while regions 3 and 4 would develop parallel arches supported on the first.

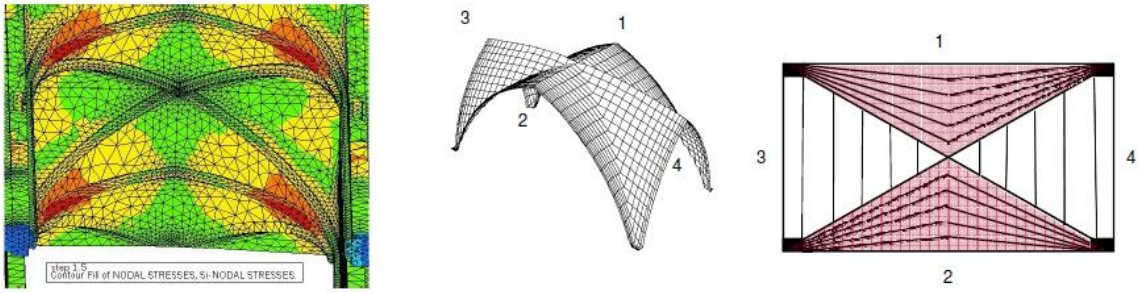

Fig. 19- Cross-vault resisting mechanism suggested by Sabouret cracks (Roca, 2018)

3. CASE OF STUDY: CATHEDRAL OF LA SEU D'URGELL

3.1. LOCATION

The object of study of this work is the Cathedral of Santa Maria d'Urgell, called Cathedral of la Seu d'Urgell. It is located in "Plaça dels Oms" in the heart of the historical part of La Seu d'Urgell which is a town of the Catalan Pyrenees in Spain, more precisely at the confluence of two rivers, Segre and Gran Valira.

Fig. 20- Location of the Cathedral (Geographic coordinates 42°21'28"N 1°27'43"E)

3.2. HISTORICAL INVESTIGATION

The city has had four different cathedrals built in as many different places over time (Puig and Cadafalch, 2003):

- Cathedral of San Justo, 5th century (in Castellciutat);
- Cathedral of the ninth century, consecrated in 839;
- Cathedral of St. Ermengol, 11th century;
- Cathedral of San Odón (actual), century XII.

The primitive episcopal church, located on the top of a hill, was destroyed by a Saracen attack, probably in 793 (Bellmunt and Figueras, 2012). This fact, followed by the adoptionism heresy of Bishop Felix de Urgel, caused a crisis in the population and the transfer from the episcopal seat to another area of the city.

The next cathedral was built on the plain side in vicus Urgelli during the dynasty of Carlo Magno as reported in a document from the episcopal archives and was consecrated in 893 by the bishop Sisebut. This building, known as Santa Maria del Vicus, was modest in nature given the great poverty that existed at that time. Surely its roof was made of wood and had a head with three apses, as recorded in the testament of Count Borrell of the year 994, the cathedral in addition to an altar dedicated to Santa María had another under the invocation of San Juan Bautista.

The bishopric of Urgell had a period of prosperity thanks to the donations of property granted by Borrell II, Count of Barcelona and Count of Urgell (927-992). This power was manifested in the buildings of Bishop Ermengol (1010-1035) who was in charge of completely reforming the cathedral in Romanesque style along with the building of other churches such as Sant Pedro and San Andrés, the San Miguel. These works were financed with the gold obtained in the conquest of the Urgell's Muslims. It is not known if the works of this cathedral had as object to extend the previous one of century IX or to reform it; it was finished and consecrated on October 22, 1040, by the successor of Ermengol, the bishop Eribau. The construction, renovation or expansion of this cathedral is believed to be due to the fact that the former was too small for the number of parishioners, as the population increased during the tenth century. During this time the cathedral received various testamentary donations (Barral and Altet, 1994). In the year 1083 the construction

of a galilea is documented. In addition to the altar dedicated to Saint Mary, it had five more: San Esteban, Santo Sepulcro, San Justo, Santiago and San Ermengol.

The building works of the current Cathedral were started under the bishopric of Odón de Urgell (1116-1122). The work was interrupted due to the continuous clashes between the clergy and the Counts of Foix. In 1175 a master builder, Ramon Llambard, was commissioned to continue with the works. Llambard committed by contract to complete the vault in a maximum period of seven years. The compromise included the completion of the dome and finishing the height of the bell towers, adding a row of stones that raised them above the vault. Llambard also collaborated in the construction of the Basilica of San Michele in Pavia (Barral and Altet, 1994). Llambard was of Italian origin so this represents an explanation of Italian influence on Romanesque style. This master basically completed the order received in 1182, when the bell tower of the main facade had been raised.

In 1195 the city suffered a siege by Arnaldo de Castellbó and Ramón Rogelio de Foix. The cathedral became the defense of the city due to its characteristics that make it almost a fortress. The city was released after the clergy paid a ransom which caused a crisis in the clerical coffers. For this reason, the works of the temple were paralyzed at the end of the 12th century and were never taken over, so the temple remained unfinished but only the works of the cloister were continued. In the Baroque period ornamentation was added to the cathedral that was later suppressed, returning it to the original appearance.

The temple has had several restorations in the twentieth century. The first was initiated in 1918 that suppressed the neoclassical decoration of the interior. Between 1955 and 1974 the church was restored again. During these works, the parts of the temple that were unfinished were covered with stone. In addition, some of the added parts were eliminated to recover the external appearance of the original temple (Bassegoda, 1990). Also, the interior was reformed, which had been somewhat disfigured by the plaster covering applied to it in the 18th century.

3.3. ARCHITECTURAL AND STRUCTURAL FEATURES

The Cathedral is dedicated to Saint Mary and it is also the seat of the diocese. Its Architectural style is Catalan Romanesque but it is considered unique because of its Italianate-style features on the ornaments of its facade and the open gallery of the head of the temple (Junyent, E., 1976).

The cathedral is not isolated and in fact it belongs to an episcopal nucleus which also includes the cloister that connects with the church of Saint Miguel (also called Saint Pedro) the Diocesan Museum of Urgell in the old church of La Piedad and the old House of the Deanery.

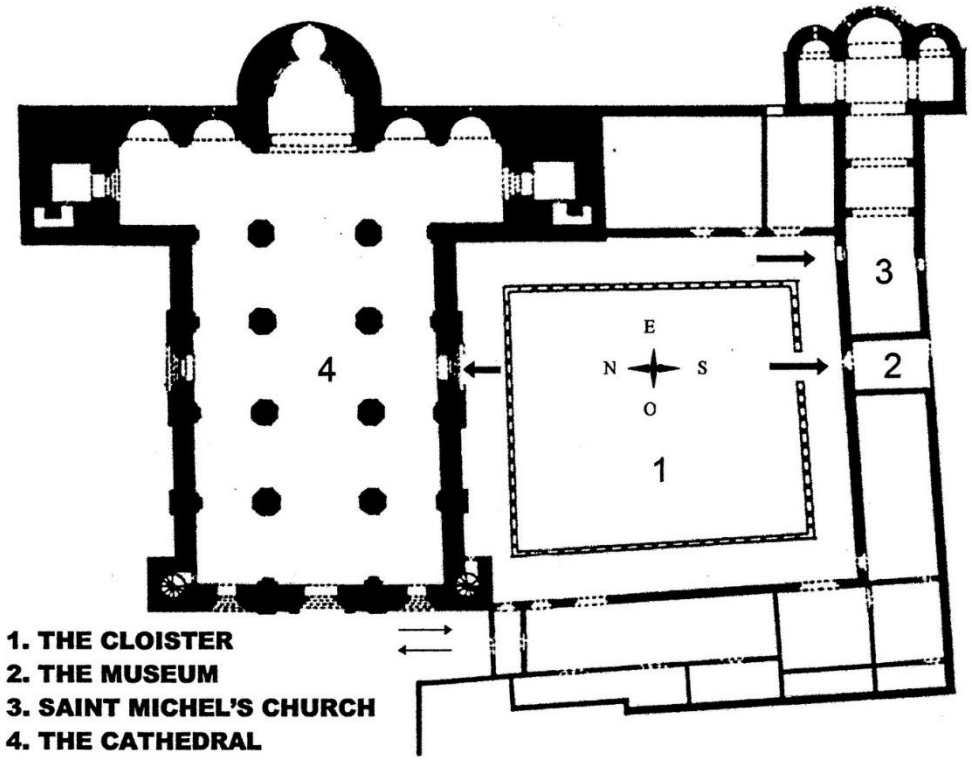

Fig. 21- Episcopal nucleus of La Seu d'Urgell

As is the norm, the church is oriented to the east and has layout in plan with three naves with a very long transept finished in two towers decorated with blind arches and lintels. The Cathedral that we can observe today, without the additions and decorations of successive times, is the result of these various restorations carried out during the 20th century, which were marked by an attempt to put in value the Romanesque past of the building.

Its walls are made of large gray granite ashlar and exceptionally there are reddish stone courses. The façade is flanked by two rectangular towers at the base and octagonal one in the upper body, and crowned by a cornice formed by three ornamental friezes. On the façade three doors open to each of the three naves. The first register of the central body is decorated, below the cornice, with three sections of blind arches, separated by columns that frame a central window and two lateral oculi while the middle register is occupied by three windows with a semicircular arch. The lower register, which contains the central entrance door to the church, is limited by a frieze sculpted with representations of animals, fantastic or not, human faces and fights of beasts and warriors or hunters (Carbonell and Cirici, 1977). On both sides of the door, in the upper part, there are represented two lions facing devouring people. The door itself has double smooth columns on which archivolts rest; the capitals are decorated with scenes of animals and characters in fight or hunting. On the front and at the apex of the façade there is the bell tower. The Italian influence can be seen in the façade in fact all these details recall the façade of the Church of San Nicola in Bari and the Church of San Michele in Pavia.

Fig. 22- Façade of the Cathedral

On the north side there is another door in the same style as the central door of the façade on which there is a series of blind archivolts. The entire structure of the building, with the two large compact towers at the ends of the transept and the two smaller ones at the ends

of the façade, together with the walls, give the effect of a fortress. In fact it is plausible to think that the original designers wanted to make it both a religious place and a fortress in case of enemy attack.

Fig. 23- Details of the door on the north side

On the South side there is another door which is inside the cloister. It is like the previous ones with two columns on each side with capitals decorated with zoomorphic and vegetal motifs. The five archivolts, all with geometric decorative representations and with human heads, form the semicircular arch of the door somewhat lower and wider than all the others of the building, as a differential feature has on its right side a pile of holy water of form octagonal.

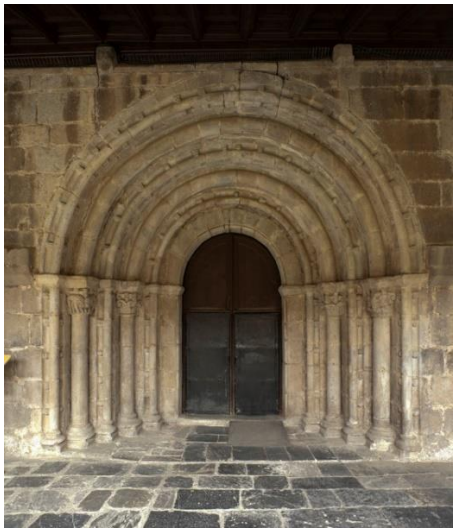

Fig. 24- Details of the door on the sur side

The total length of the Cathedral is 52.82 meters, its width is 23.42 meters and its height is 19.80 meters on the central nave and 11.18 meters on the side aisles. The transept measures 36 m and the cupola of the dome rises to 24.67 m in height. The cathedral has a basilica plan with three naves divided into four sections, leading to a large transept which has five apses (only the central forms a large semicircle to the outside and covers the entire width of the central nave). The central nave is covered with a barrel vault reinforced by sub-arches that start from an impost that runs throughout the nave, while the lateral aisles, lower than the central nave, have cross vaults. Also the transept is covered with a barrel vault. The pillars of the naves, four on each side, have a Greek cross section and start from an octagonal base. They have at each angle attached columns, which in the central nave go to the sub-arches of the vault, other two form the arches of communication between the naves in longitudinal direction and the last corner columns reach the edges of the ribbed vaults of the aisles. Besides, there are flying arches only on one side, like shown in the following figures.

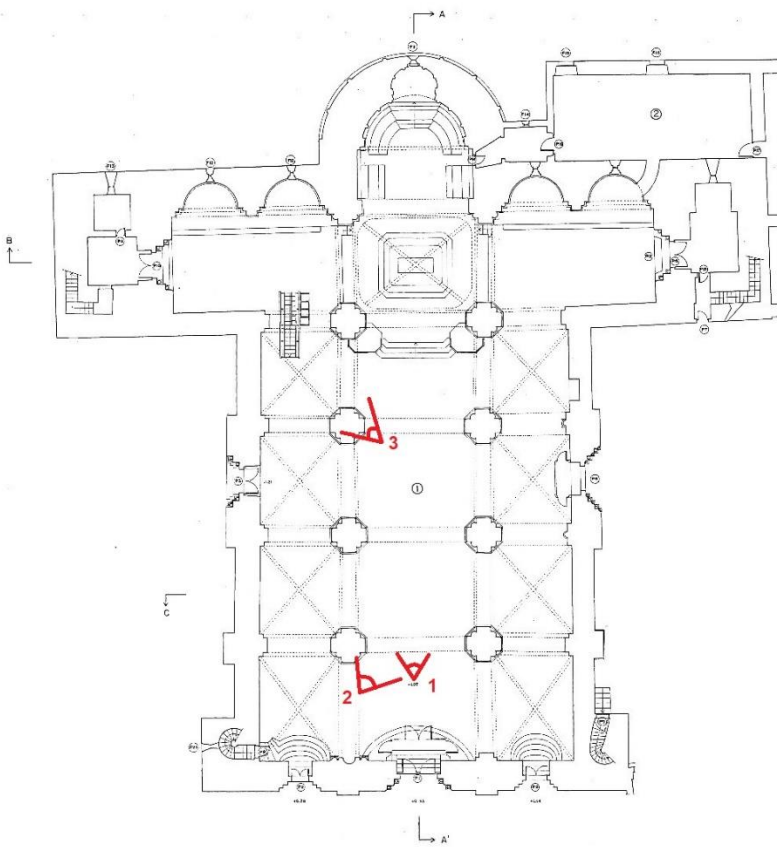

Fig. 25- Layout of the Cathedral

Fig. 26- Section A-A'

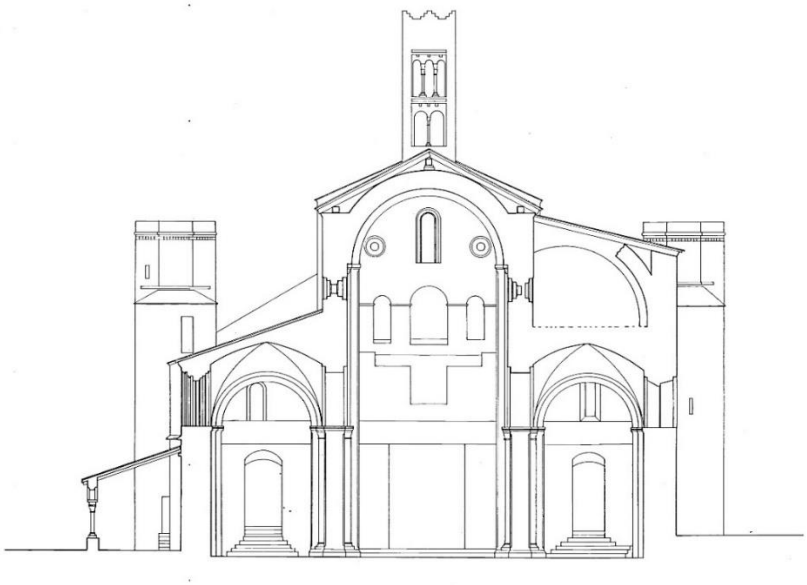

Fig. 27- Section C-C'

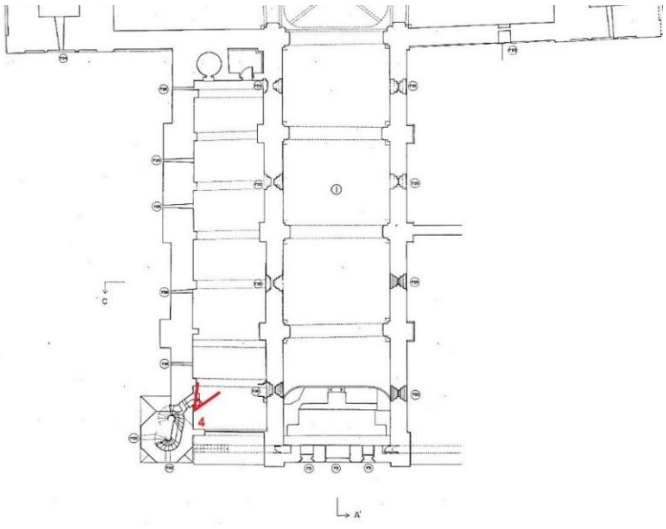

Fig. 28- Detail of flying arches

The section A-A' is a longitudinal section of the Cathedral and the longitudinal arches that connect the pillars can be seen. Besides the difference in heights between the naves can be noted. The section C-C' is a transversal section of the Cathedral that shows the barrel vault, the cross vaults and the flying arch. Finally, there is a detail of the flying arches which are placed at the pillars and halfway between them. The following photos are taken from the marks of the previous sections.

Fig. 29- Photo 1,2,3,4

4. APPLICATION OF GRAPHIC STATICS

In this work the following part of the Cathedral was analyzed which has a width of 8.175 meters.

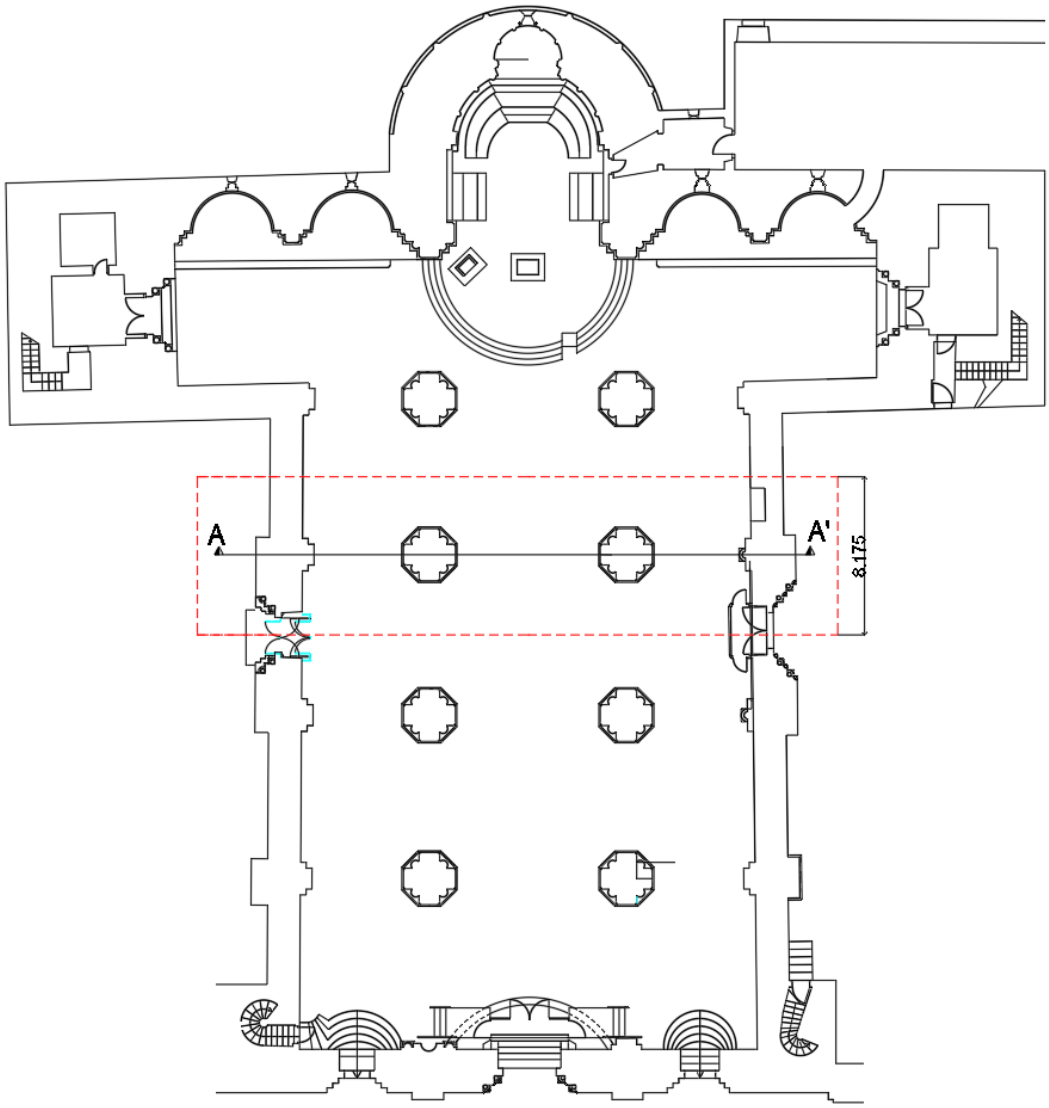

Fig. 30- Section analyzed

The development of this work was realized in different phases. First of all, the cathedral was analyzed in its original state, so an equilibrium solution was found to the case of cathedral subject to dead load; secondly the structure was studied with considering the flying arches; then the significant deformation of the barrel vault was taking into account and finally the structure was studied applying seismic action.

4.1. CALCULATION HYPOTHESIS

Some information regarding geometry and materials were unknown. So, following the inspection, it was possible to make several hypothesis.

Regarding the materials, the weight (per unit volume) of the structural blocks is assumed equal to 25 kN/m^3 while the weight (per unit volume) of the filling material is assumed equal to 18 kN/m^3. Besides, the weight (per unit area) of the roof is assumed equal to 3 kN/m^2.

The thickness of the barrel vault is unknown and a thickness of 0.6 m was assumed. Also, the thickness of the cross vault is unknown and a thickness of 0.2 m was assumed.

The thickness of the sub-arches of the barrel vault is equal to 0.4 m while its width is equal to 1.08 m. The longitudinal arches which connect the pillars in the longitudinal direction are composed by two arches with the same thickness (0.35 m) and different width (1.08 m and 1.4 m) while the wall above them has the same width of the upper arch (1.4 m). The flying arches are placed at the pillars and there is one also between the pillars, so it's like there are two flying arches in the part analyzed. Every flying arch has a width of 0.7 m so the total width considered is 1.4 m. The section area of the pillar is equal to 4.98 m^2. All these details are shown in the Annex.

It was assumed that the load of the vault is transferred to the pillars, while the longitudinal arches transmit the weight of the walls above them on their base on the pillars. Clearly the horizontal force on the pillar in longitudinal direction can be neglected because the one of an arch is canceled by means of the horizontal force of the following arch so it's more interesting calculate the weights.

4.2. CALCULATION METHOD

First of all, all the structural parts (barrel vault, flying arch, cross vault, longitudinal arch) have been studied separately by means of graphic statics.

Firstly, in according to the previous hypothesis, it was possible to calculate all the gravity loads on these structural parts. To do this, in according to graphic statics, all the structural parts have been divided into many voussoirs, so the weight of each voussoir have been

calculated taking into account the correct dimension and the weight per unit volume supposed. Clearly, also the external loads (such as the roof for the barrel vault) were also considered in the calculation. In this way, it was possible to define a thrust line in the arches/vaults; for the barrel vault the thrust line found was the minimum one, while for the others (flying arch, cross vaults) the calculation of the thrust line was connected to the thrust line in the structure, so there were more solutions for the different cases.

For the seismic case, a horizontal force has been added to each weight force calculated; these forces are proportional to the weight force by a seismic coefficient identified in the Annex in according to Italian legislation.

4.3. CASES ANALYZED

There are five cases that were analyzed: the structure subject to the gravity loads in its original state (without the flying arches); the structure with the flying arches subject to the gravity loads; the structure considering the deformations of the barrel vault subject to the gravity loads; the structure with deformations subject to gravity loads and seismic actions (one direction and opposite direction).

4.3.1. ORIGINAL STRUCTURE

In the original state the Cathedral didn’t have the flying arches, so it was analyzed the following section:

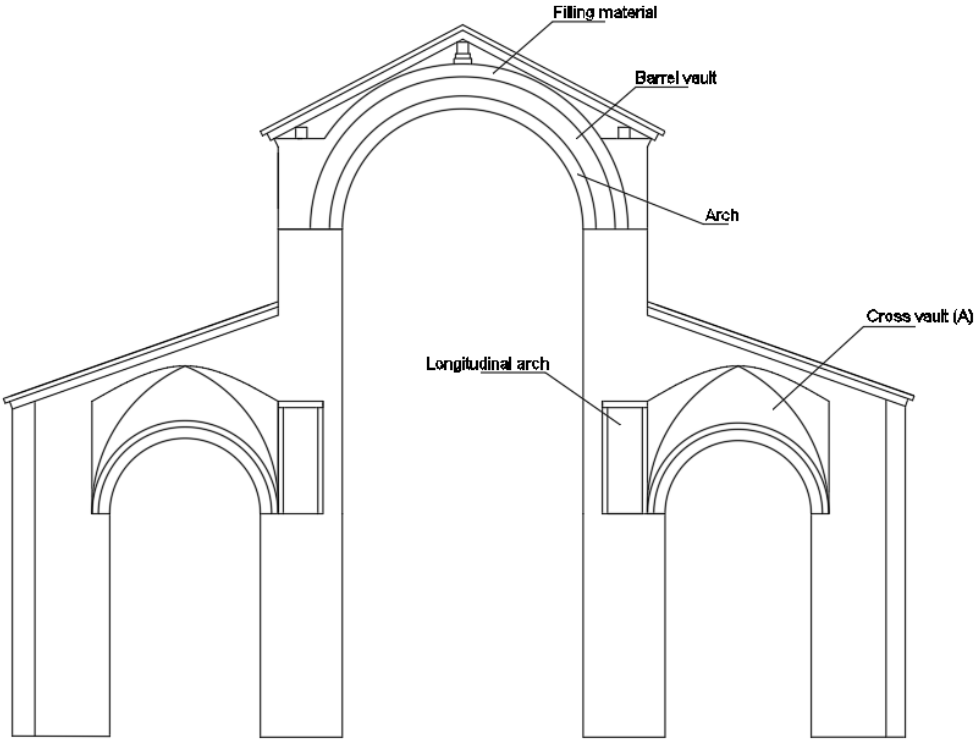

Fig. 31- Section analyzed in original state

First of all, studying the barrel vault, a minim thrust line is found for which the reactions are equal to 1471.36 kN.

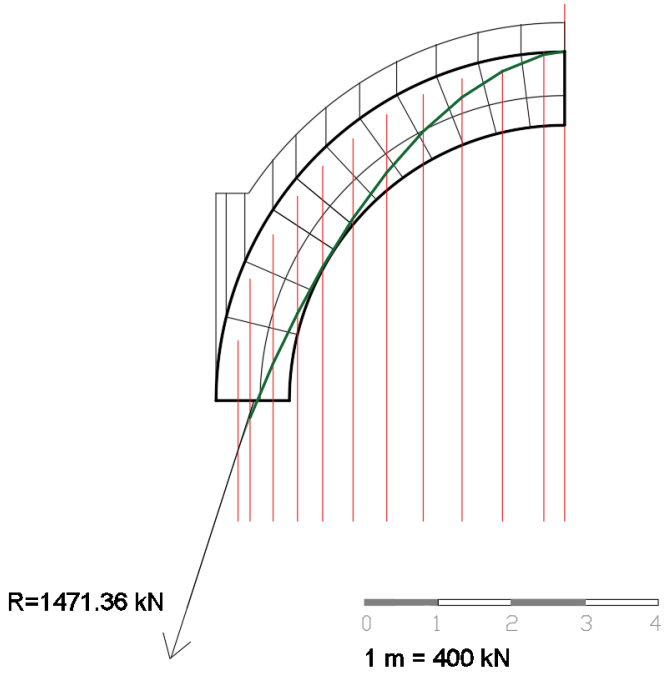

Fig. 32- Thrust line and reaction in the barrel vault

Then, studying the cross vaults, their thrust line and reactions have been determined. The cross vault was decomposed in in a system of one-dimensional arches and studied like an arch.

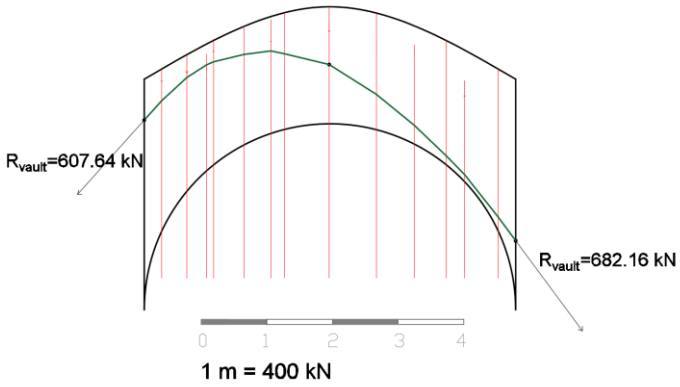

Fig. 33- Thrust line and reactions in the cross vault

Besides, the reaction transmitted by the longitudinal arches to the pillar on their base have been calculated which are equals to 1676.56 kN.

So, combining all these thrusts with the force vectors of the weights of the pillars, the thrust line of the structure in its original state has been drawn. All the passages of the application of static graphic are explained step by step in the Annex

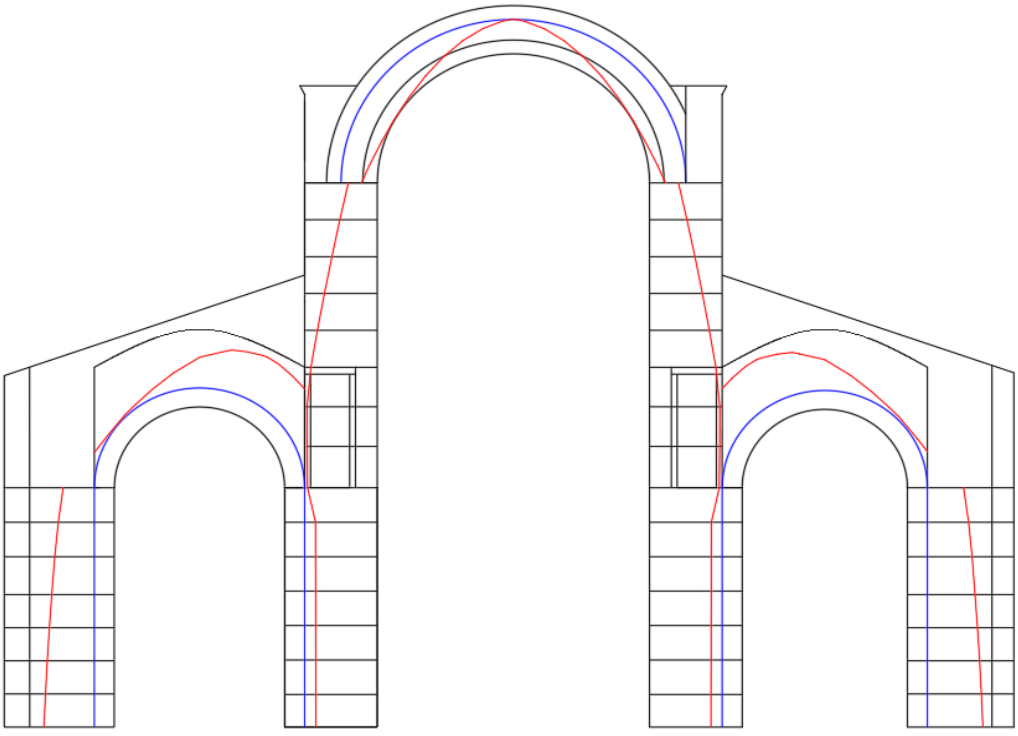

Fig. 34- Thrust line in the original structure

As seen from the previous figure, the thrust line is easily inside the structure and the current situation is far from the collapse for which ten hinges are required. Besides, the thrust line can easily be changed increasing the thrust of the cross vaults.

4.3.2. STRUCTURE WITH FLYING ARCHES

Then the structure was studied considering the flying arches which are present only on one side. So, the following section was analyzed.

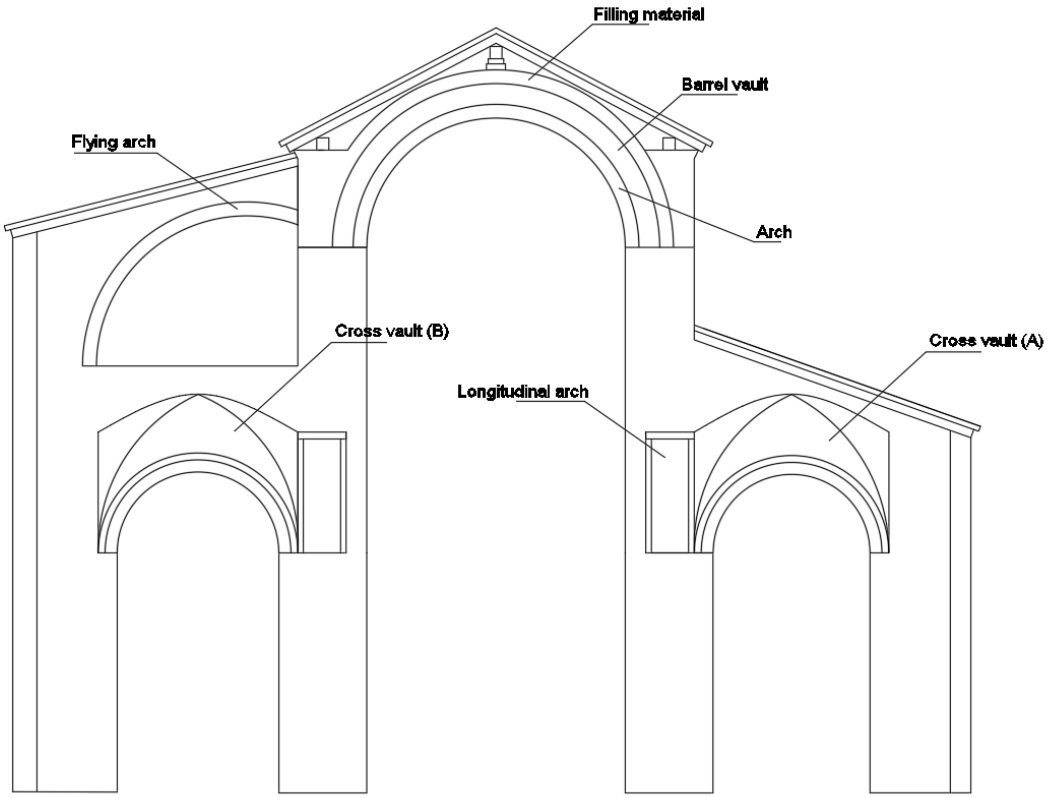

Fig. 35- Section analyzed in the current state

For this case, the thrust line of the barrel vault is considered equal to the previous one. Also, the reactions transmitted by the longitudinal arches to the pillars are the same with the previous ones. Also, the thrust line of the cross vault on the left side is the same. So it's necessary to calculate a new thrust line in the cross vault on the right side and a thrust line in the flying arch.

For the flying arch, the following thrust line and reactions have been determined.

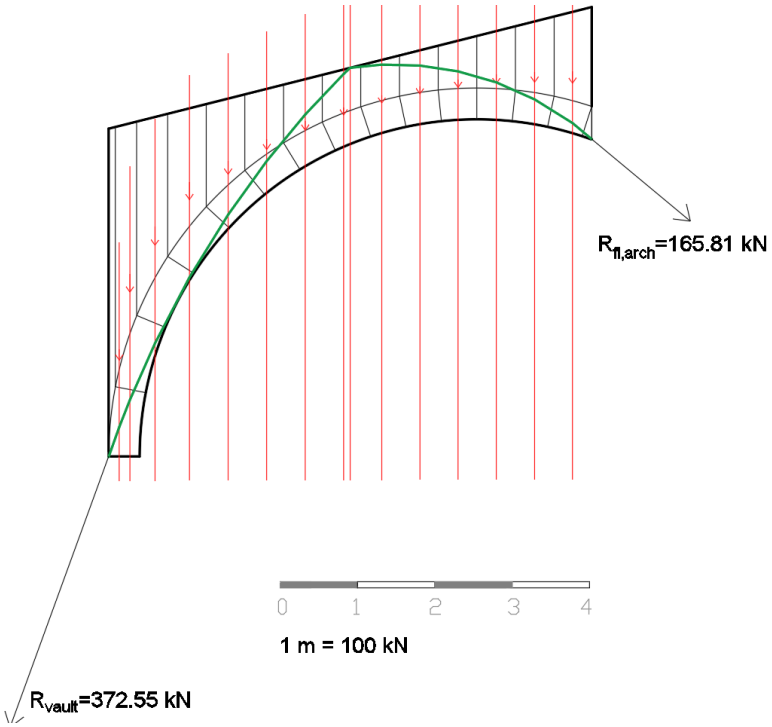

Fig. 36- Thrust line and reactions of the flying arch

Then, studying the cross vault on the left side as explicated in the previous one, the following thrust line and reactions have been determined.

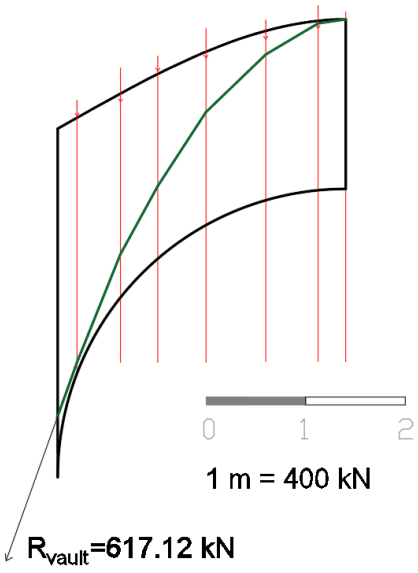

Fig. 37- Thrust line and reaction on the cross vault

So, combining all these thrusts with the force vectors of the weights of the pillars, the thrust line of the structure in its original state has been drawn. All the passages of the application of static graphic are explained step by step in the Annex.

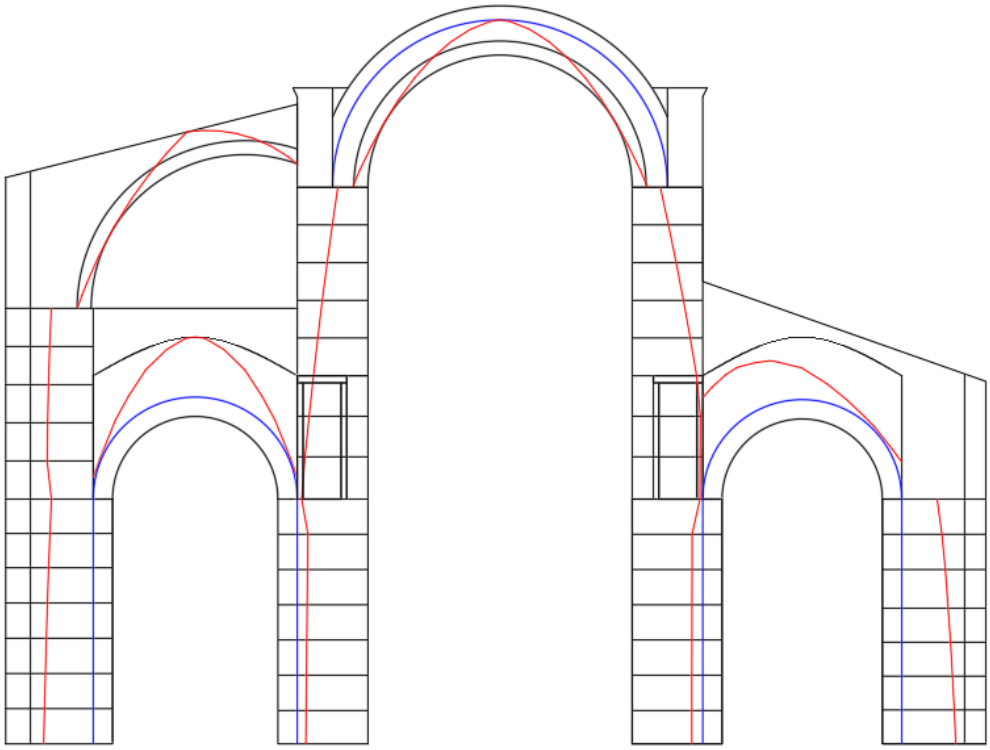

Fig. 38- Thrust line in the structure with flying arches

As seen from the previous figure, the thrust line is easily inside the structure like the previous case. As a consequence of the introduction of the flying arches it was possible to reduce the thrust in the cross vault. Even in this case the current situation is far from the collapse and the thrust line can easily be changed increasing the thrust of the cross vaults.

4.3.3. STRUCTURE WITH DEFORMATION

The structure of the nave of the cathedral is showing at present significant deformation and some damage as it can be seen in the following figure.

Fig. 39 - Photo of the deformations of the barrel vault

The differences with the previous case can be seen in the following figure:

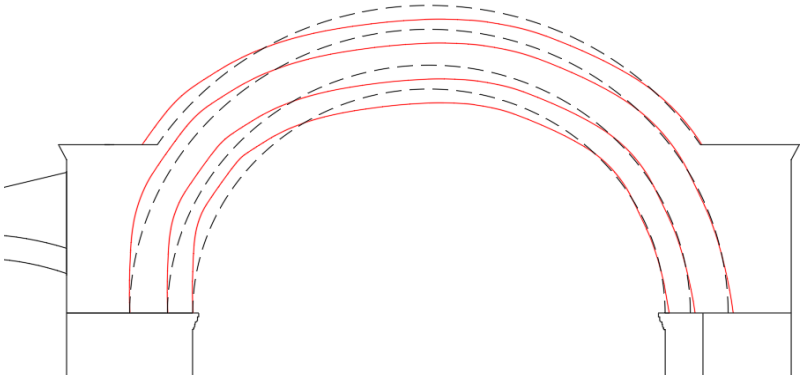

Fig. 40- Deformations in the barrel vault

The barrel vault is lowered because of these deformations. Clearly, it's necessary to calculate a new thrust line, for which new reactions have been obtained.

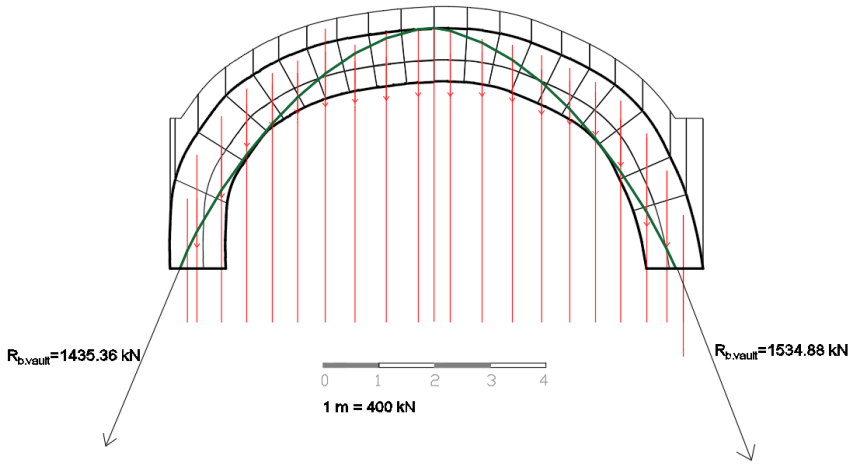

Fig. 41- Thrust line and reactions in the barrel vault with deformations

Comparing with the reactions of the previous barrel vault, these new reactions have a higher horizontal component. For this reason, it's necessary to increase the thrusts of the other structural parts.

For example, in the flying arch the following thrust line has been considered.

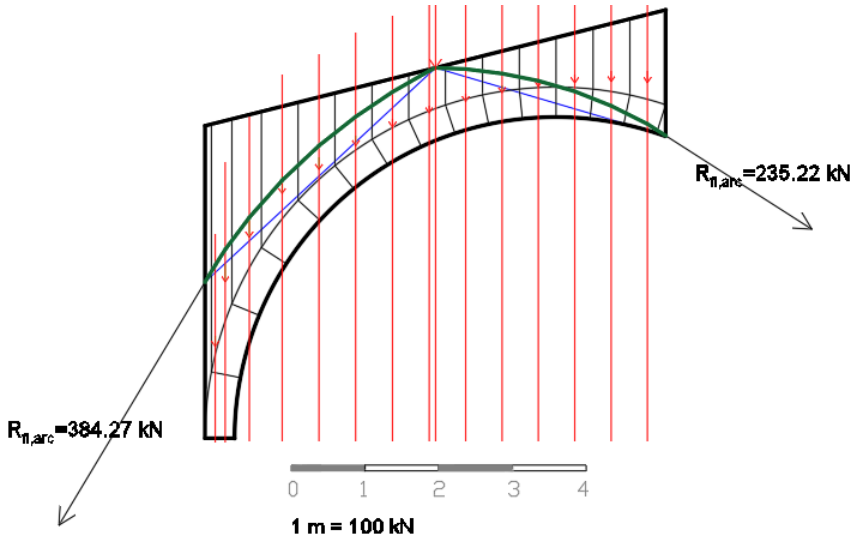

Fig. 42- Thrust line and reactions in the flying arch

For the cross vault (A) (of the right side), the following thrust line is assumed. As it can be seen, it's necessary to consider the passage of the thrust line in the upper material of the cross vault. Obviously, this is a consequence of the higher thrust in the barrel vault.

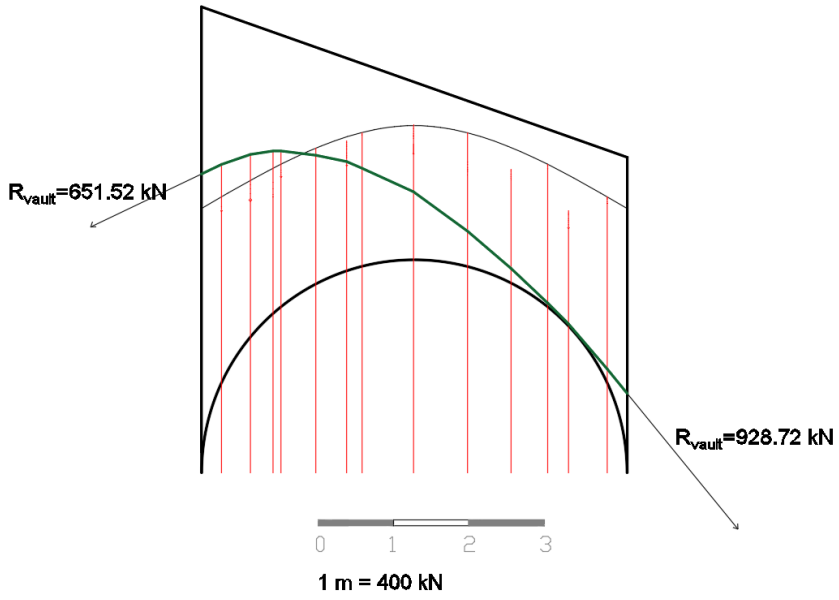

Fig. 43- Thrust line and reactions in the cross vault (A)

Finally, for the cross vault (B) (of the left side) the following thrust line has been determined.

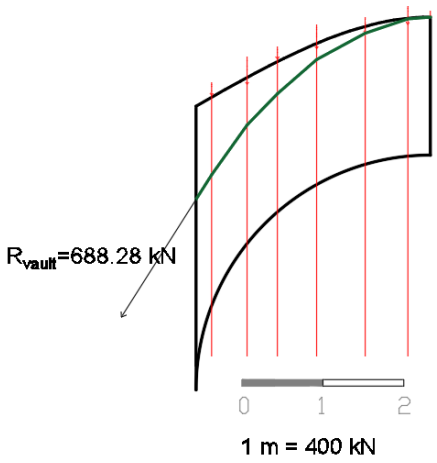

Fig. 44- Thrust line and reactions in the cross vault (B)

So, combining all these thrusts with the force vectors of the weights of the pillars, the thrust line of the structure in its original state has been drawn. All the passages of the application of static graphic are explained step by step in the Annex

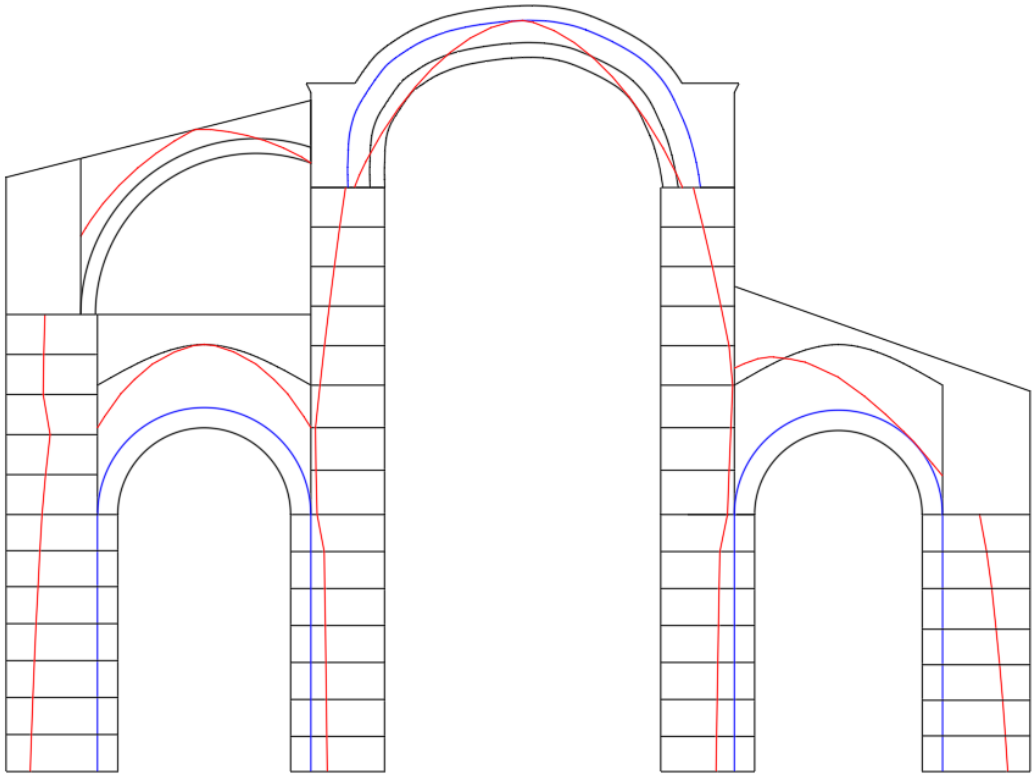

Fig. 45 - Thrust line in the structure with deformations

Also in this case the thrust line is easily inside the structure but it was necessary to consider the passage of the thrust line of the cross vault of the right side in the upper material and to increase the thrust of the flying arch. The current situation is far from the collapse and the thrust line can easily be changed increasing the thrust of the cross vaults.

4.4.4. STRUCTURE WITH SEISMIC ACTION

According to NCSE-02, the seismic acceleration to be considered is obtained as:

$$a_c = S \cdot \rho \cdot a_b$$

Where:

- a_b is the basic acceleration, which is equal to 0.06 g in La Seu de Urgell;
- ρ is the dimensionless risk coefficient, which is equal to 1.3 for a building of patrimonial character;
- S is the coefficient of extension of the ground, so a type II ground has been adopted which corresponds to fractured rock or dense granular soil, for which S is equal to 1.04.

So the seismic acceleration is equal to 0,081g.

The calculation has been made by adopting a distribution of equivalent static forces proportional in value and distribution to the mass of the structure. The horizontal acceleration applied has been calculated as:

$$a/g = a_c \cdot \alpha \cdot (1/q)$$

where:

- α is the ordinate of the response spectrum which is equal to 2.5;
- q is is a factor that measures the ductility of the structure.

The q factor has been calculated with the Italian legislation (Circolare 2 febbraio 2009, n. 619, 8.7.1.2); for buildings with not regular height the legislation states that:

$$q = 1{,}5\ \alpha_u/\alpha_1$$

Where α_u / α_1 can be equal to 1.5 in the absence of more accurate valuations, so the final value adopted of q is equal to 2.

Then the equivalent seismic force adopted (per unit volume) is equal to:

$$f = 0.081g \cdot 2.5 \cdot {}^{1}/_{2} \approx 0.1\ g$$

However, the actual seismic force adopted (per unit volume) is equal 0.05 g. Already the use of this force, will lead to the formation of a local mechanism in the structure, which will be shown later.

Therefore, a horizontal force must be added for each block:

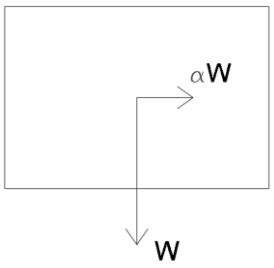

Fig. 46- Application of horizontal force to each block

Where W is the weights and $\alpha = 0.05$.

Clearly the seismic action is considered in two opposite directions (+ like to the the right and – like to the left of the section), so two different solutions have been determined.

- Seismic direction (-)

Considering the seismic direction (-) to the left, obviously the reactions on the left side are higher, like their horizontal component. So it will be more critical the left side of the section. For the barrel vault, the following thrust line and reactions have been obtained.

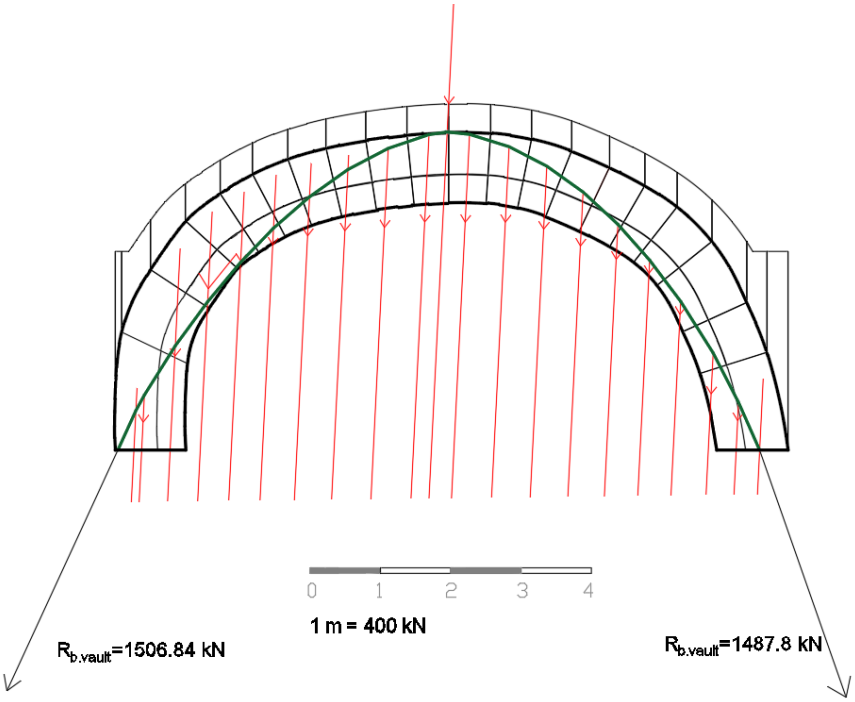

Fig. 47- Thrust line and reactions of the barrel vault - seismic direction (-)

Considering the flying arch, the following thrust line and reaction have been determined. As a consequence of the seismic action in the left direction, the reaction of the right clearly has a higher horizontal component than the previous cases while the reaction of the left side was minimized.

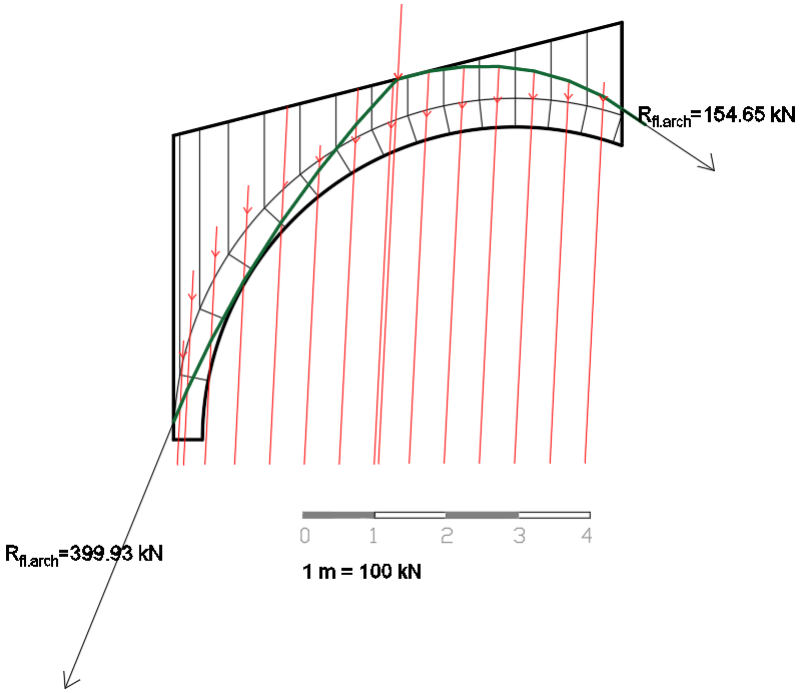

Fig. 48- Thrust line and reactions of the flying arch - seismic direction (-)

The cross vault (B) has the following thrust line and reactions.

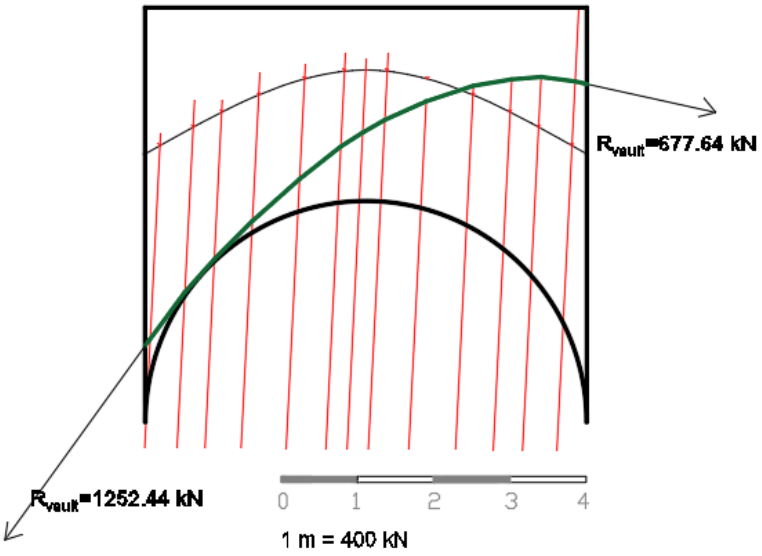

Fig. 49- Thrust line and reactions of the cross vault (B) - seismic direction (-)

Clearly, it was necessary to increase the reaction on the right side and minimize the reaction on the left side for the same reason explicated in the flying arch.

Finally, the thrust line and the reactions of the cross vault (A) are the following.

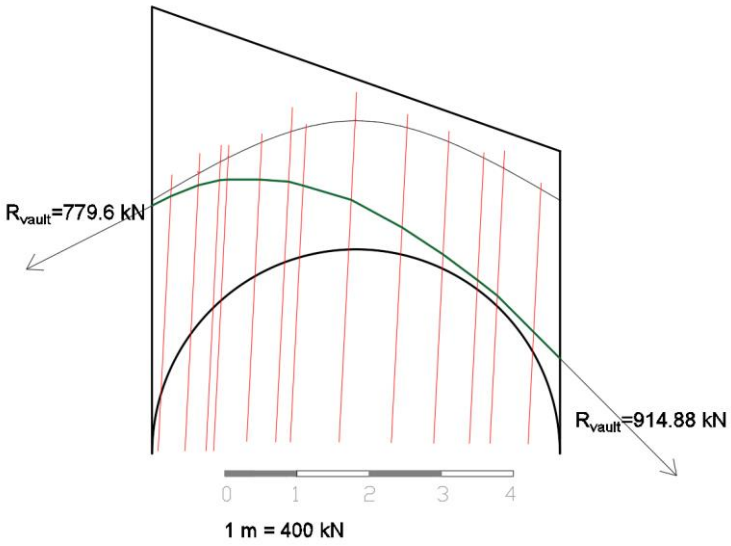

Fig. 50- Thrust line and reactions of the cross vault (A) - seismic direction (-)

So, combining all these thrusts with the force vectors of the weights of the pillars, the thrust line of the structure in its original state has been drawn. All the passages of the application of static graphic are explained step by step in the Annex

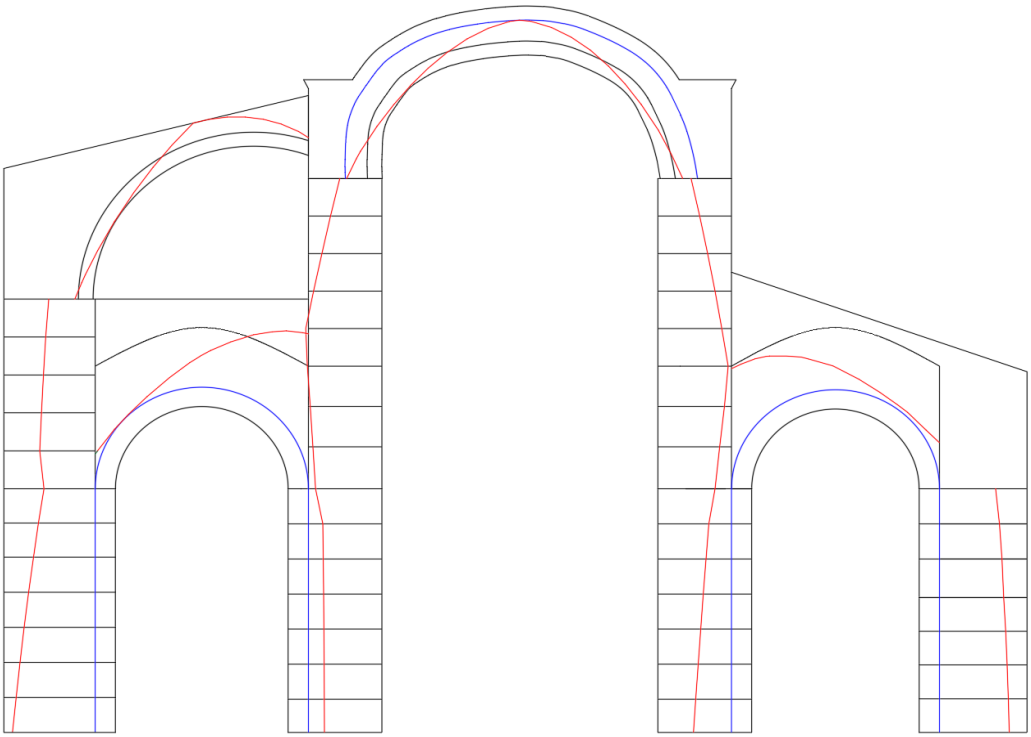

Fig. 51- Thrust line in the structure - seismic direction (-)

In this case, a local mechanism is formed and it's not possible to avoid it. For this reason, it's not allowed to use a higher seismic coefficient as said previously.

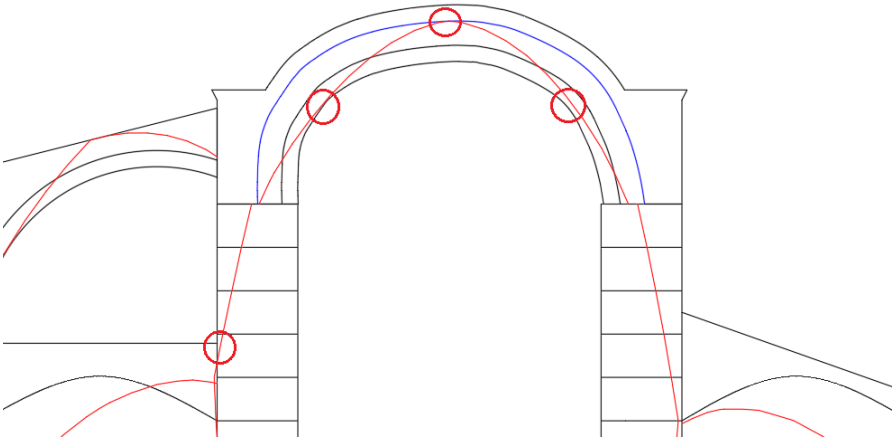

Fig. 52- Local mechanism formed in the seismic direction (-) case

- Seismic direction (+)

Considering the seismic direction (+) to the right, obviously the reactions on the right side are higher, like their horizontal component. So, it will be more critical the right side of

the section. For the barrel vault, the following thrust line and reactions have been obtained.

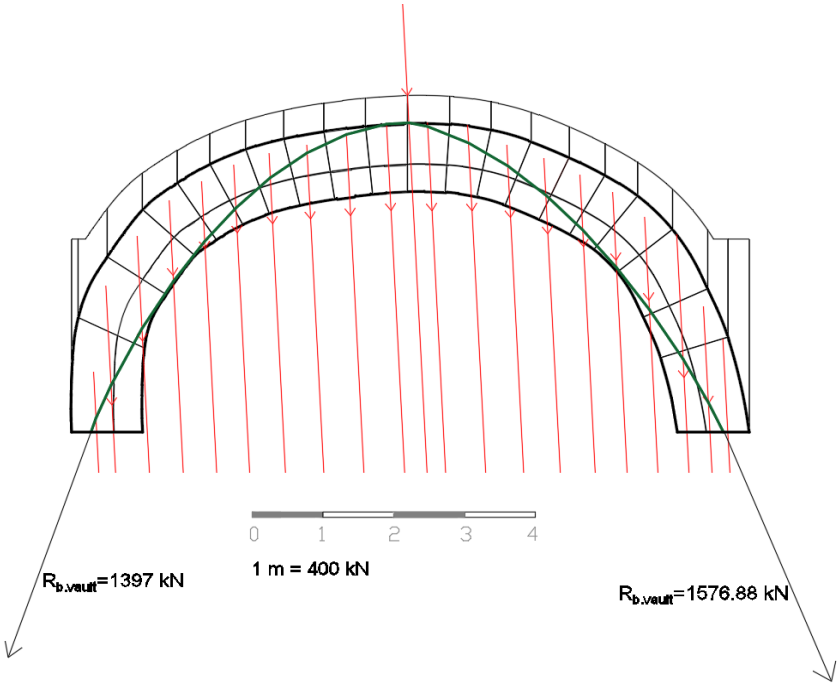

Fig. 53- Thrust line and reactions of the barrel vault - seismic direction (+)

In the flying arch the following thrust line and reactions have been determined.

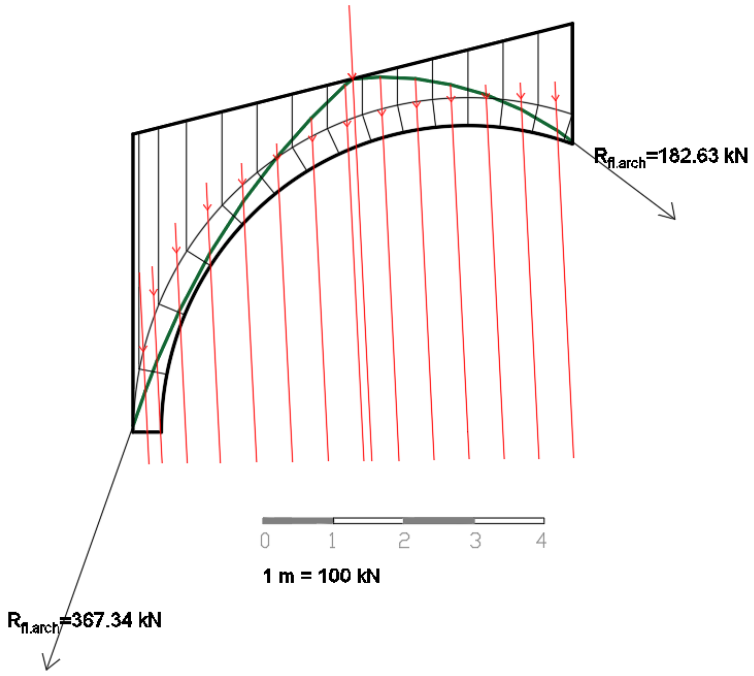

Fig. 54- Thrust line and reactions of the flying arch - seismic direction (+)

For the cross vault (A) (of the right side), the following thrust line is assumed.

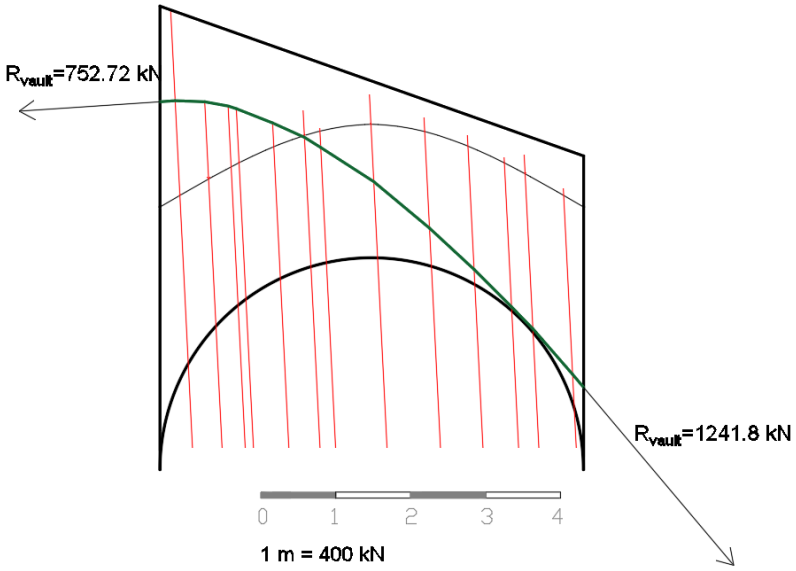

Fig. 55- Thrust line and reactions of the cross vault (A) - seismic direction (+)

For the cross vault (B) (of the left side), the following thrust line is assumed.

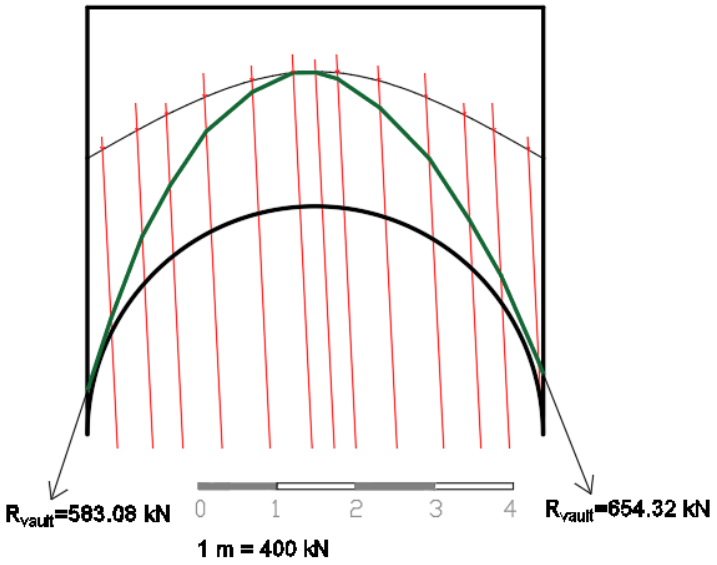

Fig. 56- Thrust line and reactions of the cross vault (B) - seismic direction (+)

So, combining all these thrusts with the force vectors of the weights of the pillars, the thrust line of the structure in its original state has been drawn. All the passages of the application of static graphic are explained step by step in the Annex

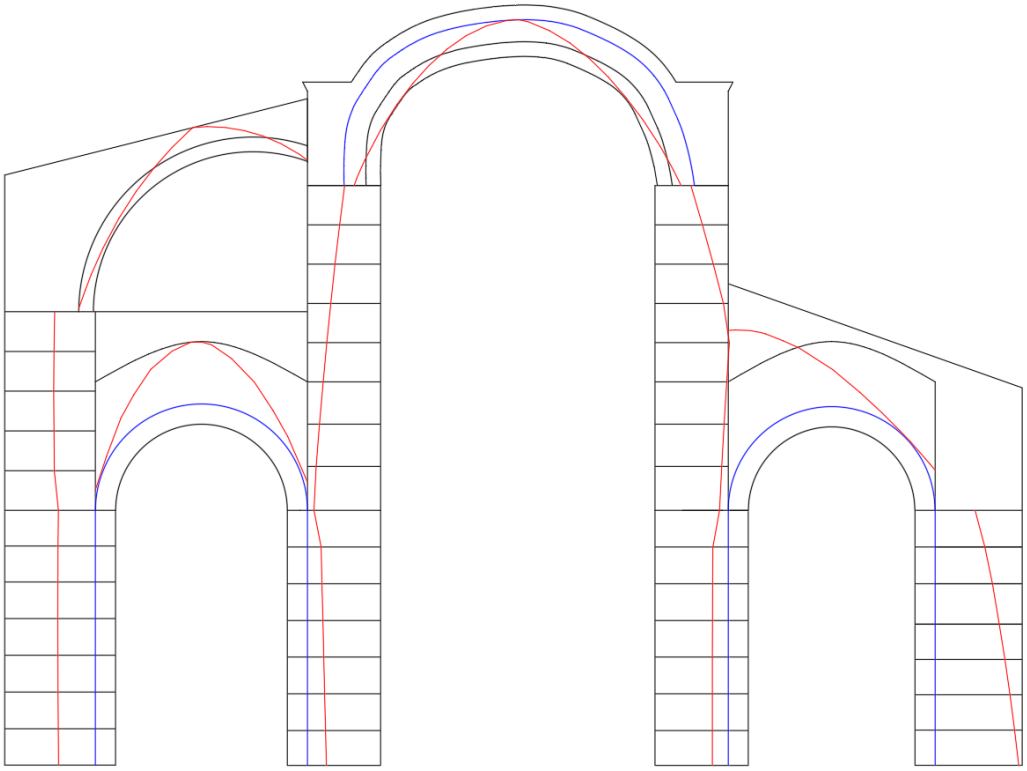

Fig. 57- Thrust line in the structure - seismic direction (+)

In this case the thrust line is easily inside the structure.

4.5. POSSIBLE STRENGTHENING INTERVENTIONS

This simple analysis testifies the need for possible strengthening interventions in order to increase the condition of the structure.

An initial idea could be the introduction of the flying arches on the other side. In this way the structure will be able to work in symmetric conditions and would guarantee a better distribution of loads.

Otherwise, a more effective and less demanding solution may be the use of ties placed in correspondence of the springer of the vault. The use of ties would prevent the formation of this local mechanism and would reduce the thrusts of the barrel vault transmitted to the pillars. This type of intervention is certainly efficient (from the structural point of view) but compromises the aesthetic appearance.

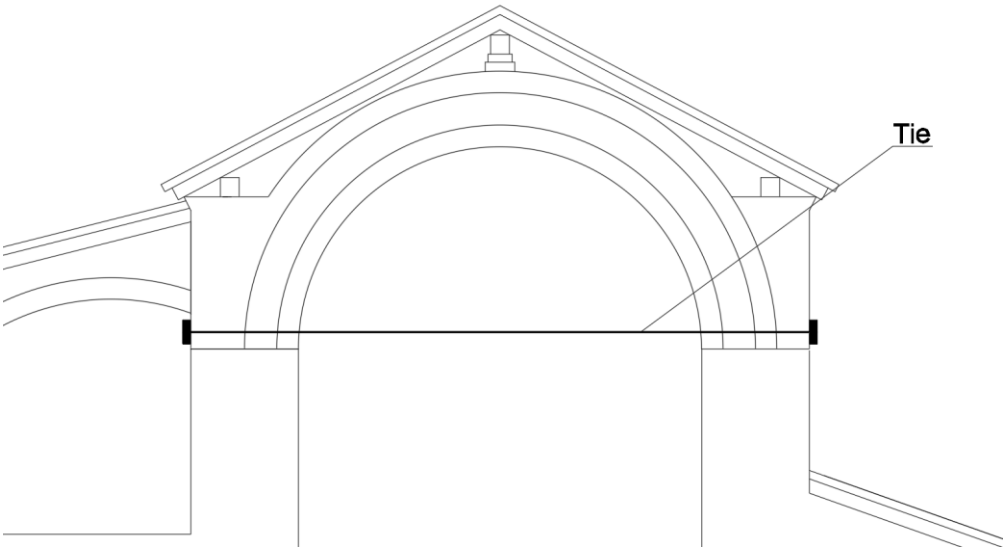

Fig. 58- Introduction of ties

Finally, other method for the consolidation of the barrel vault can be the “clamp method” which provides for the creation of a "metal clamp" at the extrados of the arch or vault, composed of a horizontal element (a metal beam) and two inclined lateral ties, inserted in the walls. This method is more complicated but allows to not compromise the aesthetic appearance.

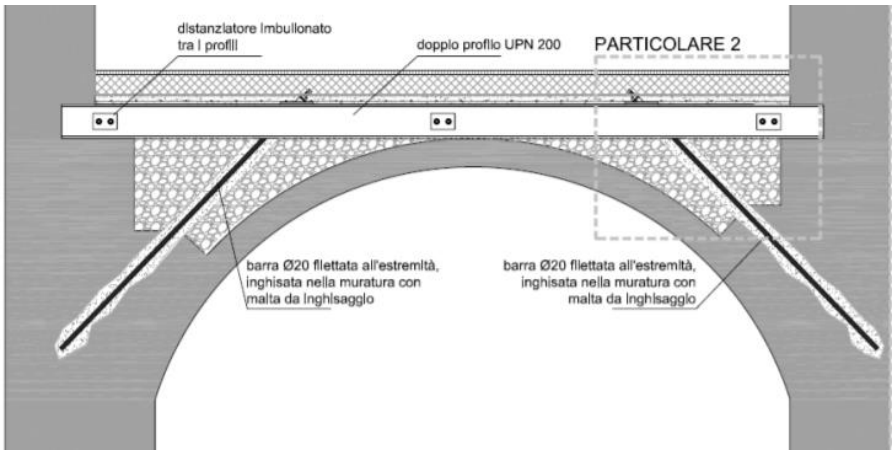

Fig. 59- Example of clamp method

5. CONCLUSIONS

Limit analysis constitutes a very reliable and powerful tool and can be used to assess masonry structures (in combination with other possible tools). In fact, this graphic approach can be useful to understand and validate the result of the computational analysis.

As shown in the work, the application of graphic static is very simple and useful and it allowed to evaluate the safety of the Cathedral subjected to gravity loads and seismic action.

Firs of all, it was possible to understand how the deformations and damages of the central nave affect the behavior of the structure. In fact, studying the structure with deformations subjected only to gravity loads, it was more complicated to find a solution in comparison to the previous case (without considering the deformations), as a consequence of the higher reactions of the barrel vault. In particular, the greatest difficulty involved the right side of the studied section, which is the one without flying arches. This showed how the addition of flying arches only one side, is useless and senseless. However, it was easy enough to find a thrust line inside the structure considering only the gravity loads.

Instead, in the seismic cases, it was more difficult to find a thrust line inside the structure and it was necessary to change the hypotheses on the thrust lines of the various structural elements several times. Besides, as shown in the seismic case (direction -), a local mechanism is formed that has not allowed to use a higher seismic coefficient, although according to Italian law it was possible for this structure. For this reason, there is some concern about long-term stability of the Cathedral under gravity loads and under earthquake and it would be appropriate to consider strengthening interventions.

6. REFERENCES

- Asteris et al. (2015). Numerical Modeling of Historic Masonry Structures. Handbook of Research on Seismic Assessment and Rehabilitation of Historic Structures, Chapter: 7; Editors: Panagiotis G. Asteris, Vagelis Plevris, pp.213-256
- Barral and Altet, X. (1994). Les catedrals de Catalunya, Editorial: Edicions 62, Barcelona
- Bassegoda J. (1990). Proyectos barrocos para la Seu d'Urgell. Revistas Espacio, Tiempo y Forma. Series I-VII, Madrid
- Bellmunt and Figueras. (2012). Catedral de la Seu d'Urgell from: http://www.lleidatur.com/Turismo/Visita/Turismo-religioso-lAlt-Urgell---Catedral-de-la-Seu-dUrgell/29.aspx
- Carbonell and Cirici (1977). Grans monuments romanics i gotics, Editorial: Edicions 62, Barcelona
- Carrero Santamaría, E. (2010). La Seu d'Urgell, el último conjunto de iglesias. Liturgia, paisaje urbano y arquitectura. Anuario de estudios medievales (AEM), pp. 251-291
- Heyman J. (1998). Structural Analysis: A Historical Approach. Cambridge University Press
- Junyent, E. (1976). Catalunya romànica: l'arquitectura del segle XII. Publicacions de l'Abadia de Montserrat
- Jurin L. (2011). Re-descovering a consolidation technique for arches and vaults: the “new clamp” method. From: http://www.jurina.it/10/2012/02/2011_La-riscoperta-del-metodo-delle-graffette-per-il-consolidamento-di-archi-e-volte.pdf
- Kömürcü et al. (2017). Macro and Micro Modelling of the Unreinforced Masonry Shear Walls. Periodicals of Engineering and Natural Sciences. 5, pp. 314-321
- Magenes G. (2003). Edifici con strutture in muratura. IX Corso di aggiornamento professionale. L’Ingegneria e la Sicurezza Sismica.

- NCSE-02. Norma de Construccion Sismorresistente: Parte general y edificacion
- Puig and Cadafalch, J. (2003). Escrits d'arquitectura, art i política. Volumen 62 de Memòries de la Secció Històrico-Arqueològica. Barcelona Institut d'Estudis Catalans
- Roca P. (2018). Ancient Rules and Classical Approaches- Part 1-4. SA1 Lectures. Advanced Masters in Structural Analysis of Monuments and Historical Constructions, Barcelona.
- Sabia D. (2018). Costruzioni in muratura. Politecnico di Torino, Italia.

7. ANNEX

In this annex there is a detailed explanation of the calculations for each case analyzed. Each case is shown in a step-by-step scheme following the sequence of passages followed with the use of graphic statics.

The structural parts have been studied separately. First of all, they have been divided into some voussoirs; after the calculation of the weight of each voussoirs, it was possible to determine a force polygon and a funicular polygon in order to obtain the thrust line and the corresponding reactions. Finally, combining all the thrust with the force vectors of the pillars and the walls, it was possible to draw a thrust line inside the structure.

1) ORIGINAL STRUCTURE

In its original state the structure didn't have the flying arches. So, the section analyzed is the following:

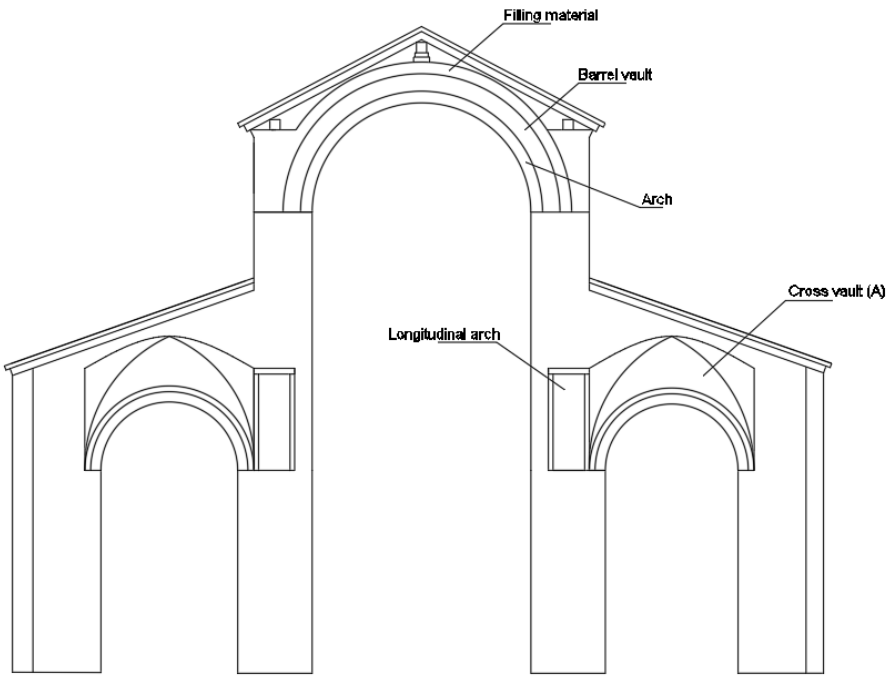

Fig. A. 1- Section analyzed in original state

It starts with the barrel vault which is the central in the section. Above this there is a roof that leans on three supports. The weight of the roof is assumed equal to 3 kN/m^2 so

considering a width of 8.175 m it is obtained a linear weight of 24.525 kN/m. In this way it's possible to calculate the reactions of the roof on the barrel vault which are expressed in the following figure:

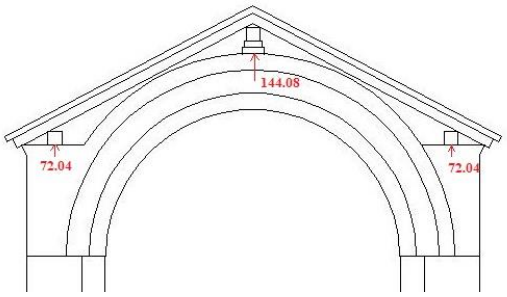

Fig. A. 2- Reactions of roof on the barrel vault

BARREL VAULT

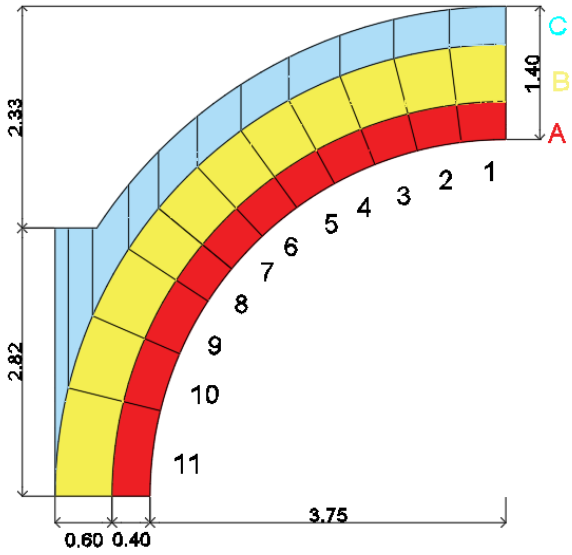

Fig. A. 3- Division of the barrel vault

In this figure the part A represents the arch which rests on the pillars under the vault; it has a width of 1.08 m and has a thickness of 0.4 m. The part B represents the barrel vault with a width of 8.175 m and a thickness of 0.6 m. Finally, there is the filling material (part C). The weight assumed for the materials is 25 kN/m^3 for the structural part and 18 kN/m^3 for the filling material. So, it's possible to calculate the weight of each voussoirs:

Areas [m^2]	Weights [kN]
A1= 0.1985= A2=...=A7	A1= 5.359= A2=...=A7
A8= 0.1775	A8= 4.793
A9=0.2659	A9=7.18
A10=0.2663	A10=7.19
A11=0.3823	A11=10.32
B1= 0.3355= B2=B3...=B7	B1= 68.57= B2=B3...=B7
B8= 0.2993	B8= 61.17
B9=0.45	B9=91.97
B10= 0.45	B10=91.97
B11=0.646	B11=132.03
C1=0.2387	C1=35.12
C2=0.2384	C2=35.08
C3=0.2378	C3=34.99
C4=0.2367	C4=34.83
C5=0.2351	C5=34.59
C6=0.2327	C6=34.24
C7=0.229	C7=33.7
C8=0.1992	C8=29.31
C9=0.2872	C9=42.26
C10=0.3248	C10=47.79
C11=0.2848	C11=41.91

Table 1- Weights of the barrel vault

So the following force vectors have been obtained considering the scale 1 m = 100 kN:

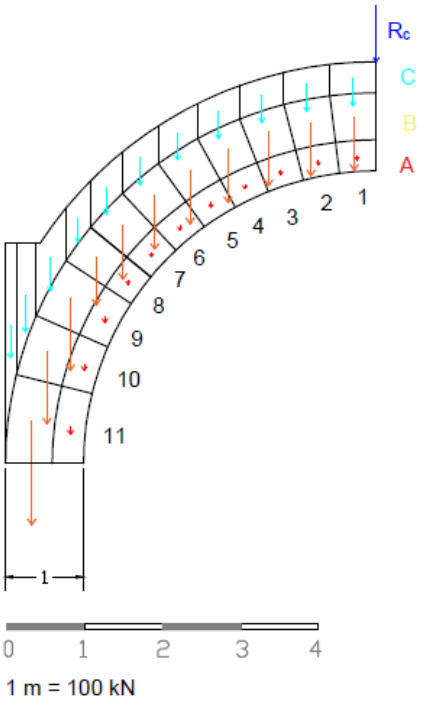

Fig. A. 4- Force vectors of the weights of the barrel vault (1)

In order to simplify the graphic operation, the different parts (A, B, C) are combined so as to determine one equivalent force for each voussoirs:

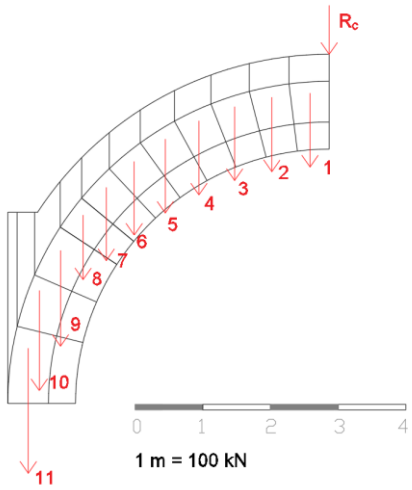

Fig. A. 5- Force vectors of the weights of the barrel vault (2)

Then the force polygon and the funicular polygon has been realized:

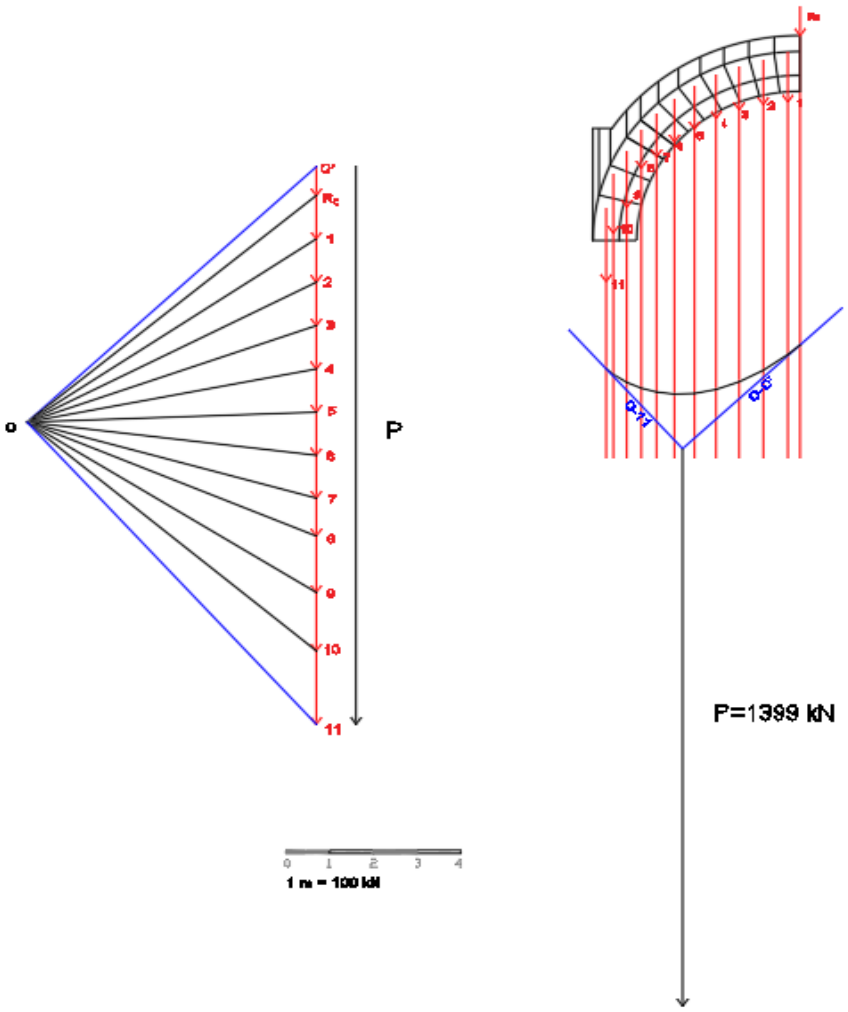

Fig. A. 6- Force polygon and funicular polygon of half barrel vault

Where P is the total weight of half arch, barrel vault and filling material that is equal to 1399.99 kN.

In this case a horizontal force is assumed passing for the extrados of the keystone. Assuming a series of values of this force, it's possible to find the one which gives the minimum thrust.

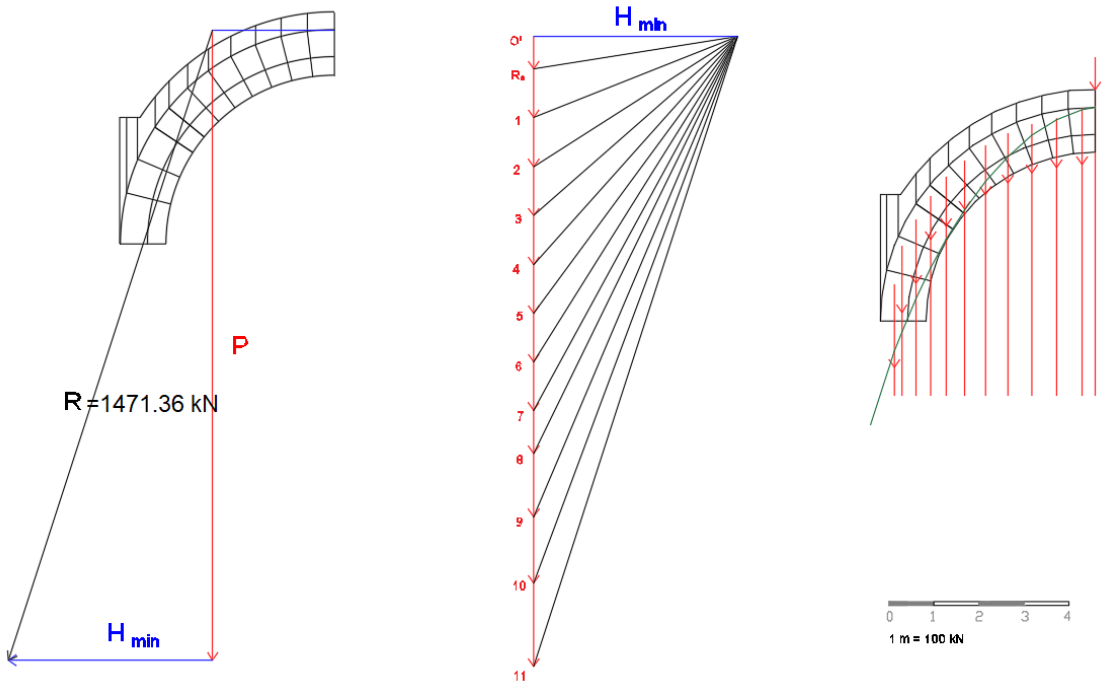

Fig. A. 7- Minimum thrust line in the barrel vault

Where H_{min} is equal to 452.69 kN.

ARCH IN LONGITUDINAL DIRECTION

In the longitudinal direction there are arches between the pillars above which there is a wall so it's necessary to calculate their weights and thrust.

The arches are composed by two arches with the same thickness (0.35 m) and different width (1.08 m and 1.4 m) while the wall has the same width of the upper arch (1.4 m).

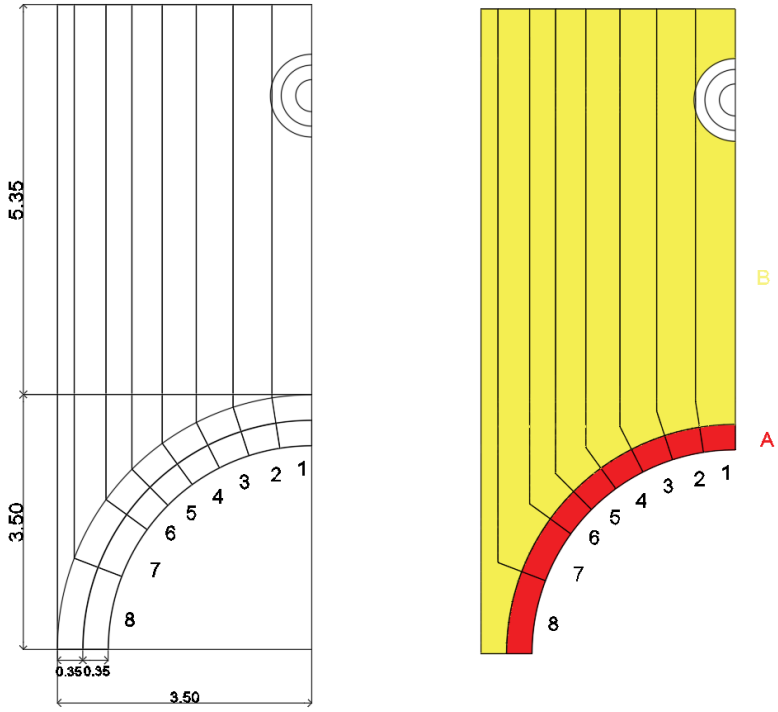

Fig. A. 8- Longitudinal arch

The weight (per unit volume) assumed for the material is 25 kN/m3 so it's possible to calculate the weight of each voussoirs:

Area [m^2]	Weights [kN]
A1= 0.1635=A2=..=A6	A1=A6= 4.41
A7= 0.2733	A7=7.38
A8= 0.3807	A8= 10.28
B1= 2.6333	B1= 92.17
B2= 3.0926	B2= 108.24
B3= 3.0331	B3= 106.16
B4= 2.9293	B4= 102.53
B5= 2.7661	B5= 96.81
B6= 2.5265	B6= 88.43
B7= 3.4299	B7= 120.05
B8= 2.2791	B8= 79.77

Table 2- Weights of the longitudinal arch

In order to simplify the graphic operation, the different parts (A, B) are combined so as to determine one equivalent force for each voussoirs.

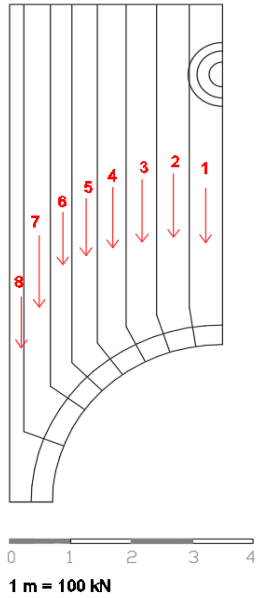

Fig. A. 9- Force vectors of the longitudinal arch

Finally the force polygon and the funicular polygon have been determined. The resultant weight of half part (P) is equal to 838.28 kN.

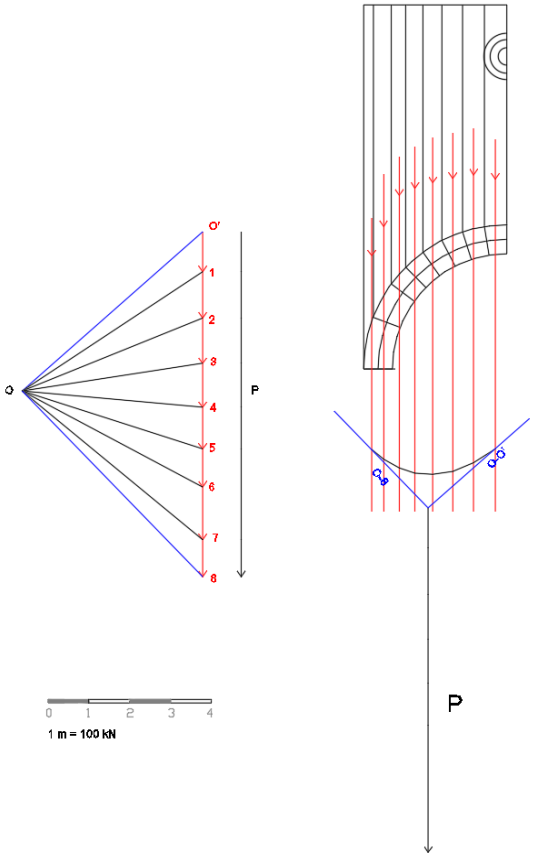

Fig. A. 10- Force polygon and funicular polygon of longitudinal arch

CROSS VAULT

The application of limit analysis isn't simple to cross vault as seen for the arch. In accord to Beranek (1988) it's possible to decompose the vault in a system of one-dimensional arches in which the diagonal arches are critical and receive all the weight of the vault.

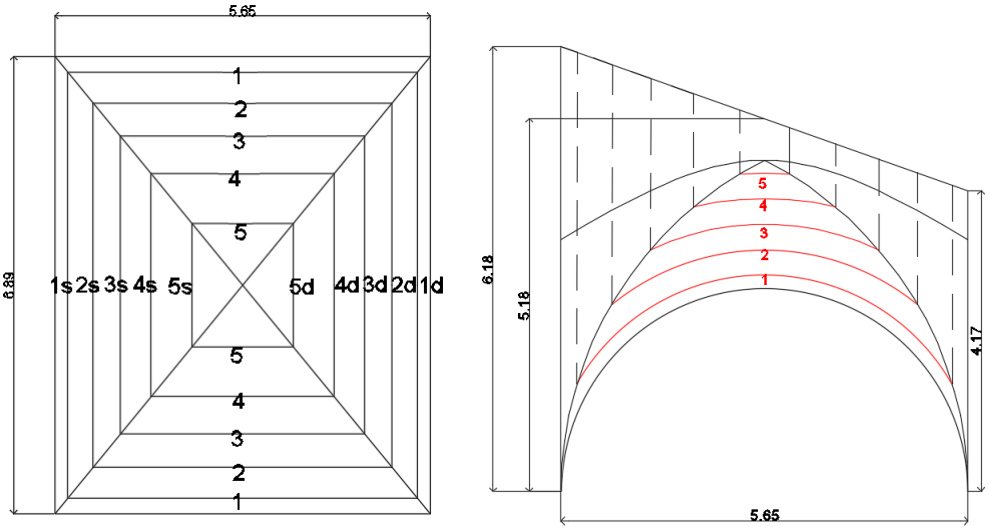

Fig. A. 11- Cross vault (A)

Arch 1: It has a width of 0.237 m, the weight of part A is 25 kN/m^3 while the weight of part B is 18 kN/m^3. Beside above this, there is a roof that leans uniformly, so it's necessary to consider his weight which is 3 kN/m^2 (Part C).

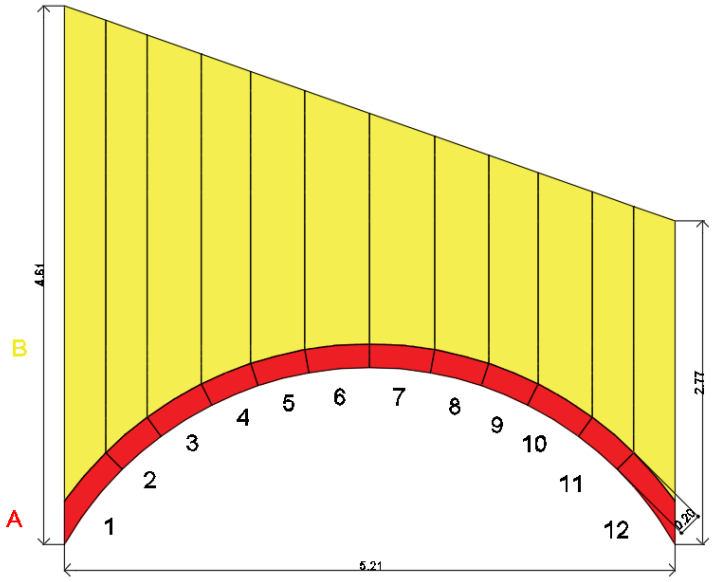

Fig. A. 12- Arch 1 (of the cross vault A)

Area [m^2]	Weights [kN]
A1= 0.1345=A12	A1= 0.79=A12
A2=0.0903=A11	A2=0.53=A11
A3=0.1056=A10	A3=0.62=A10
A4=0.0882=A9	A4=0.52=A9
A5=0.0928=A8	A5=0.55=A8
A6=0.1080=A7	A6=0.64=A7
B1= 1.4215	B1= 6.06
B2= 1.2619	B2= 5.38
B3= 1.4521	B3= 6.19
B4= 1.1531	B4= 4.92
B5=1.1849	B5=5.05
B6= 1.1424	B6= 4.87
B7= 1.1005	B7= 4.69
B8= 0.8764	B8= 3.74
B9=0.789	B9=3.36
B10=0.9049	B10=3.86
B11=0.743	B11=3.17
B12=0.8186	B12=3.49
	C1= 0.26=C12
	C2=0.24=C11
	C3=0.35=C10
	C4=0.31=C9
	C5=0.35=C8
	C6=0.42=C7

Table 3- Weights of arch 1

From the combination of the weights force vectors, force polygon and funicular polygon has been determined.

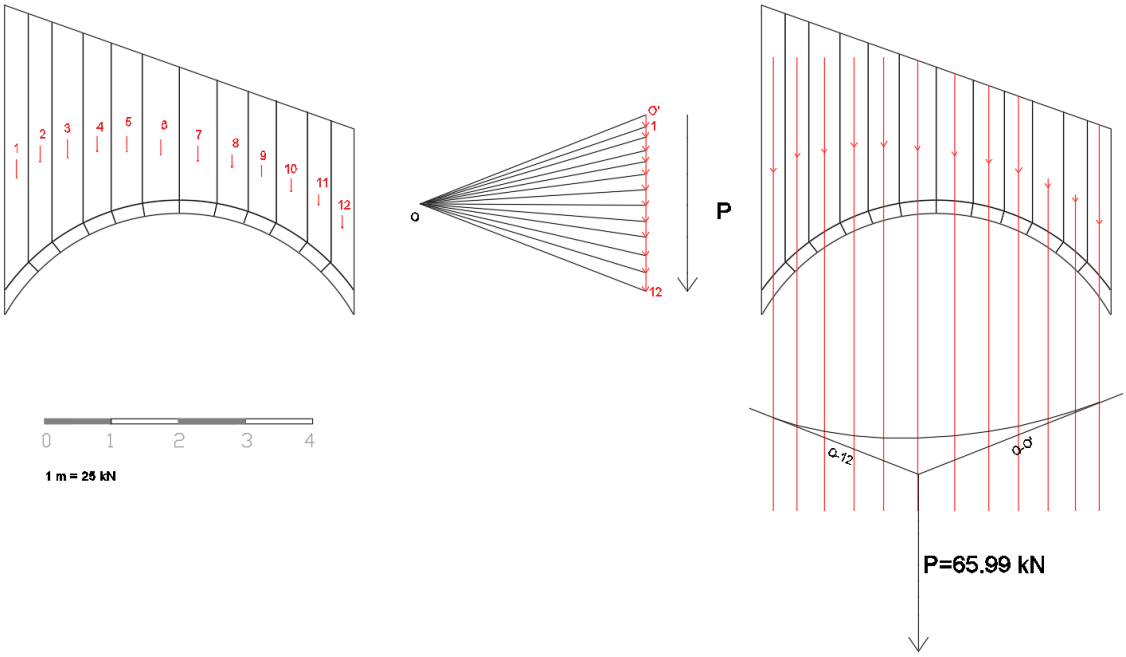

Fig. A. 13- Force polygon and funicular polygon of arch 1 (1)

So it's possible to find a minimum thrust supposing the passage of the thrust line for three points (A, B, C):

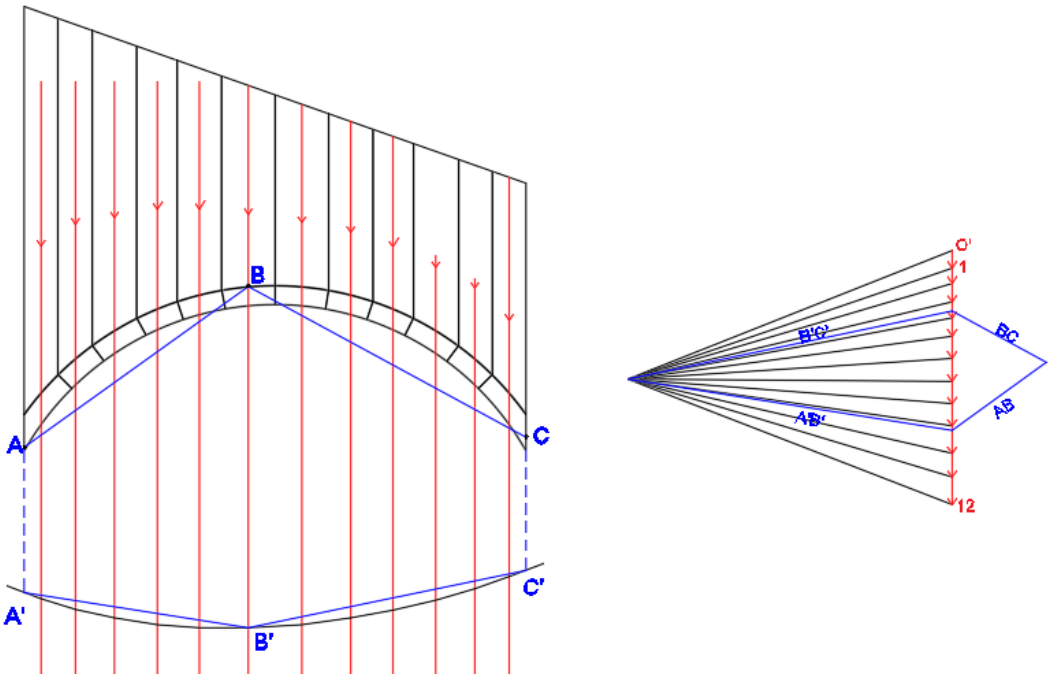

Fig. A. 14- Force polygon and funicular polygon of arch 1 (2)

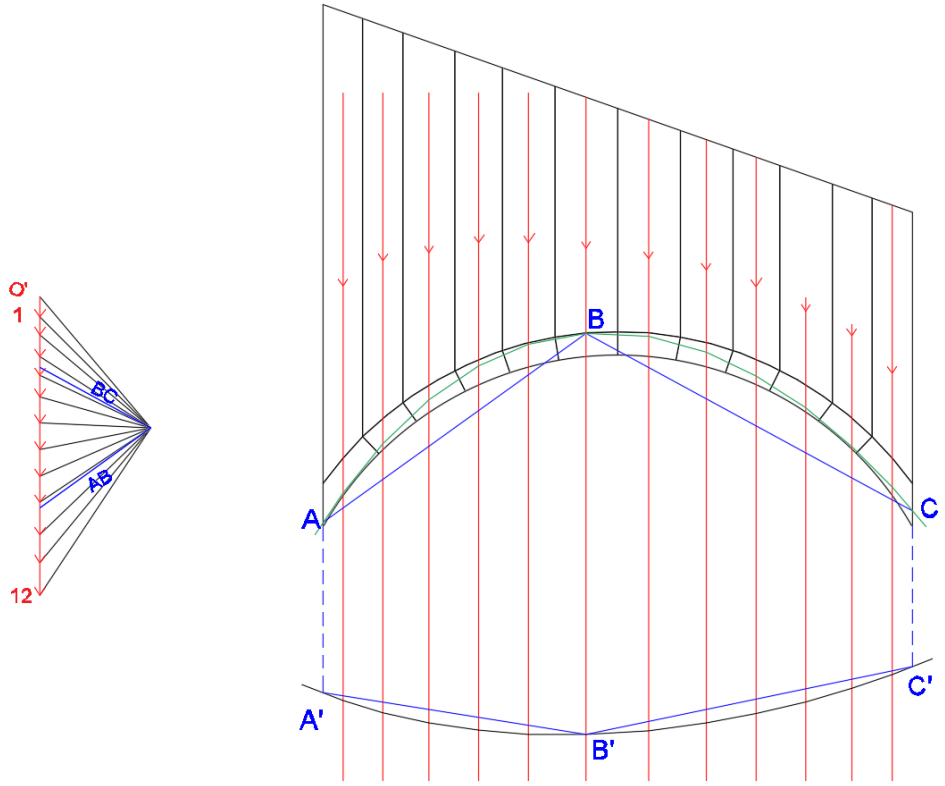

Fig. A. 15- Thrust line in the arch 1

Arch 2: It has a width of 0.47 m, the weight of part A is 25 kN/m^3 while the weight of part B is 18 kN/m^3. Beside above this, there is a roof that leans uniformly, so it's necessary to consider his weight which is 3 kN/m^2 (Part C).

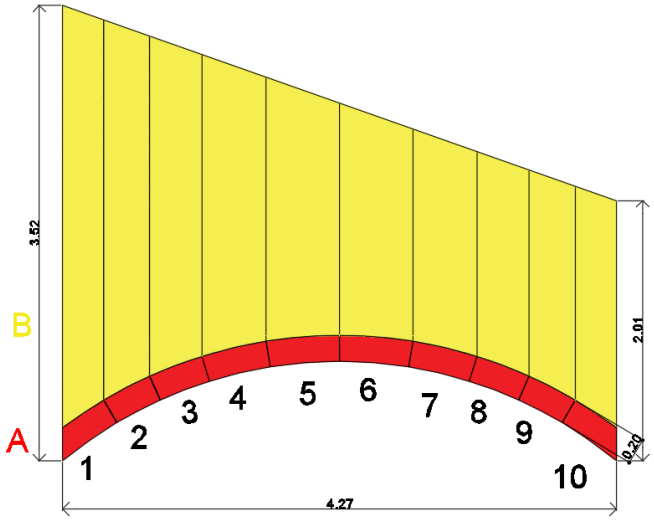

Fig. A. 16- Arch 2 (of the cross vault A)

Area [m^2]	Weights [kN]
A1= 0.0895=A10	A1= 1.04=A10
A2=0.078=A9	A2=0.91=A9
A3=0.0837=A8	A3=0.98=A8
A4=0.0989=A7	A4=1.16=A7
A5=0.1107=A6	A5=1.29=A6
B1= 0.9821	B1= 8.26
B2= 0.9881	B2= 8.31
B3= 0.995	B3= 8.37
B4= 1.0789	B4= 9.08
B5=1.0829	B5=9.11
B6= 0.9694	B6= 8.16
B7= 0.7943	B7=6.68
B8= 0.6365	B8= 5.36
B9=0.5758	B9=4.84
B10=0.539	B10=4.53
	C1= 0.47=C10
	C2=0.52=C9
	C3=0.6=C8
	C4=0.73=C7
	C5=0.84=C6

Table 4- Weights on the arch 2

From the combination of the weights, the following force vectors, force polygon and funicular polygon have been obtained:

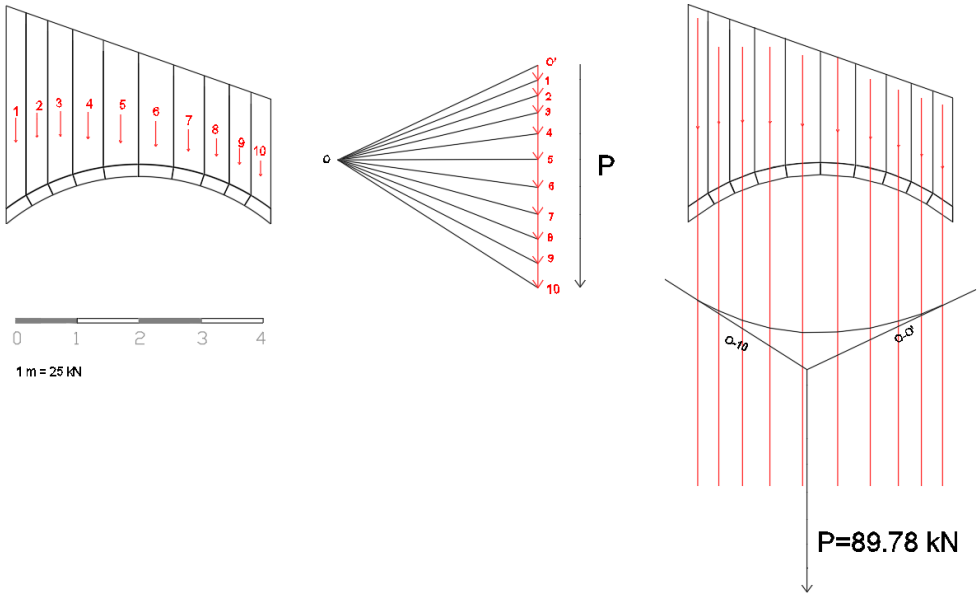

Fig. A. 17- Force polygon and funicular polygon of arch 2 (1)

So it's possible to find a minimum thrust supposing the passage of the thrust line for three points (A, B, C):

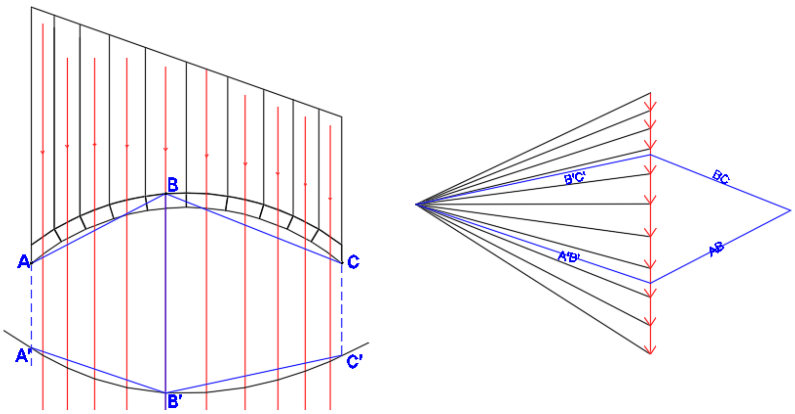

Fig. A. 18- Force polygon and funicular polygon of arch 1 (2)

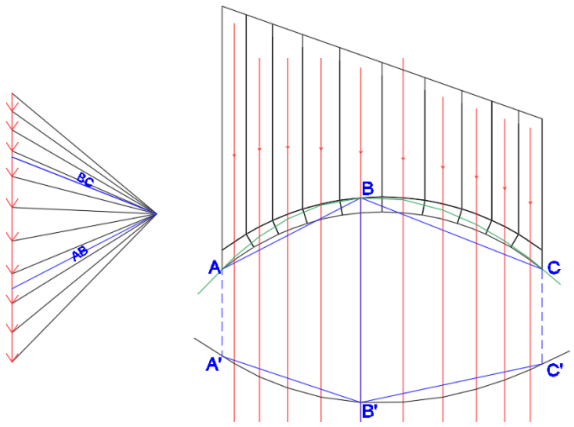

Fig. A. 19- Thrust line in the arch 2

Arch 3: It has a width of 0.5 m, the weight of part A is 25 kN/m^3 while the weight of part B is 18 kN/m^3. Beside above this, there is a roof that leans uniformly, so it's necessary to consider his weight which is 3 kN/m^2 (Part C).

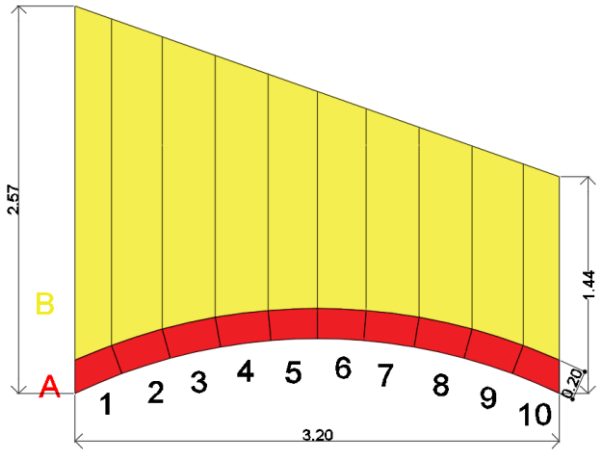

Fig. A. 20- Arch 3 (of the cross vault A)

Area [m^2]	Weights [kN]
A1= 0.0597=A10	A1= 0.74=A10
A2=0.0689=A9	A2=0.86=A9
A3=0.07=A8	A3=0.87=A8
A4=0.0689=A7	A4=0.86=A7
A5=0.0632=A6	A5=0.79=A6
B1= 0.5425	B1= 4.85
B2= 0.6889	B2= 6.16
B3= 0.6425	B3= 5.75
B4= 0.5775	B4= 5.16
B5=0.4854	B5=4.34
B6= 0.4484	B6= 4.01
B7= 0.4547	B7= 4.07
B8= 0.4322	B8= 3.86
B9=0.4054	B9=3.63
B10=0.2907	B10=2.6
	C1= 0.38=C10
	C2=0.53=C9
	C3=0.55=C8
	C4=0.55=C7
	C5=0.51=C6

Table 5- Weights on the arch 3

From the combination of the weights, the following force vectors, force polygon and funicular polygon have been obtained.

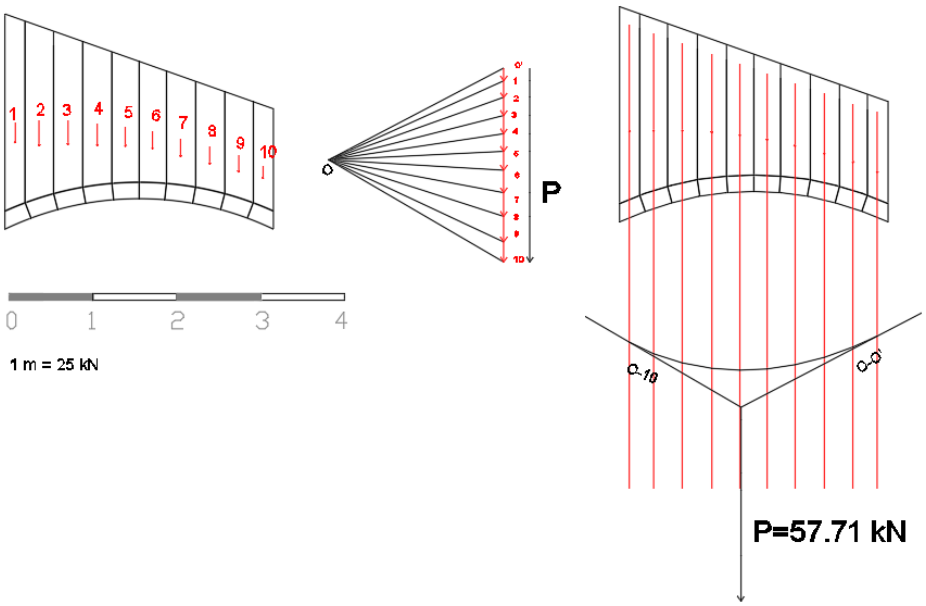

Fig. A. 21- Force polygon and funicular polygon of arch 3 (1)

So it's possible to find a minimum thrust supposing the passage of the thrust line for three points (A, B, C):

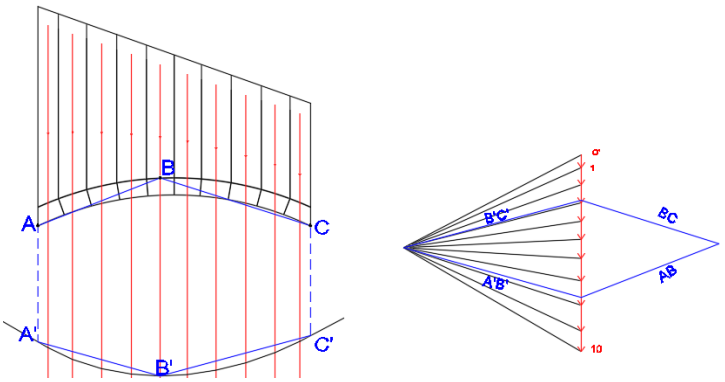

Fig. A. 22- Force polygon and funicular polygon of arch 3 (2)

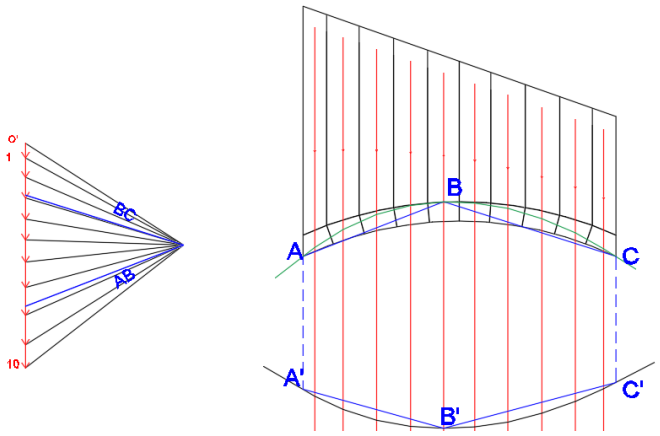

Fig. A. 23- Thrust line in the arch 3

Arch 4: It has a width of 0.564 m, the weight of part A is 25 kN/m^3 while the weight of part B is 18 kN/m^3. Beside above this, there is a roof that leans uniformly, so it's necessary to consider his weight which is 3 kN/m^2 (Part C).

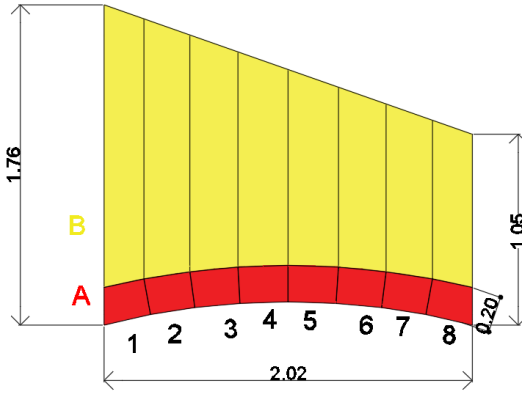

Fig. A. 24- Arch 4 (of the cross vault A)

Area [m^2]	Weights [kN]
A1= 0.0485=A8	A1= 0.68=A8
A2=0.0503=A7	A2=0.71=A7
A3=0.0515=A6	A3=0.73=A6
A4=0.0541=A5	A4=0.76=A5
B1= 0.3262	B1= 3.31
B2= 0.348	B2= 3.53
B3= 0.3266	B3= 3.31
B4= 0.3132	B4= 3.17
B5=0.2861	B5=2.9
B6= 0.251	B6= 2.55
B7= 0.2283	B7=2.32
B8= 0.1871	B8= 1.9
	C1= 0.39=C8
	C2=0.46=C7
	C3=0.47=C6
	C4=0.49=C5

Table 6- Weights of arch 4

From the combination of the weights, the following force vectors, force polygon and funicular polygon have been obtained.

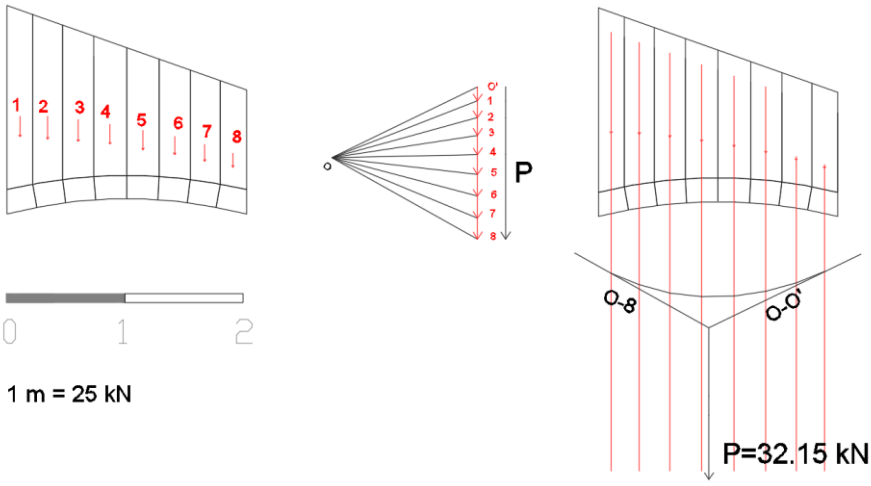

Fig. A. 25- Force polygon and funicular polygon of arch 4 (1)

So it's possible to find a minimum thrust supposing the passage of the thrust line for three points (A, B, C):

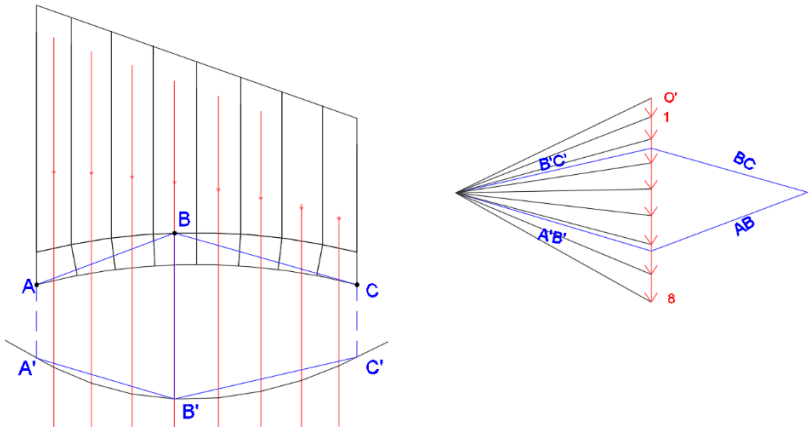

Fig. A. 26- Force polygon and funicular polygon of arch 4 (2)

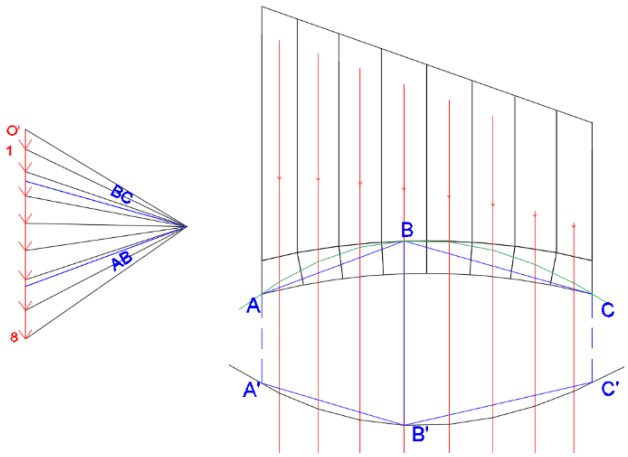

Fig. A. 27- Thrust line in the arch 4

Arch 5: It has a width of 0.75 m, the weight of part A is 25 kN/m^3 while the weight of part B is 18 kN/m^3. Beside above this, there is a roof that leans uniformly, so it's necessary to consider his weight which is 3 kN/m^2 (Part C).

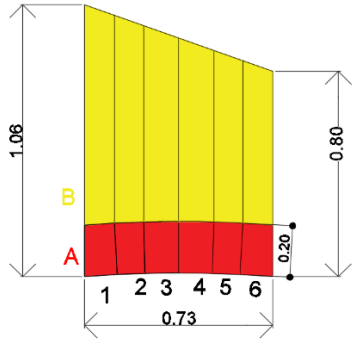

Fig. A. 28- Arch 5 (of the cross vault A)

Area m2	Weights [kN]
A1= 0.0244=A6	A1= 0.46=A6
A2=0.0222=A5	A2=0.42=A5
A3=0.0268=A4	A3=0.5=A4
B1= 0.0969	B1= 1.31
B2= 0.0889	B2= 1.2
B3= 0.101	B3= 1.36
B4= 0.0944	B4= 1.27
B5=0.0735	B5=0.99
B6= 0.0716	B6= 0.97
	C1= 0.28=C6
	C2=0.27=C5
	C3=0.31=C4

Table 7- Weights of arch 5

From the combination of the weights, it obtains the following force vectors, force polygon and funicular polygon.

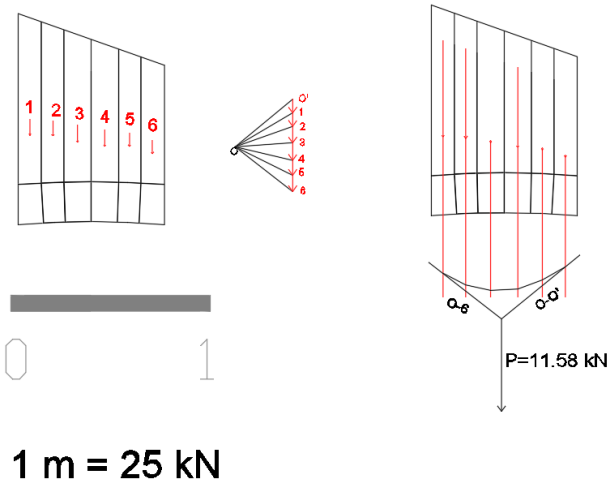

Fig. A. 29- Force polygon and funicular polygon of arch 5 (1)

So it's possible to find a minimum thrust supposing the passage of the thrust line for three points (A, B, C):

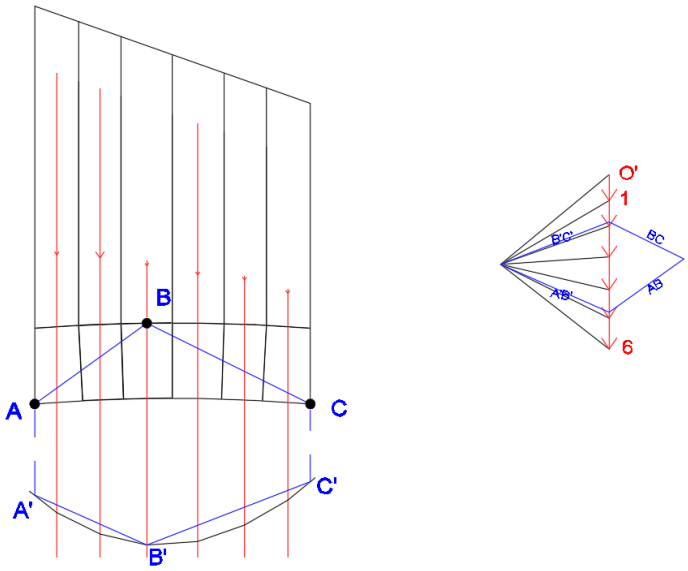

Fig. A. 30- Force polygon and funicular polygon of arch 5 (2)

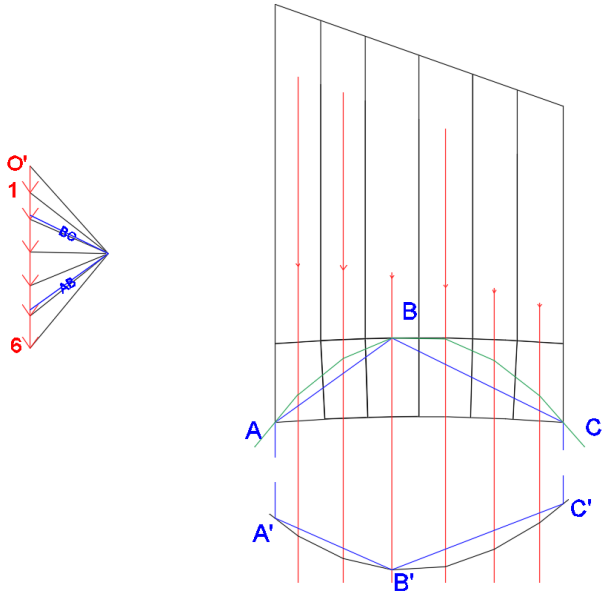

Fig. A. 31- Thrust line in arch 5

Repeating this procedure to the other parts it obtains the total weights of the cross vault and the reactions of all these arches transmitted to the diagonal arches.

In the next table all the arches are summarized:

Arch	Weight [kN]
1	65.99
2	89.78
3	57.71
4	32.15
5	11.58

Arch	Weight [kN]
1s	78.02
2s	112.18
3s	70.54
4s	47.34
5s	14.7

Arch	Weight [kN]
1d	34.7
2d	46.36
3d	27.86
4d	17.06
5d	7

Table 8- Weights of the cross vault (A)

So considering the central part that is about 30 kN, the global weight is 1000.18 kN.

In order to determine the reactions of these cross vaults it can be possible to study them like arch; so combining all the weights calculated in the previous arches, it can be studied the cross vault like an arch. In this way it can be defined the force polygon and the funicular polygon.

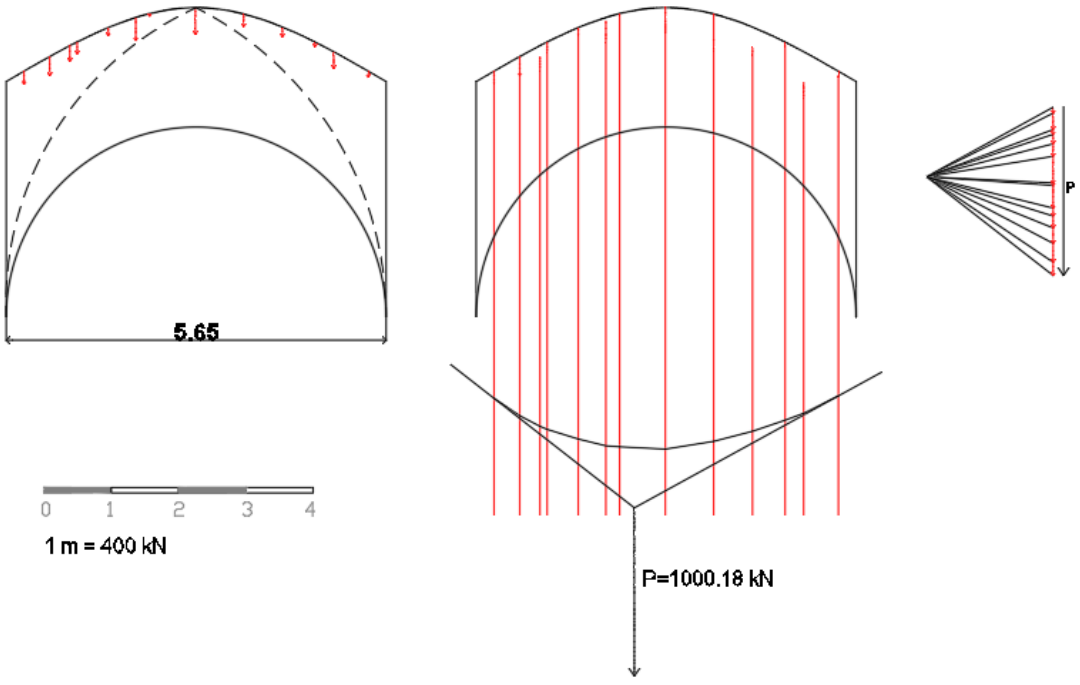

Fig. A. 32- Cross vault (A) like arch

So, it's possible to find a thrust in the cross vault supposing the passage of the thrust line for three points (A, B, C); the choice of these points is linked to the thrust line that is generated in the structure:

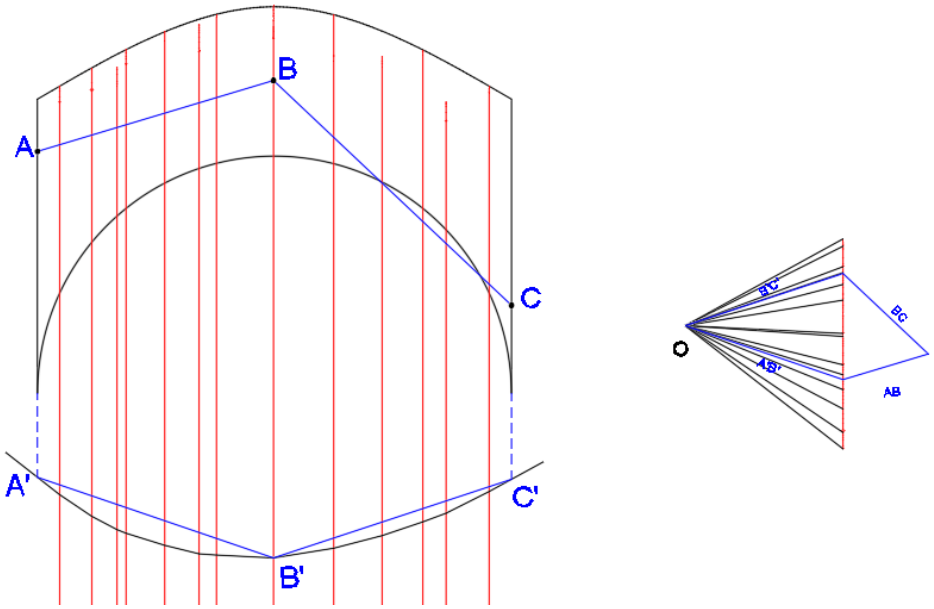

Fig. A. 33- Force polygon and funicular polygon of cross vault (A)

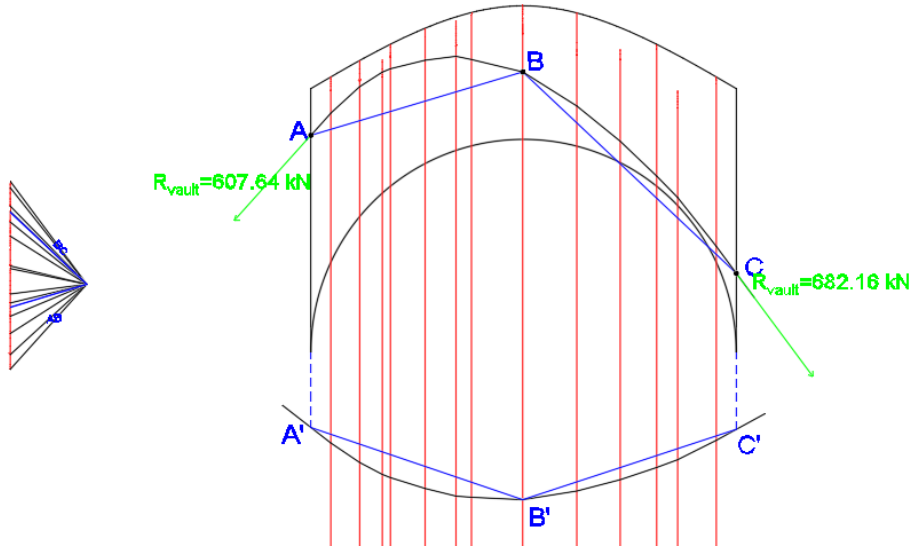

Fig. A. 34- Thrust line in the cross vault (A)

THRUST LINE OF THE STRUCTURE

Now it can be possible to draw the thrust line inside of the structure, considering and calculating the weights of other parts.

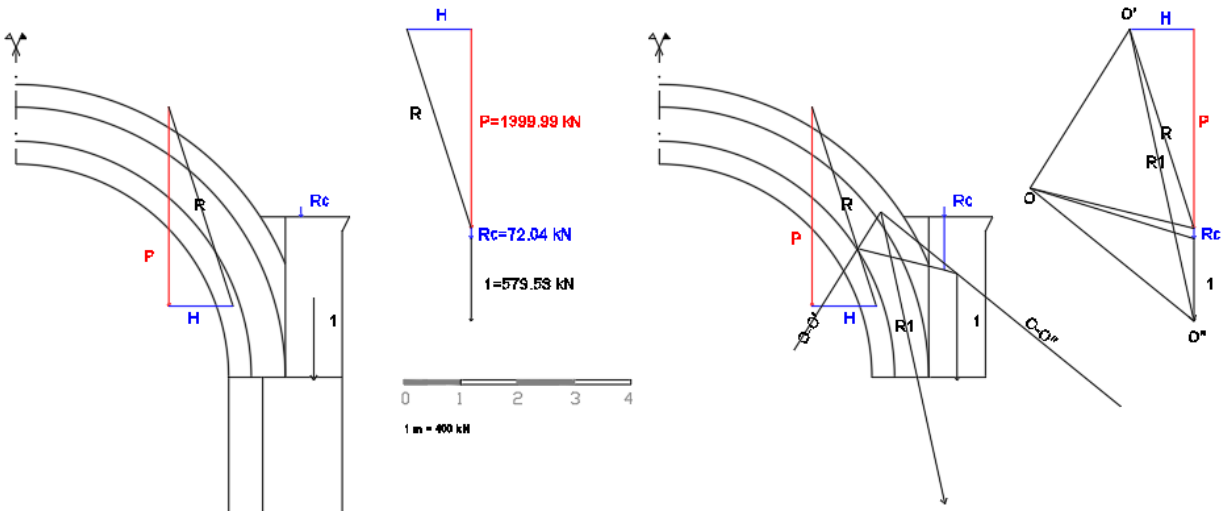

Fig. A. 35- Thrust line in the original structure (1)

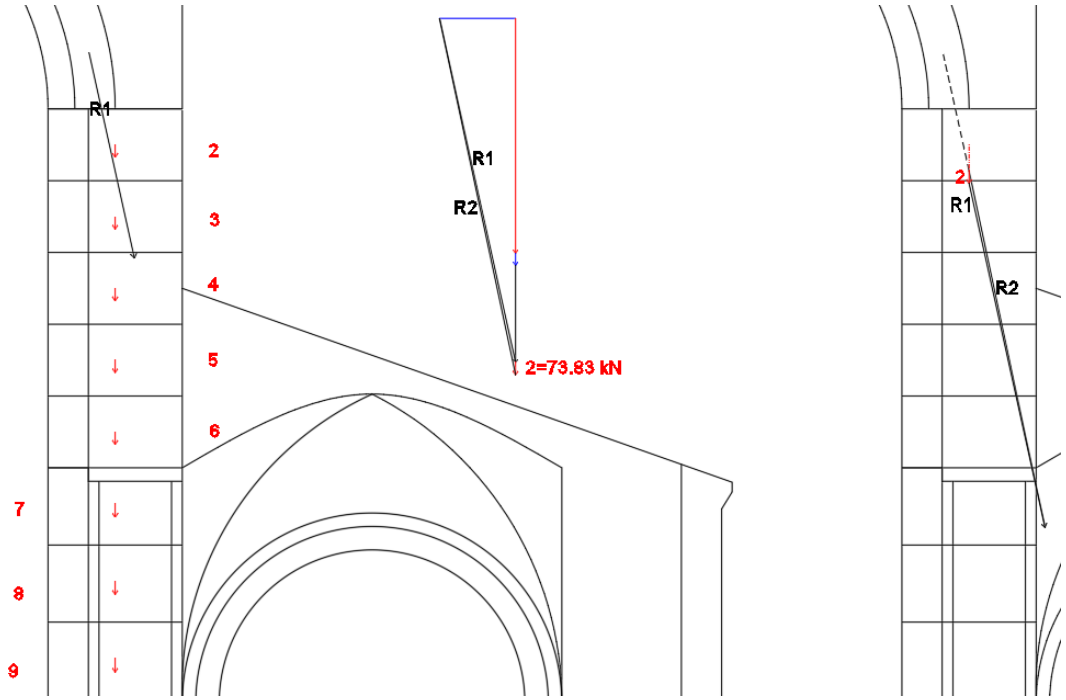

Fig. A. 36- Thrust line in the original structure (2)

In this case the resultant R2 can be obtained (combination of R1 and 2) and represented with the parallelogram rule. So the procedure keeps going on with other blocks.

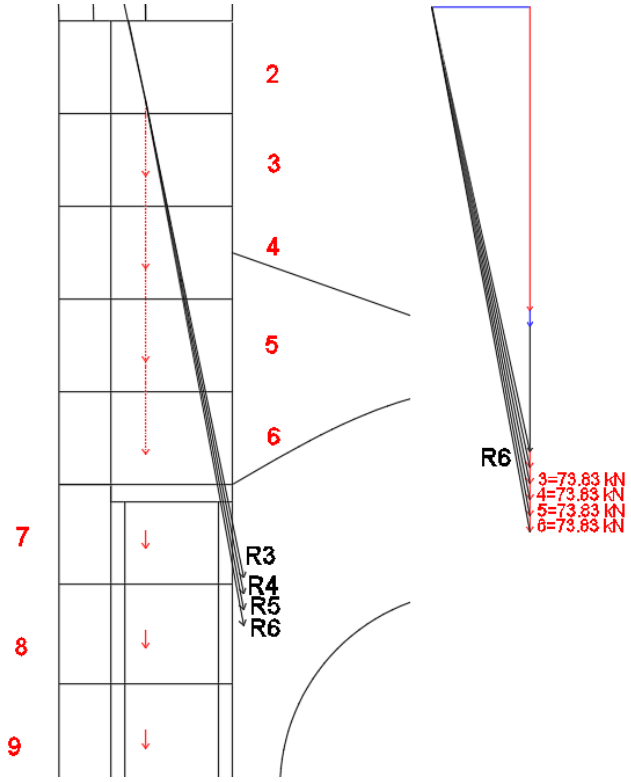

Fig. A. 37- Thrust line in the original structure (3)

In this case it is considered the thrust force of the cross vault calculated previously.

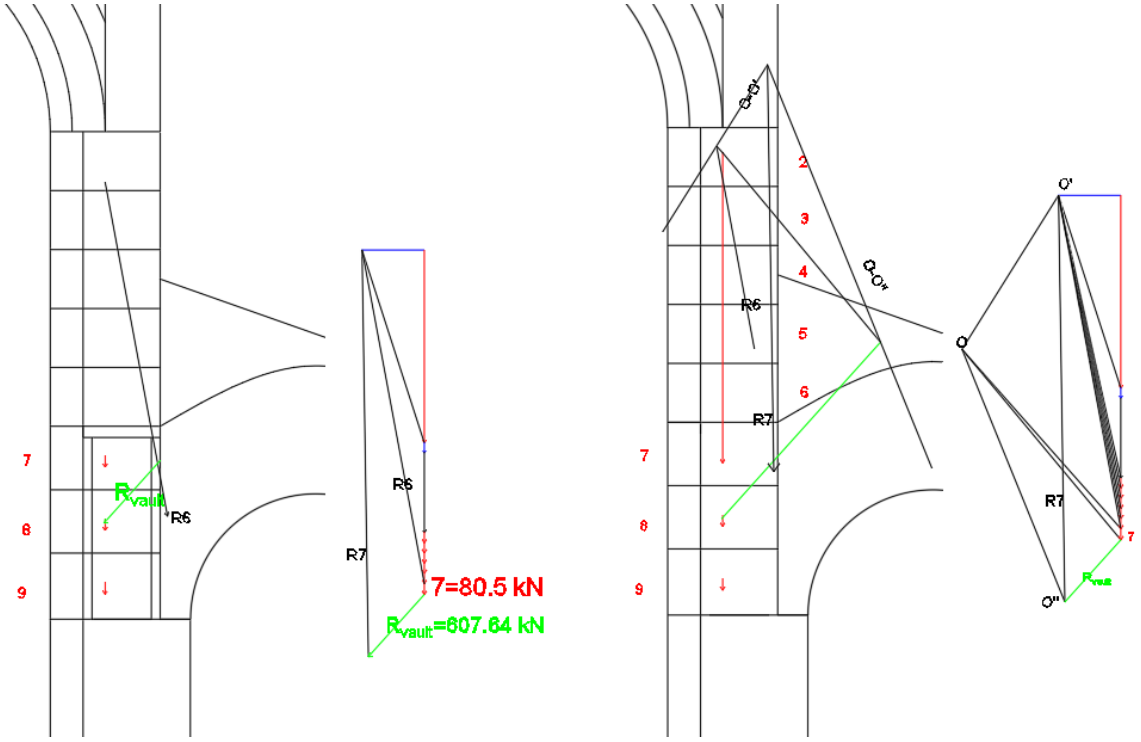

Fig. A. 38- Thrust line in the original structure (4)

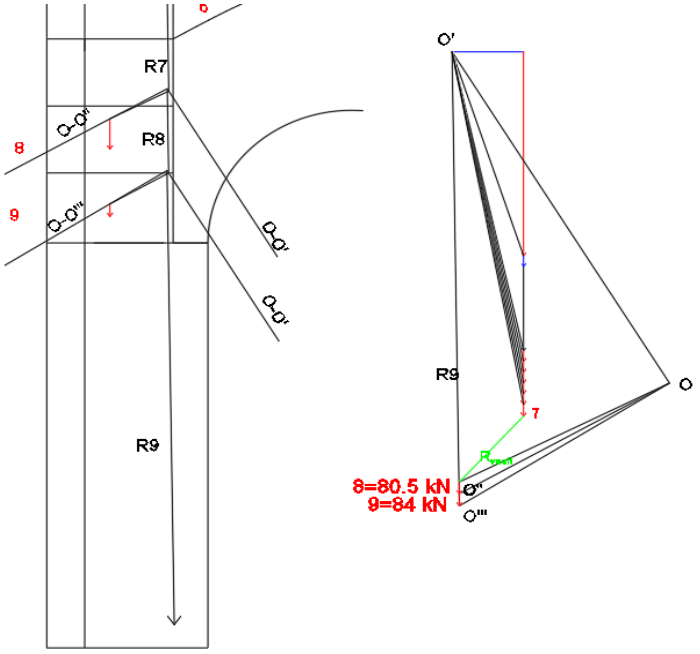

Fig. A. 39- Thrust line in the original structure (5)

Now it must consider the reaction of the longitudinal arch and it is supposed that this arch transmits his reaction on its base to the pillar.

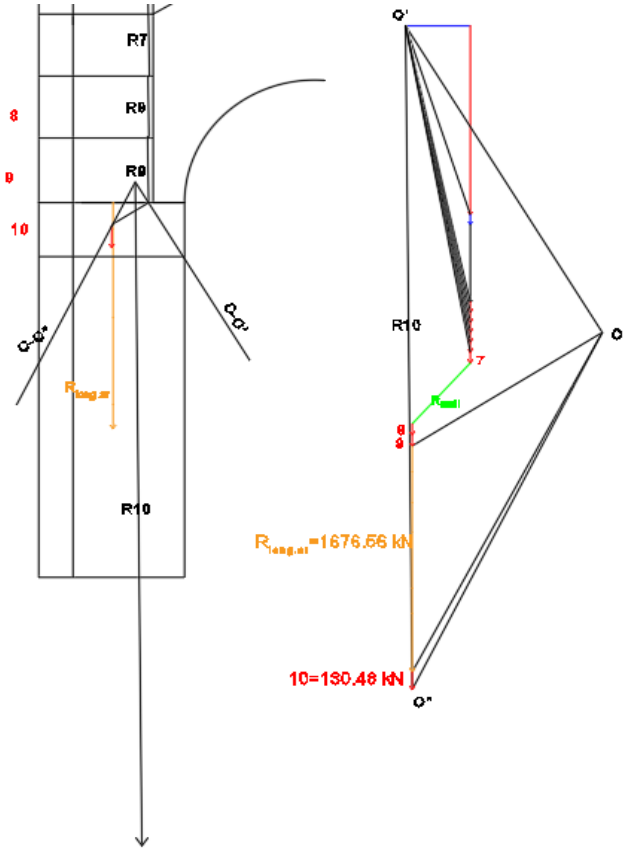

Fig. A. 40- Thrust line in the original structure (6)

So it is over with the final part of the pillar. In this figure the resultant forces are already cut.

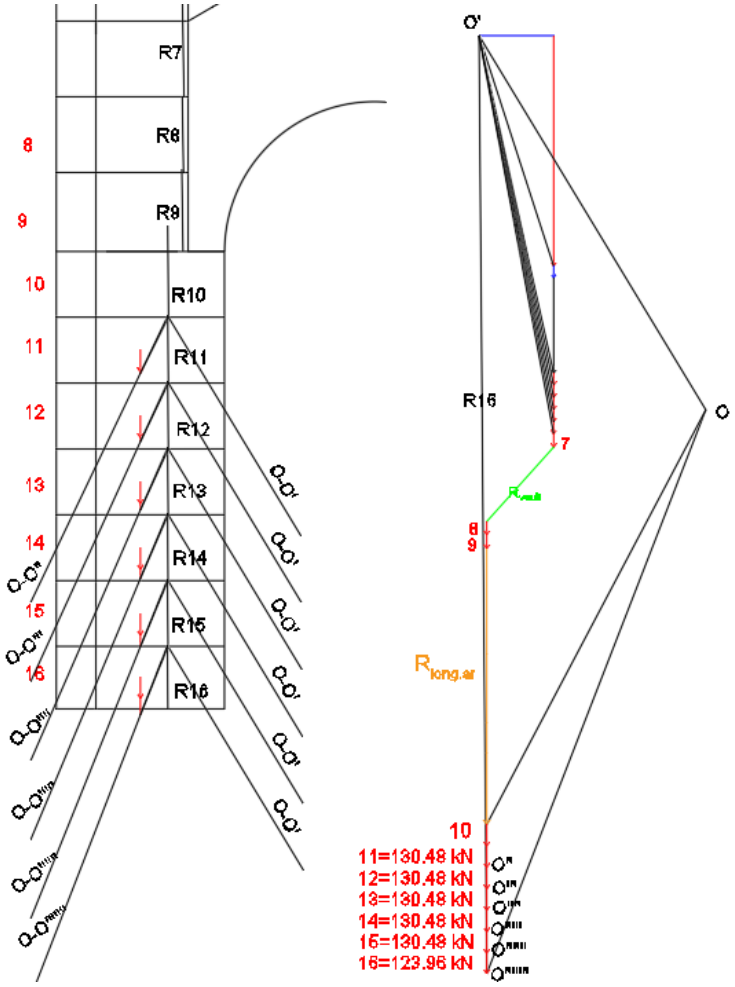

Fig. A. 41- Thrust line in the original structure (7)

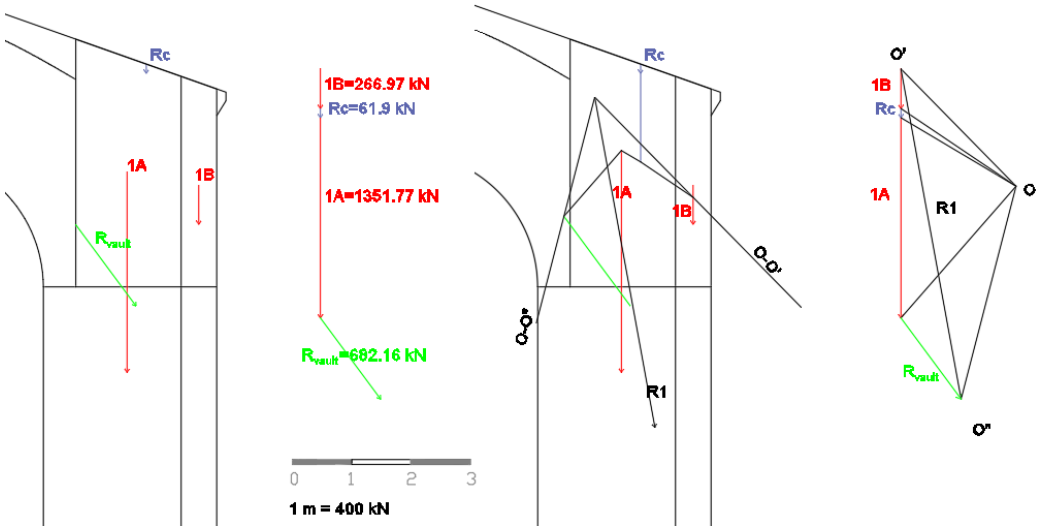

Fig. A. 42- Thrust line in the original structure (8)

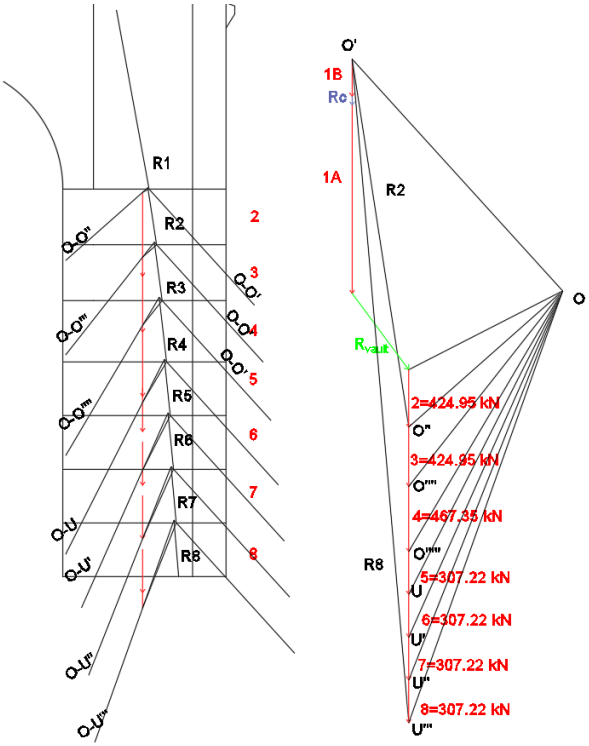

Fig. A. 43- Thrust line in the original structure (9)

Repeating the procedure on the left side, the thrust line has been determined.

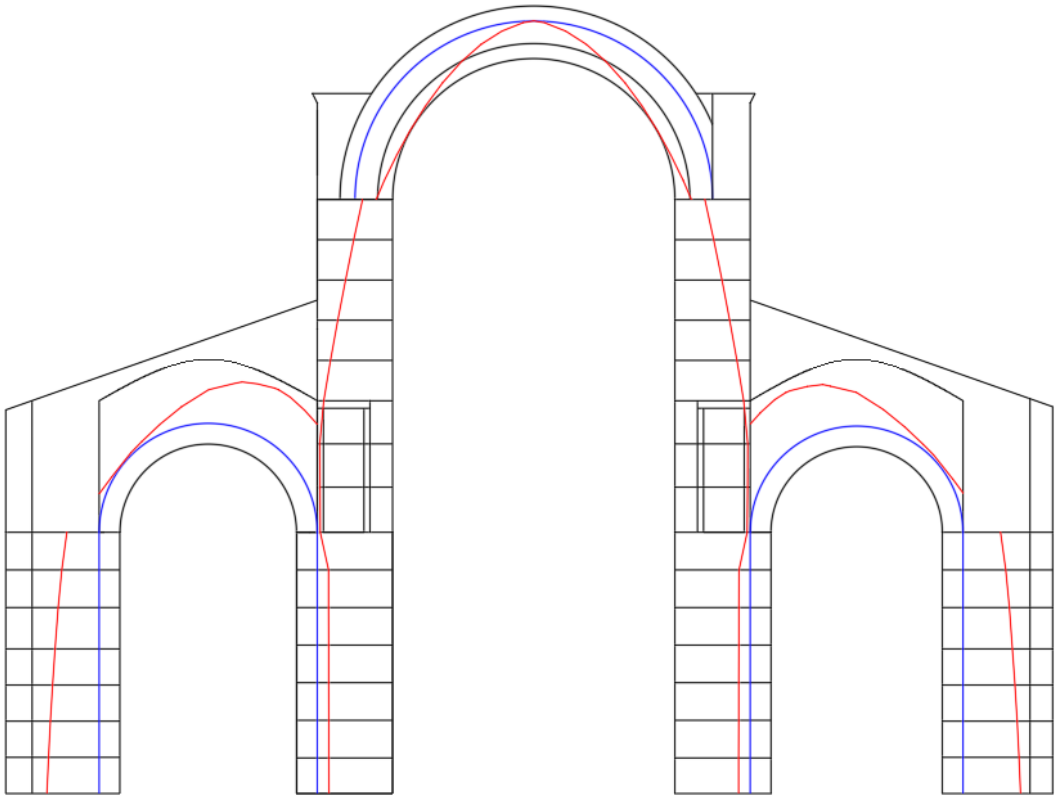

Fig. A. 44- Thrust line in the original structure (10)

2) STRUCTURE WITH FLYING ARCH

In this case the structure with flying arches has been analyzed. So, the section is the following:

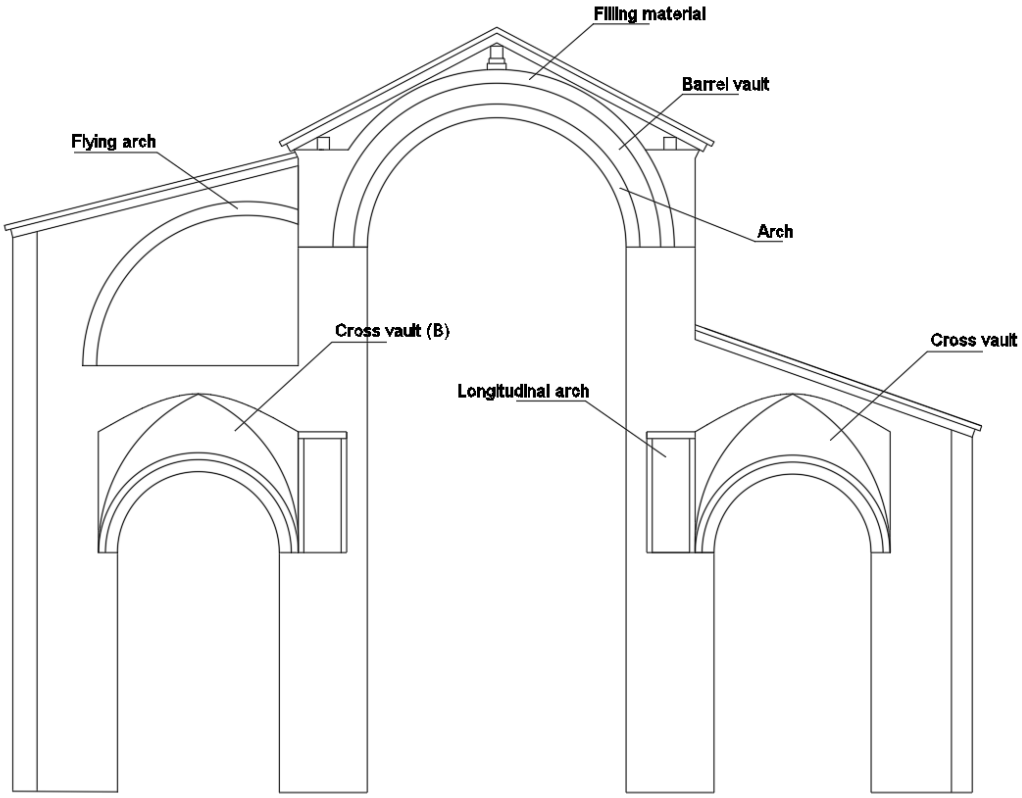

Fig. A. 45- Section analyzed in the current state

The right part remains the same as the previous one. On the flying arches there is a roof that leans on three supports, two on the walls and one in the middle of the flying arches. The weight of the roof is assumed equal to 3 kN/m^2 so considering a width of 8.175 m it is obtained a linear weight of 24.525 kN/m. In this way it's possible to calculate the reactions on the flying arch which is equal to 104.23 kN while the reactions on the walls are equal to 52.12 kN.

FLYING ARCH

The flying arches are placed at the pillars and there is one also between the pillars, so it's like there are two flying arches in the part analyzed. Every flying arch has a width of 0.7 m so the total width considered is 1.4 m.

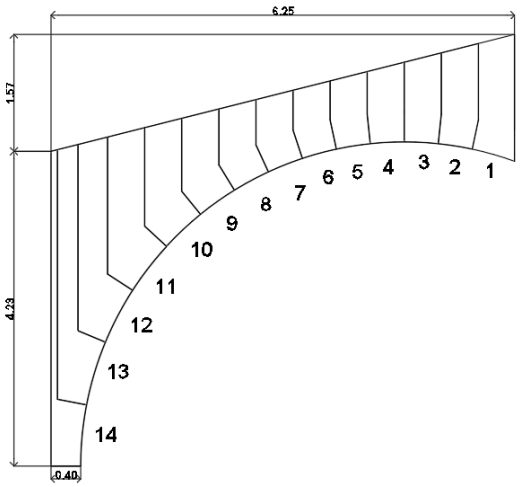

Fig. A. 46- Flying arch

Area [m^2]	Weights [kN]
1= 0.7544	1=26.41
2= 0.6549	2=22.93
3= 0.5633	3=19.72
4= 0.5005	4=17.52
5= 0.4662	5= 16.31
6= 0.4617	6= 16.15
7= 0.4896	7= 17.13
8= 0.5543	8= 19.41
9= 0.6638	9= 23.24
10= 0.8331	10= 29.16
11= 1.0948	11= 38.33
12= 1.1882	12= 41.58
13= 1.1637	13= 40.72
14= 0.6614	14= 23.15

Table 9- Weights on the flying arch

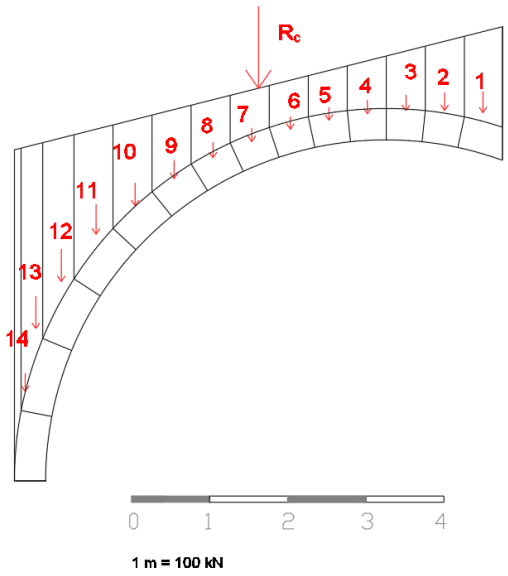

Fig. A. 47- Force vectors of the weights in the flying arch

Then the force polygon and the funicular polygon have been realized:

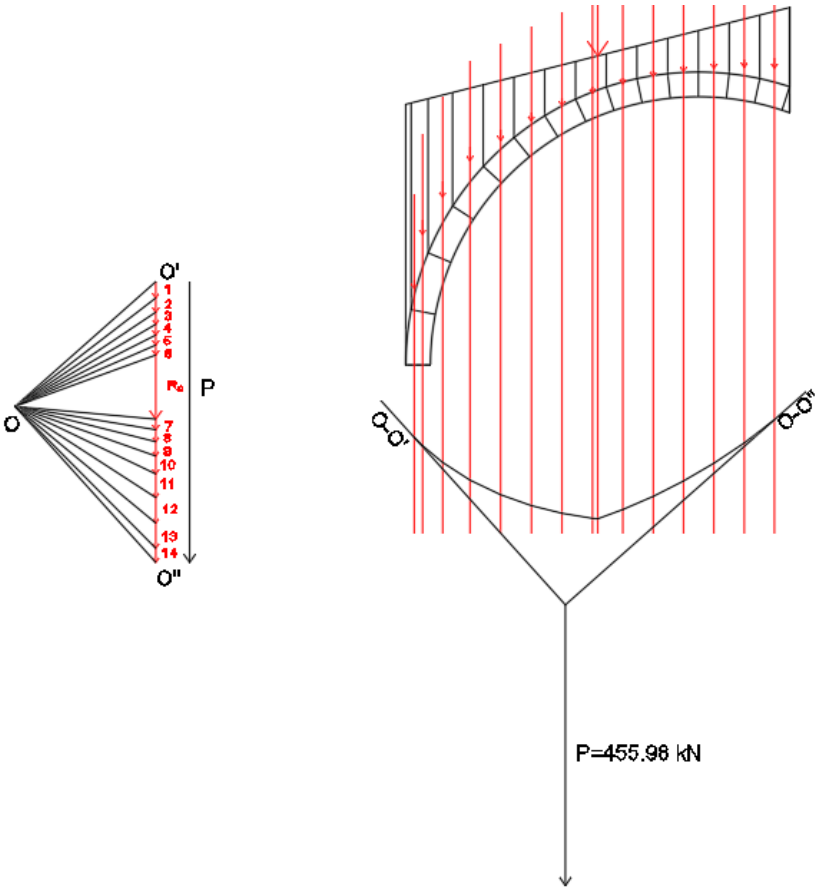

Fig. A. 48- Force polygon and funicular polygon of the flying arch (1)

So it's possible to find a minimum thrust in the flying arch supposing the passage of the thrust line for three points (A, B, C):

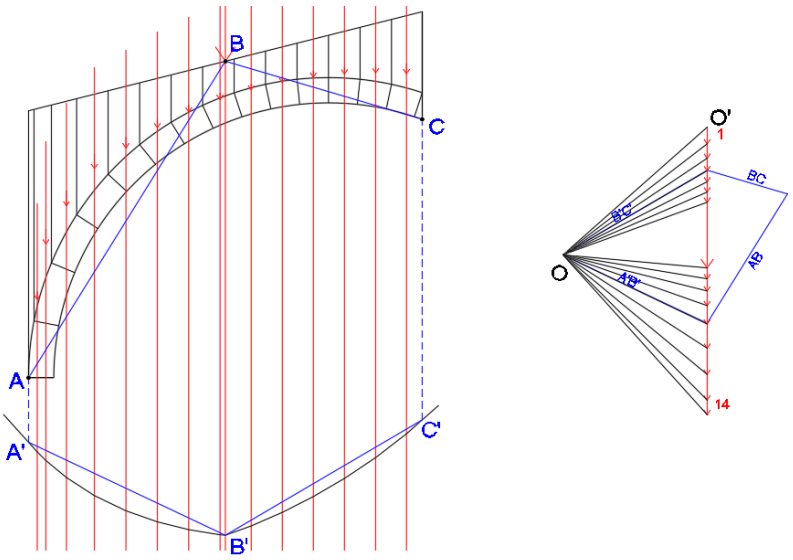

Fig. A. 49- Force polygon and funicular polygon of the flying arch (2)

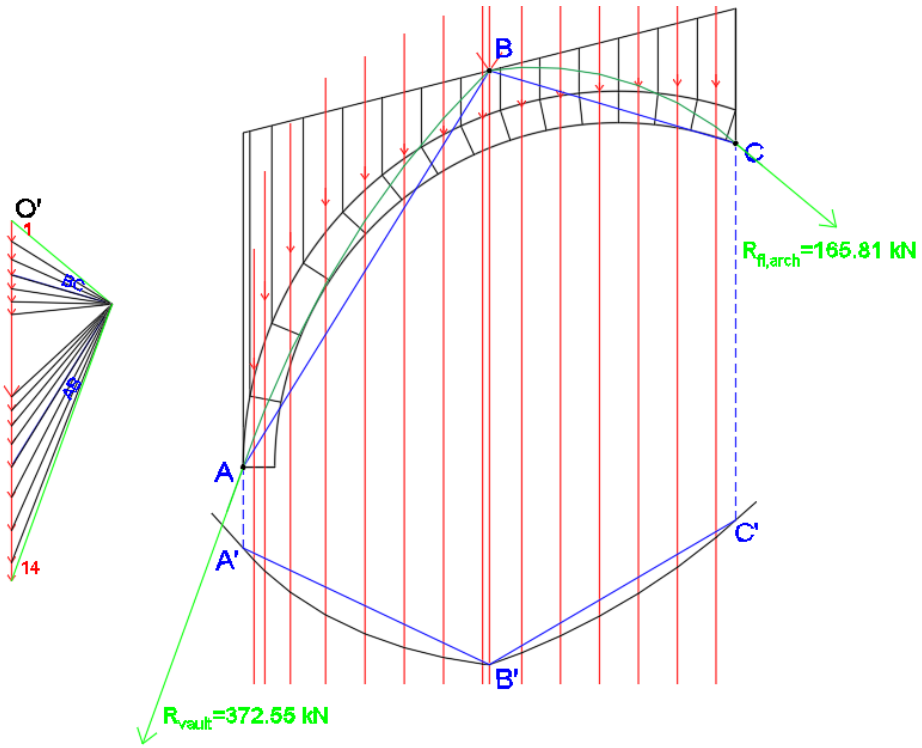

Fig. A. 50- Thrust line in the flying arch

CROSS VAULT

First of all, it's necessary to apply the procedure utilizing on the right cross vault so it has been divided in many arches.

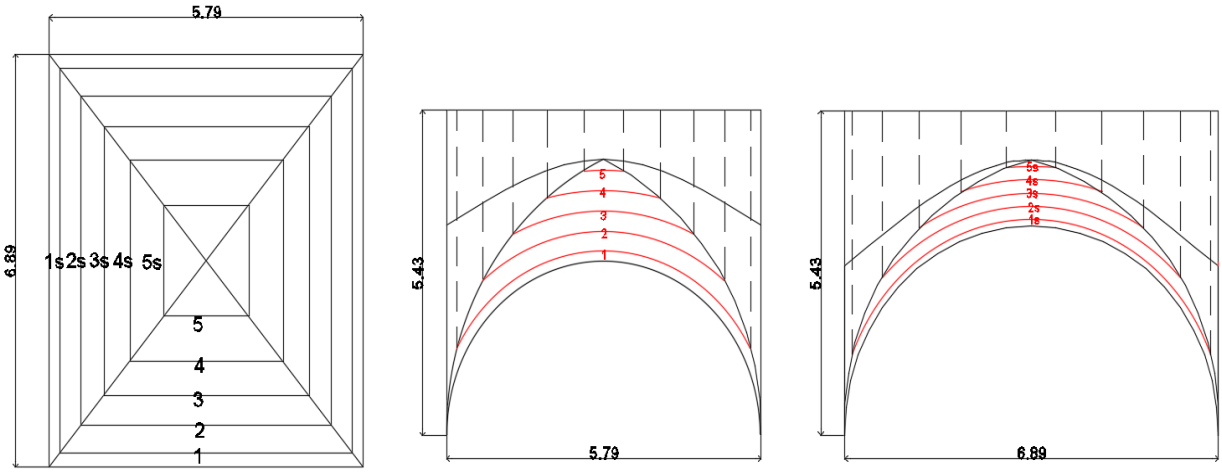

Fig. A. 51- Cross vault (B)

Skipping all the steps, the following weights have been found:

Arch	Weight [kN]
1	71.1
2	100.66
3	66
4	37.9
5	13.64

Arch	Weight [kN]
1s	63.28
2s	90.72
3s	60.42
4s	34.06
5s	13.18

Table 10- Weights of the cross vault (B)

So the total weight, considering the remaining central part of 60 kN, it's 1161.92 kN.

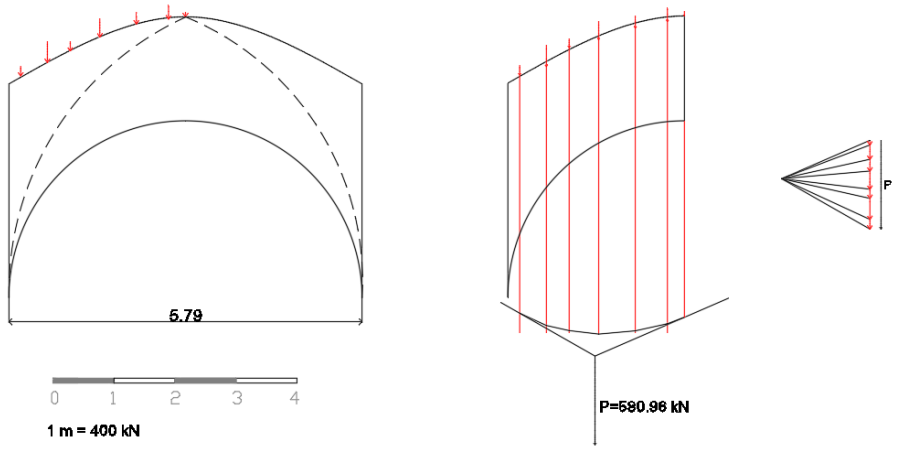

Fig. A. 52- Cross vault (B) like arch

In this case it is assumed a horizontal force passing for the extrados of the keystone; changing its value, a thrust line is determined.

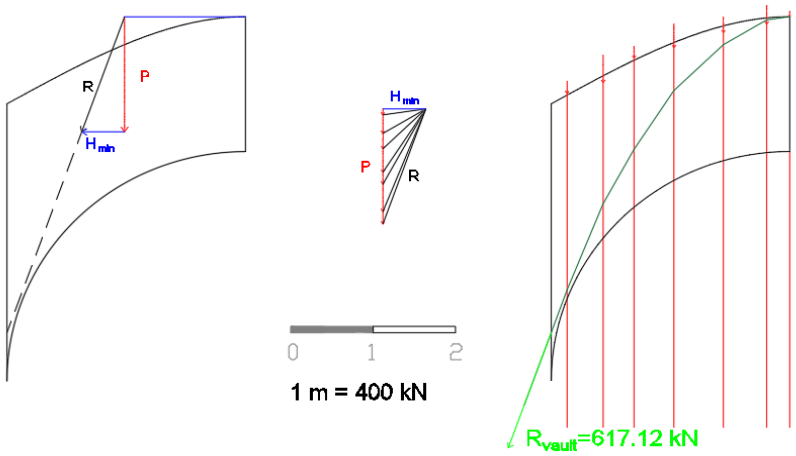

Fig. A. 53- Thrust line in cross vault (B)

THRUST LINE OF THE STRUCTURE

Now it can be possible to the realize the thrust line inside of the structure, considering and calculating the weights of other parts. As already mentioned above, the right part remains the same as the previous one, for which the left side is analyzed.

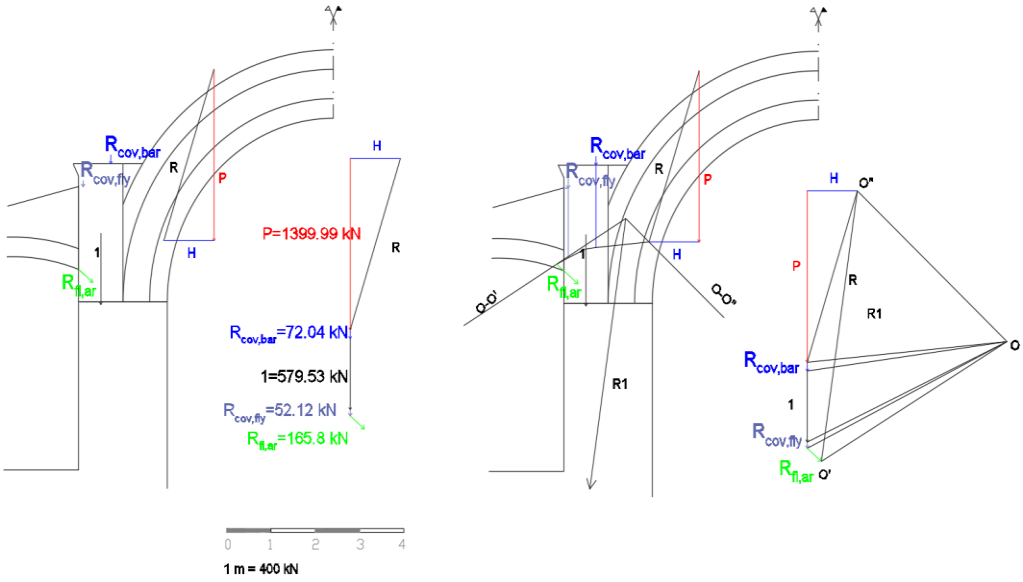

Fig. A. 54- Thrust line in the structure with flying arch (1)

So it can be defined the thrust line in the structure considering all the weights like shown in the following figure with the application of parallelogram rule.

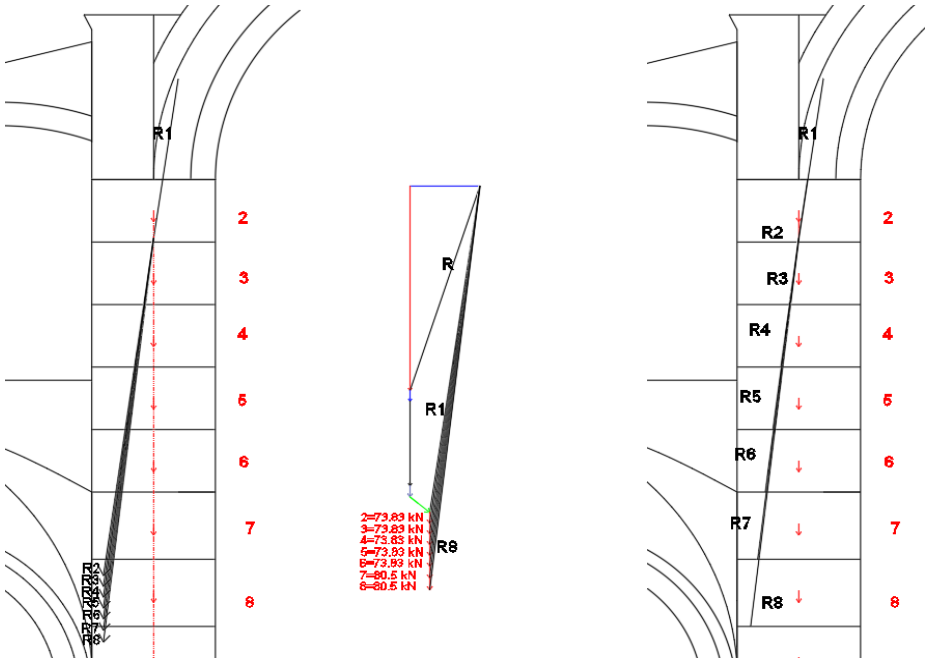

Fig. A. 55- Thrust line in the structure with flying arch (2)

In this case it is considered the thrust force of the cross vault calculated previously.

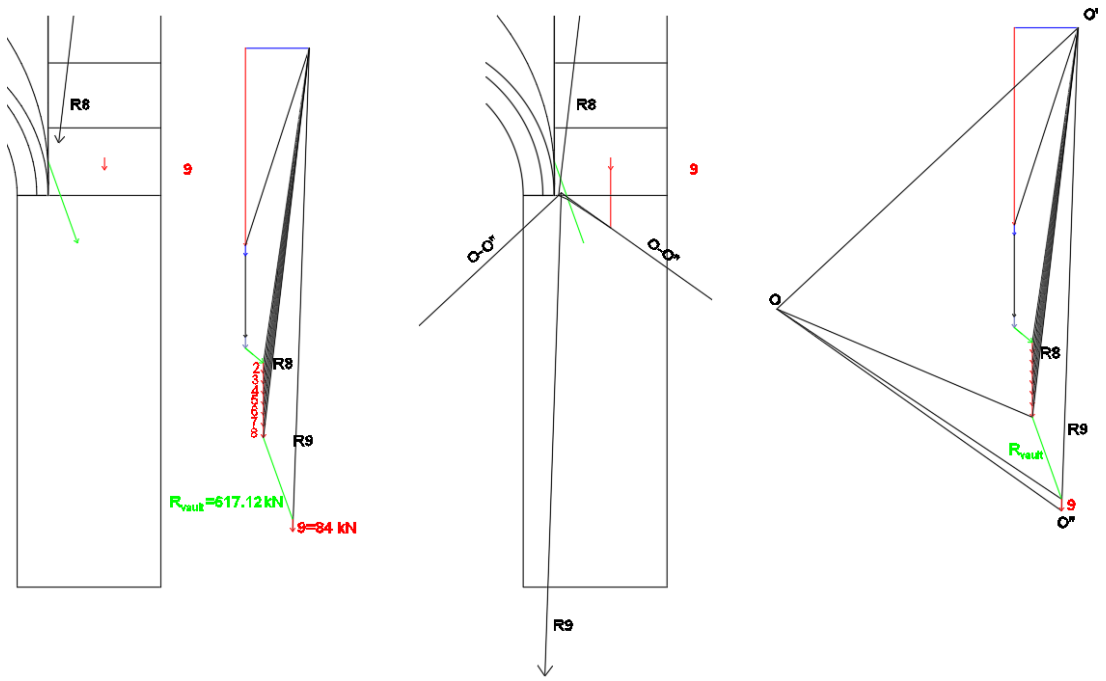

Fig. A. 56- Thrust line in the structure with flying arch (3)

Now it must consider the reaction of the longitudinal arch and it is supposed that this arch transmits his reaction on its base to the pillar.

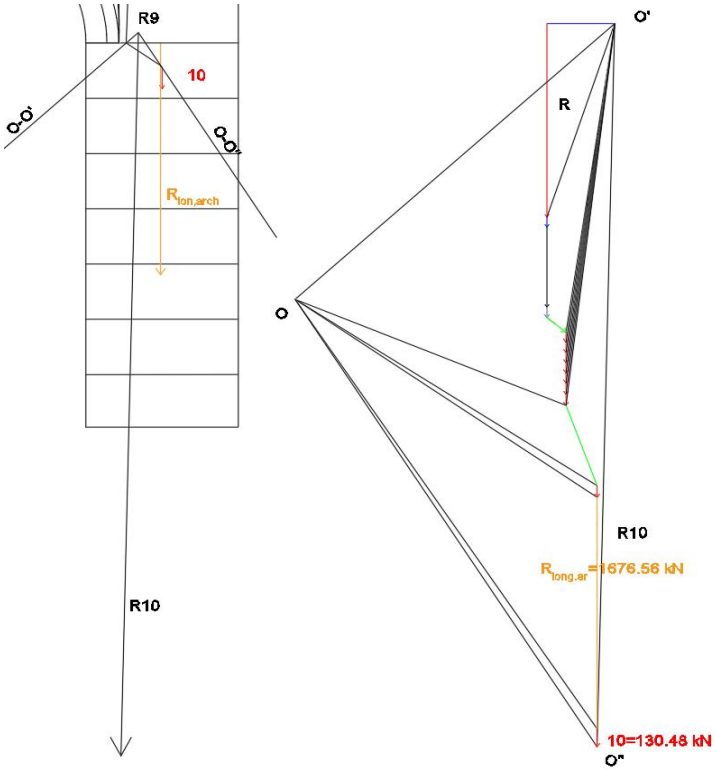

Fig. A. 57- Thrust line in the structure with flying arch (4)

So it is over with the final part of the pillar. The resultant forces are already cut in figure.

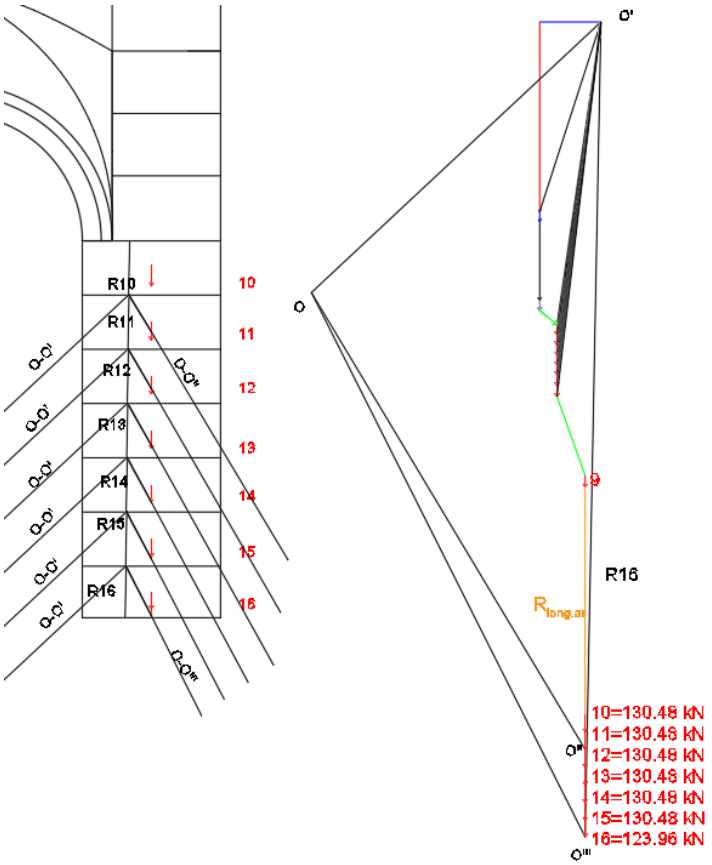

Fig. A. 58- Thrust line in the structure with flying arch (5)

The procedure continues to the left of the flying arch. Here there is the polygon force which include the reaction of the flying arch and the weights of the wall.

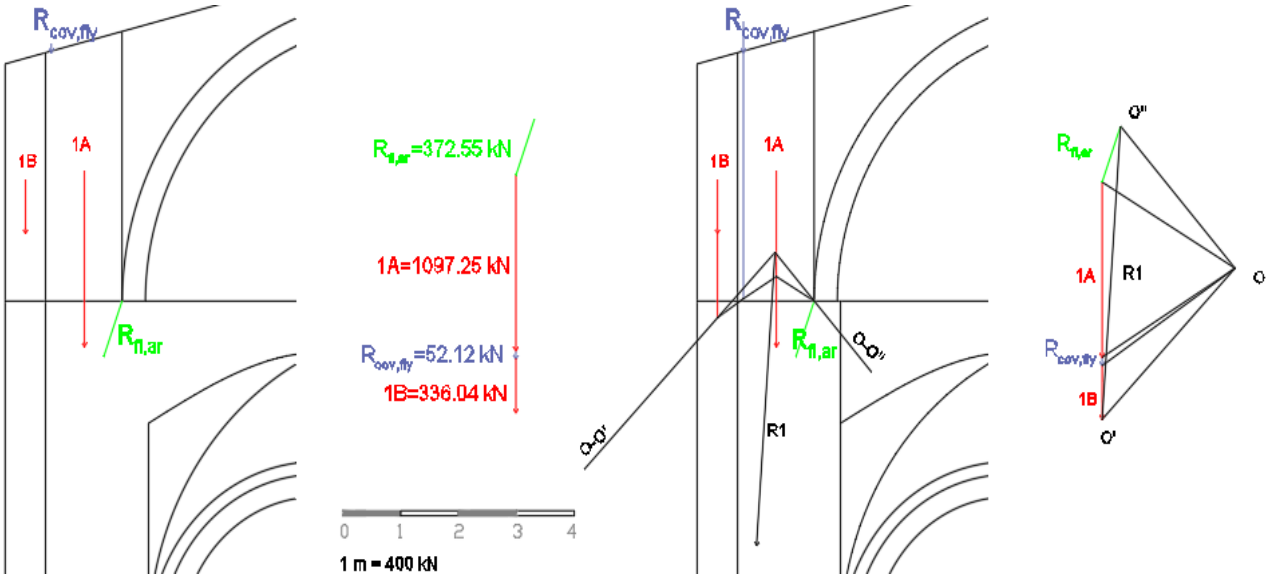

Fig. A. 59- Thrust line in the structure with flying arch (6)

So it can be defined the thrust line in the structure considering all the weight of the wall like shown in the following figure with the application of parallelogram rule.

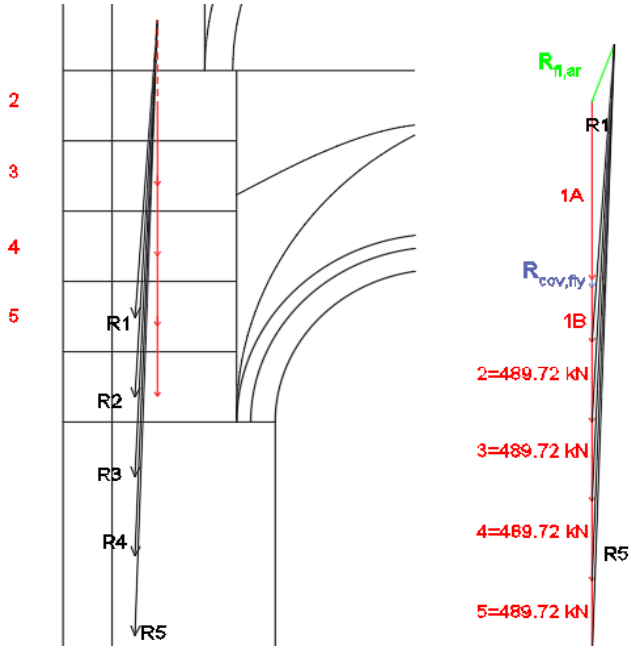

Fig. A. 60- Thrust line in the structure with flying arch (7)

Then, the reaction of the cross vault is taking into account. So, in order to determine the resultant, the polygon force is used.

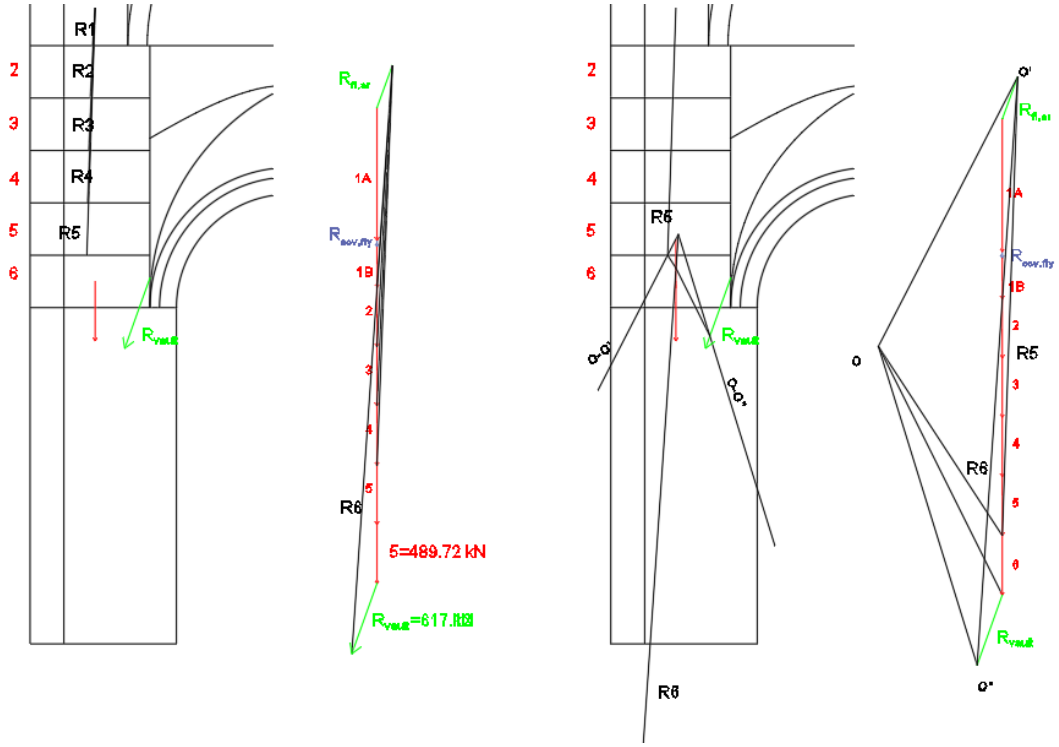

Fig. A. 61- Thrust line in the structure with flying arch (8)

So it is over with the final part of the pillar. The resultant forces are already cut in figure.

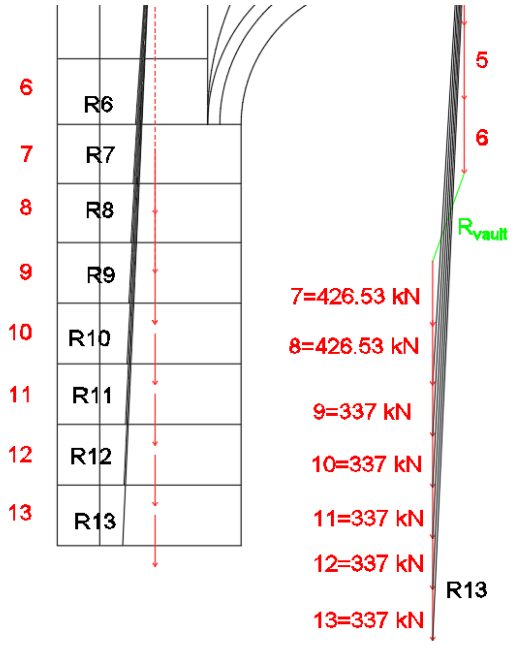

Fig. A. 62- Thrust line in the structure with flying arch (9)

Finally the thrust line inside the structure with flying arch can be drawn.

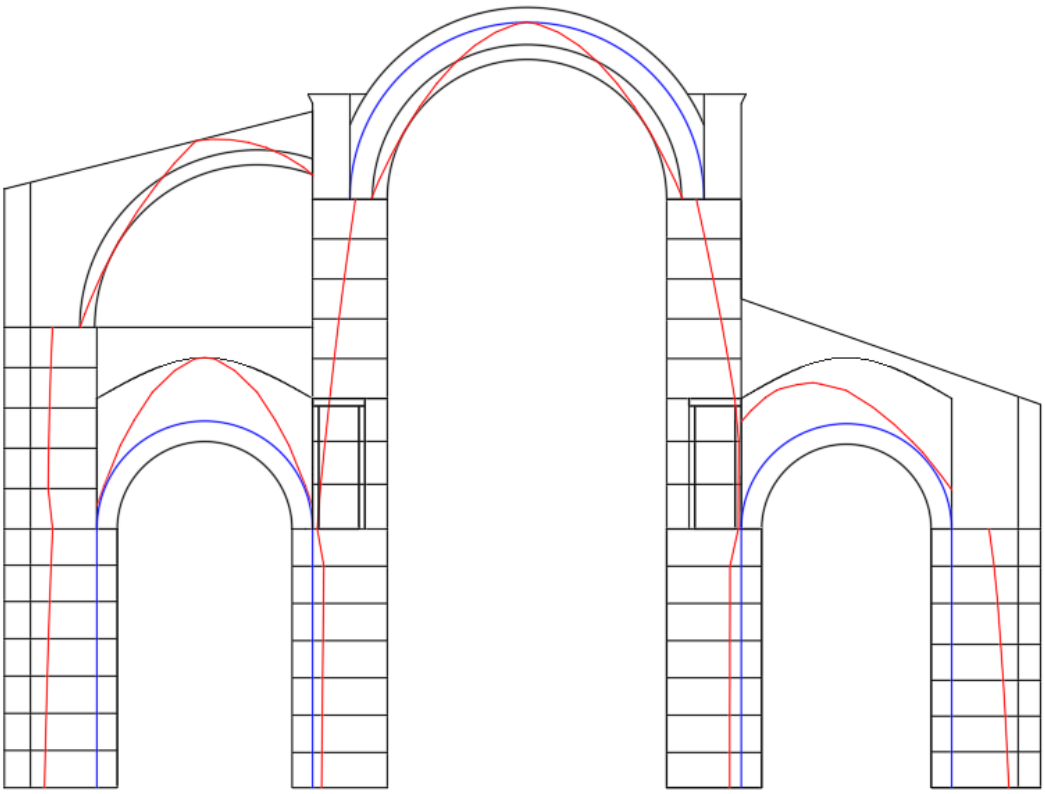

Fig. A. 63- Thrust line in the structure with flying arch (10)

3) STRUCTURE WITH DEFORMATIONS

BARREL VAULT

In this case the barrel vault is analyzed with its real deformations which are very important like shown in the following figure in comparison to the previous case:

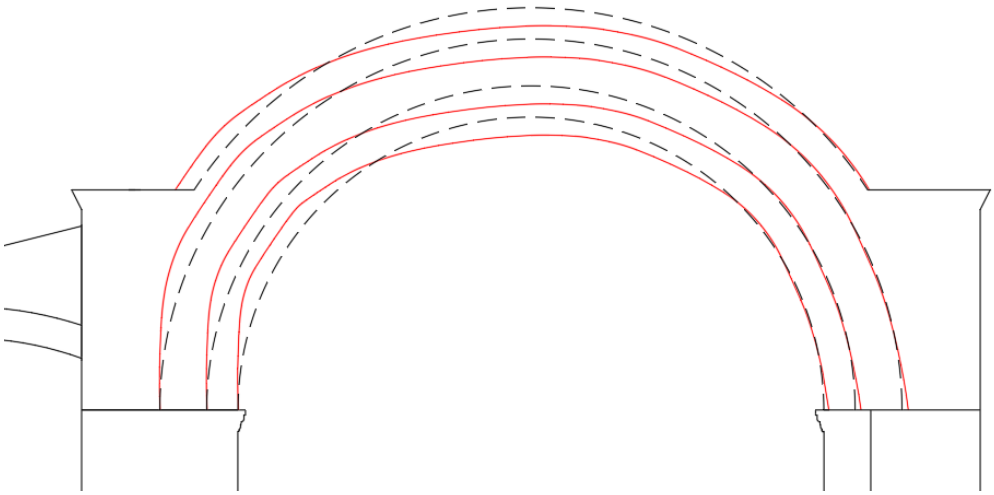

Fig. A. 64- Deformations in the barrel vault

So, it's necessary to calculate a thrust line in the barrel vault that will be actually different. First of all, the barrel vault with deformations is divided in many voussoirs, so the weights of each ones can be calculated.

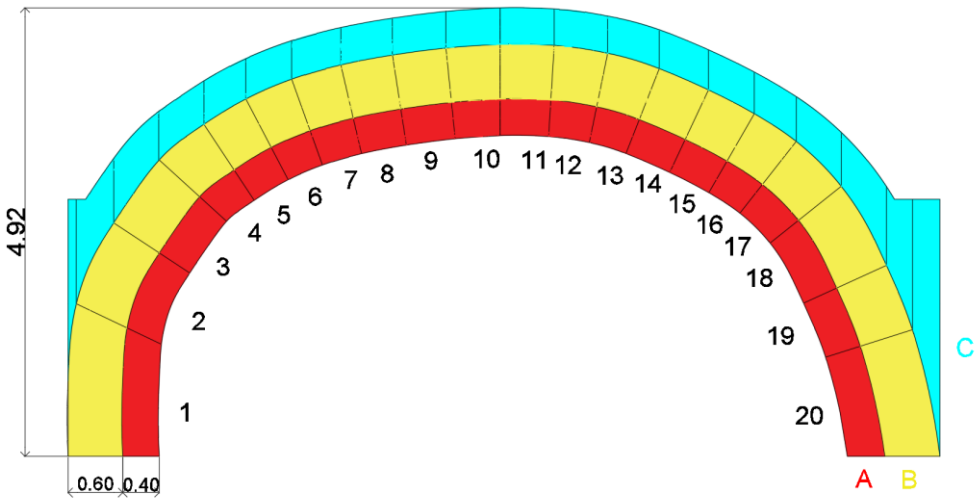

Fig. A. 65- Division of the barrel vault with deformations

Remembering that the part A, B, C represent respectively the arch under the barrel vault, the barrel vault and the filling material, it's possible to calculate the weights of each voussoirs:

Area [m²]	Weights [kN]
A1=0.6286	A1=14.27
A2=0.3507	A2=9.47
A3=0.2914	A3=7.87
A4=0.1725	A4=4.66
A5=0.1827	A5=4.93
A6=0.1749	A6=4.72
A7=0.1882	A7=5.08
A8=0.2068	A8=5.58
A9=0.2199	A9=5.94
A10=0.206	A10=5.56
A11=0.2184	A11=5.9
A12=0.1922	A12=5.19
A13=0.1817	A13=4.91
A14=0.2146	A14=5.79
A15= 0.2004	A15= 5.41
A16=0.1746	A16=4.71
A17=0.2058	A17=5.56
A18=0.3226	A18=8.71
A19=0.2659	A19=7.18
A20=0.4745	A20=12.81

Area [m²]	Weights [kN]
B1=0.9224	B1=188.52
B2= 0.566	B2= 115.68
B3=0.4837	B3=98.86
B4=0.3331	B4=68.08
B5=0.3043	B5=62.19
B6=0.3043	B6=62.19
B7=0.3167	B7=64.73
B8=0.333	B8=68.06
B9=0.3454	B9=70.59
B10=0.3396	B10=69.41
B11=0.3462	B11=70.75
B12=0.3304	B12=67.53
B13=0.3246	B13=66.34
B14=0.3412	B14=69.73
B15=0.3255	B15=66.52
B16=0.3049	B16=62.31
B17=0.3783	B17=77.32
B18=0.5574	B18=113.92
B19=0.4353	B19=88.96
B20=0.7986	B20=163.21

Area [m²]	Weights [kN]
C1=0.1292	C1=19.01
C2=0.3285	C2=48.34
C3=0.3142	C3=46.23
C4=0.2445	C4=35.98
C5=0.2119	C5=31.16
C6=0.2177	C6=32.03
C7=0.2241	C7=32.98
C8=0.2309	C8=33.98
C9=0.2363	C9=34.77
C10=0.2387	C10=35.12
C11=0.2383	C11=35.07
C12=0.2369	C12=34.86
C13=0.236	C13=34.73
C14=0.2342	C14=34.46
C15=0.2264	C15=33.17
C16=0.2163	C16=31.83
C17=0.265	C17=38.99
C18=0.3496	C18=51.44
C19=0.3089	C19=45.45
C20=0.609	C20=89.61

Table 11- Weights of the barrel vault with deformations

So the following force vectors have been obtained:

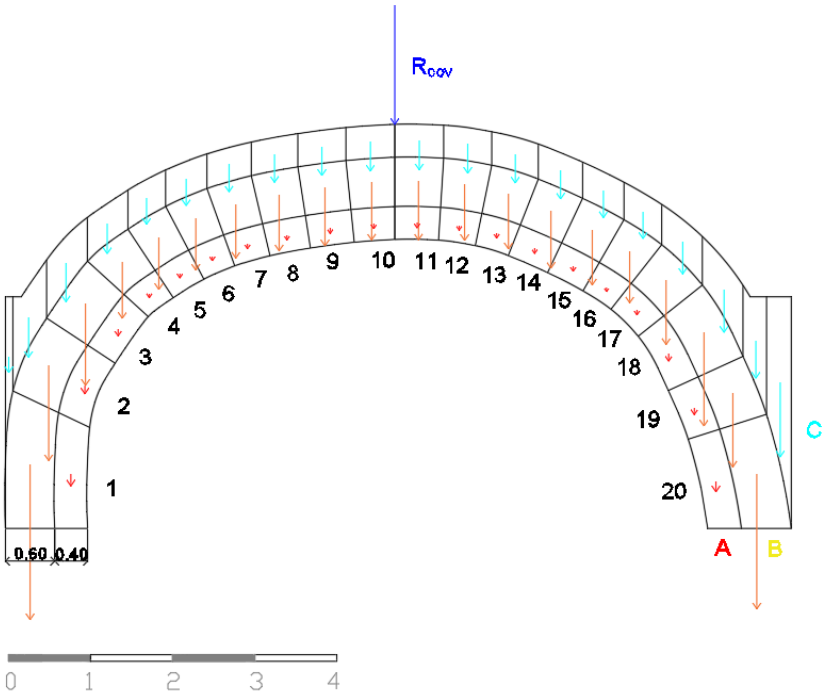

Fig. A. 66- Force vectors of the weights on the barrel vault with deformations (1)

In order to simplify the graphic operation, the different parts (A, B, C) are combined so as to determine one equivalent force for each voussoirs:

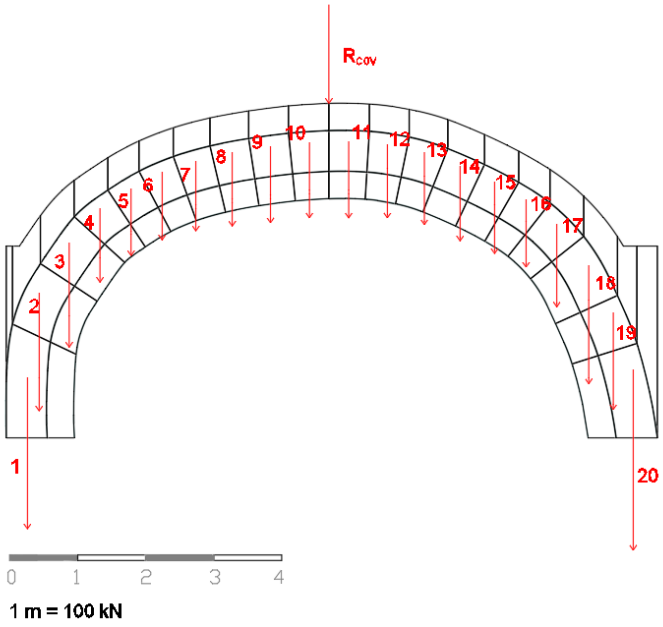

Fig. A. 67- Force vectors of the weights on the barrel vault with deformations (2)

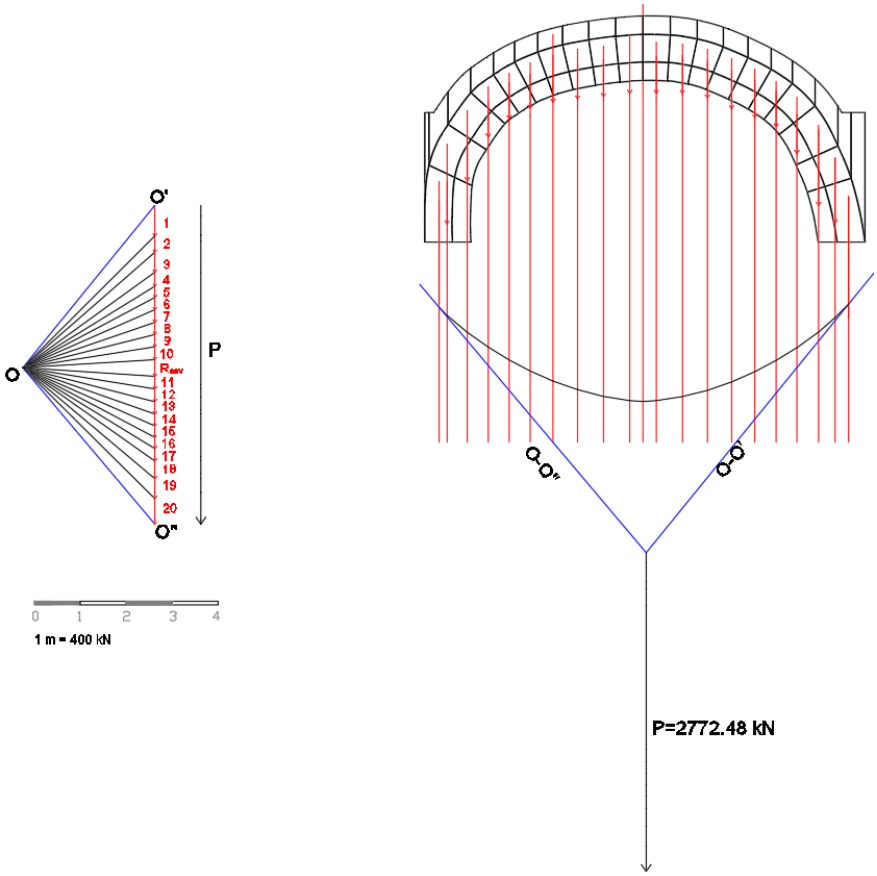

Fig. A. 68- Force polygon and funicular polygon in the barrel vault with deformations (1)

So it's possible to find a minimum thrust line supposing the passage of the thrust line for three points (A, B, C):

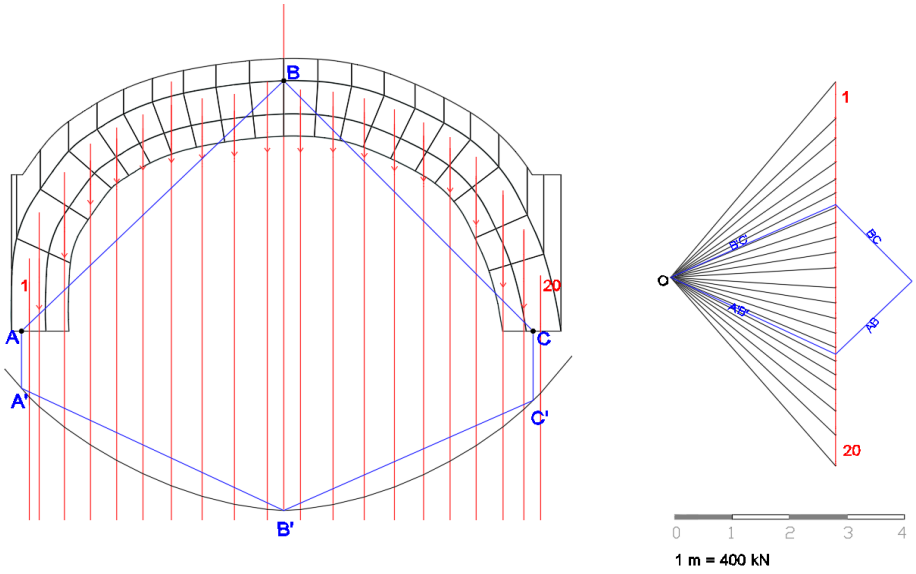

Fig. A. 69- Force polygon and funicular polygon in the barrel vault with deformations (2)

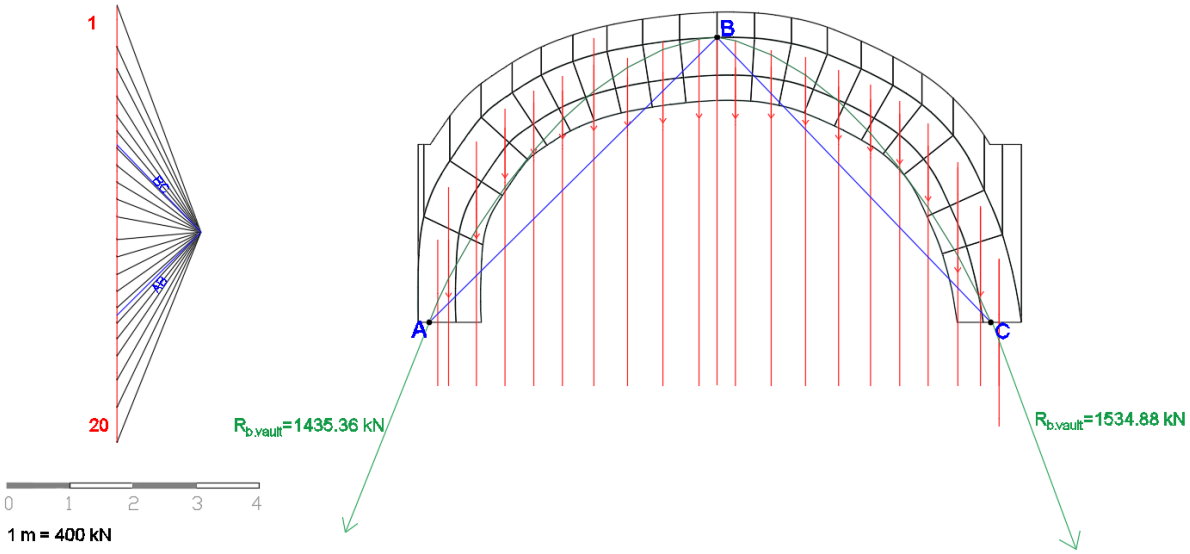

Fig. A. 70- Thrust line in the barrel vault with deformations

FLYING ARCH

Comparing with the previous case, now a new thrust line has been determined in the flying arch because of the increase of the thrust in the barrel vault.

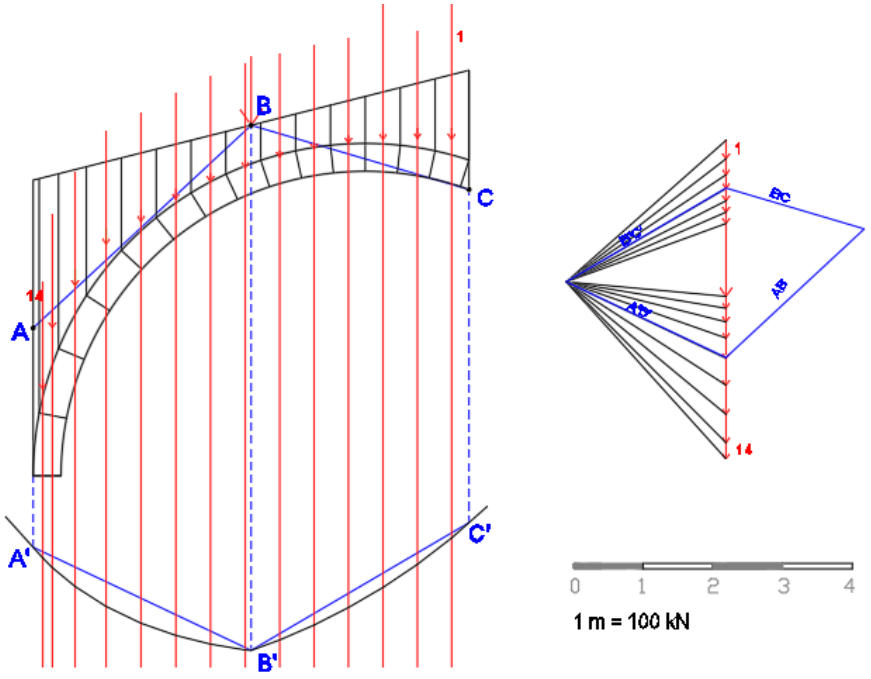

Fig. A. 71- Force polygon and funicular polygon of the flying arch

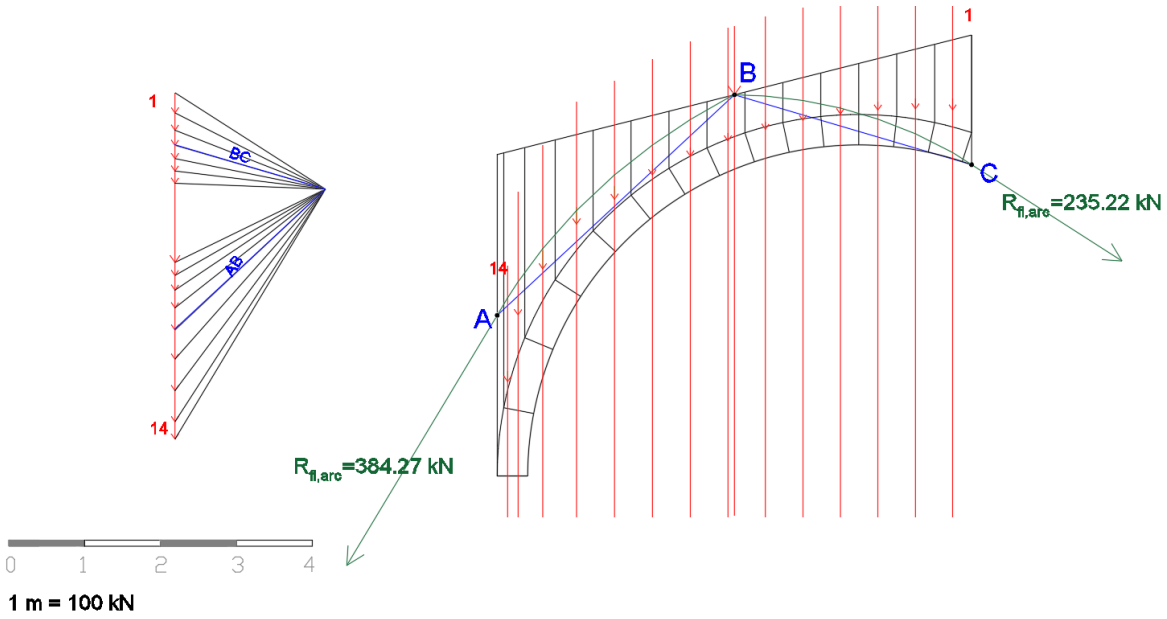

Fig. A. 72- Thrust line in flying arch

CROSS VAULTS

Also for the cross vaults it's necessary to calculate different thrust lines in order to obtain sufficient thrusts to satisfy the equilibrium of the structure. Even for the vault of the right

side, it is necessary to consider the passage of the thrust line for the upper part as it will be shown.

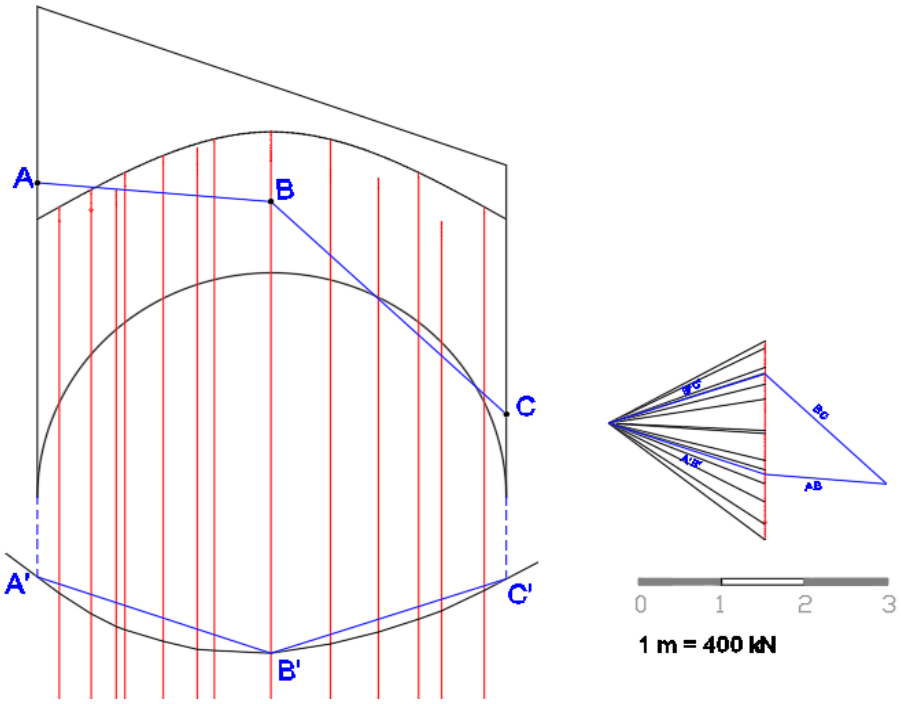

Fig. A. 73- Force polygon and funicular polygon of the cross vault (A)

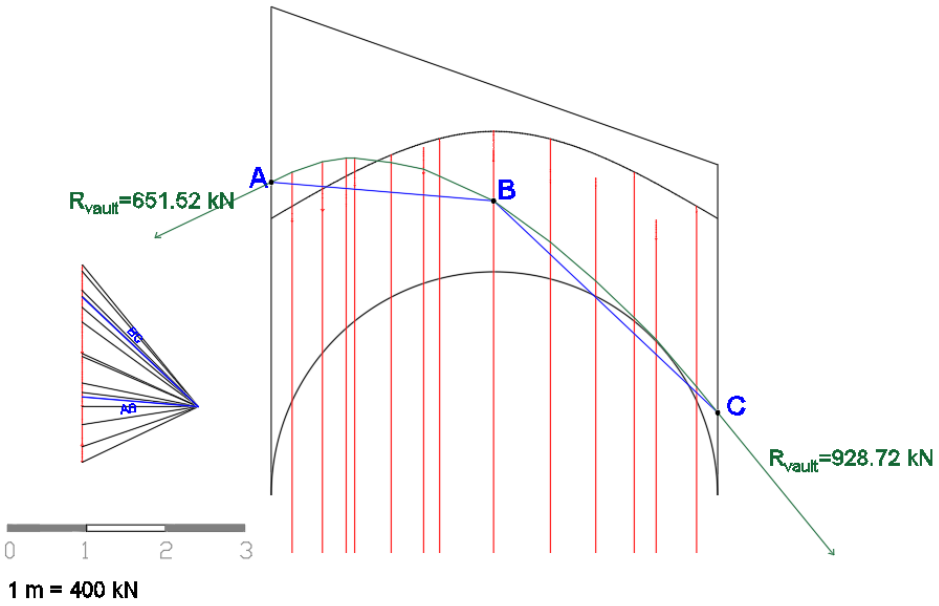

Fig. A. 74- Thrust line in cross vault (A)

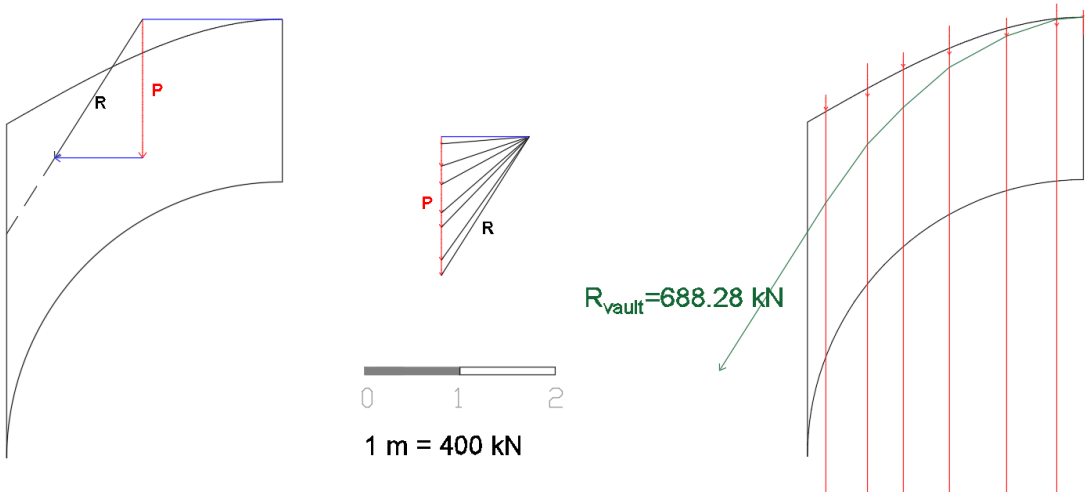

Fig. A. 75- Thrust line in cross vault (B)

THRUST LINE OF THE STRUCTURE

Once found the thrust lines in the arches, it's possible to draw the thrust line of the structure as shown in the previous cases.

In the following figure, with the force polygon the resultant R1 is found. This is obtained from the sum of the reaction of the barrel vault, the weight of the block 1 and the reaction of the roof.

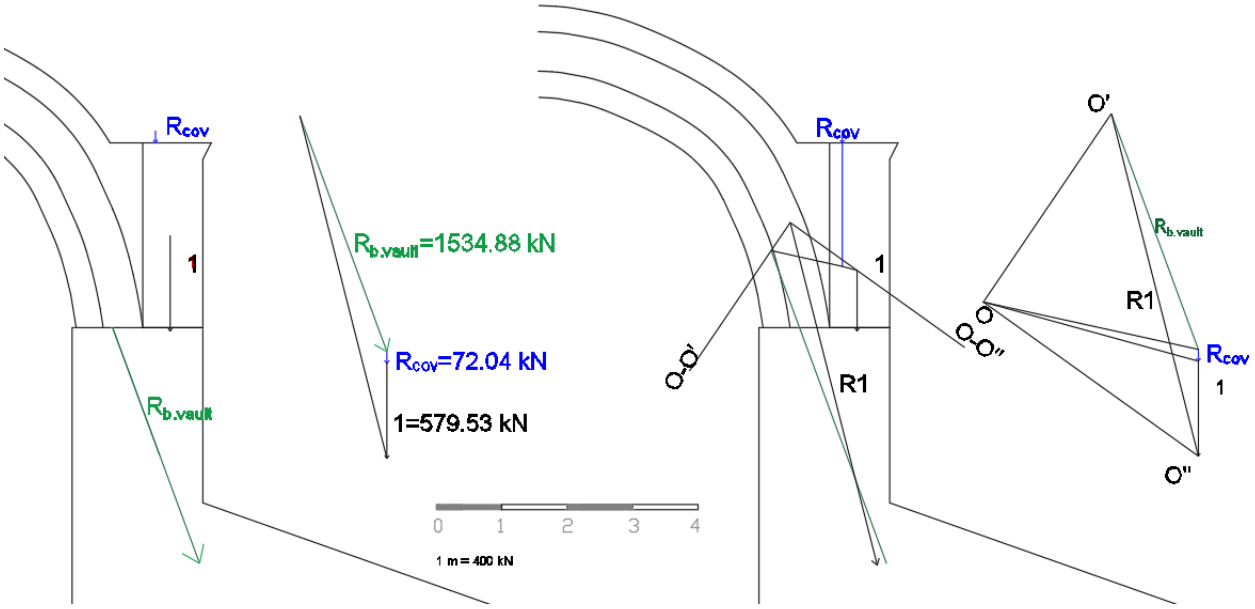

Fig. A. 76- Thrust line in the structure with deformations (1)

Here is the application of the parallelogram rule with the block of the pillars, the sum of the resultant with the reaction of the cross vault and then the sum with the reaction of longitudinal arch; finally, the final part of the pillar.

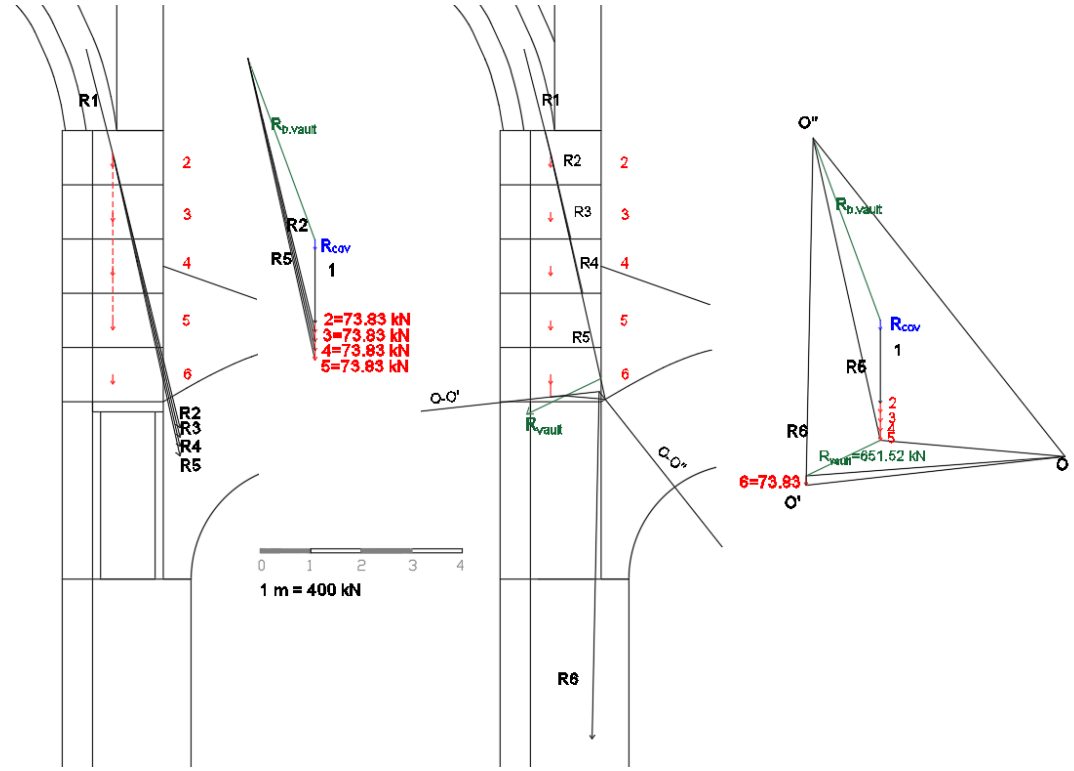

Fig. A. 77- Thrust line in the structure with deformations (2)

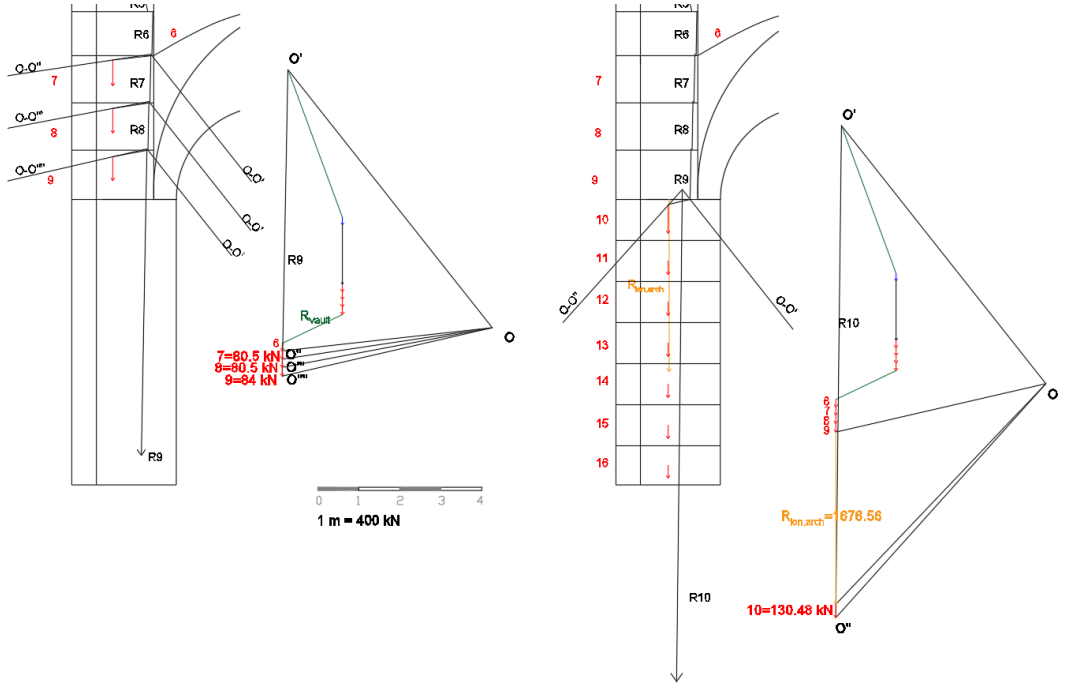

Fig. A. 78- Thrust line in the structure with deformations (3)

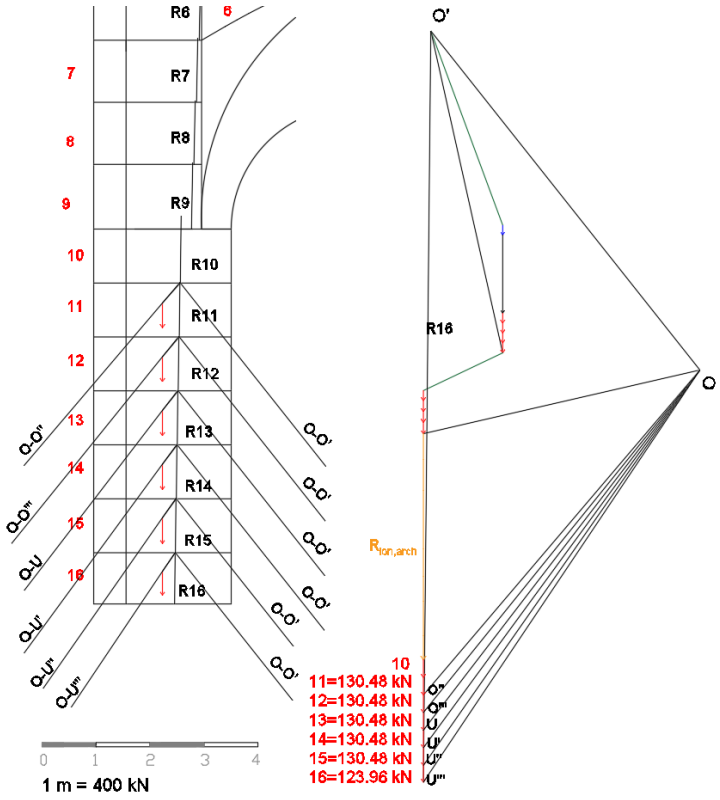

Fig. A. 79- Thrust line in the structure with deformations (4)

Here the right side is analyzed, starting from the resultant R1 summing the reaction of the cross vault, the blocks of the wall (1A and 1B) and the reaction of the roof with force polygon.

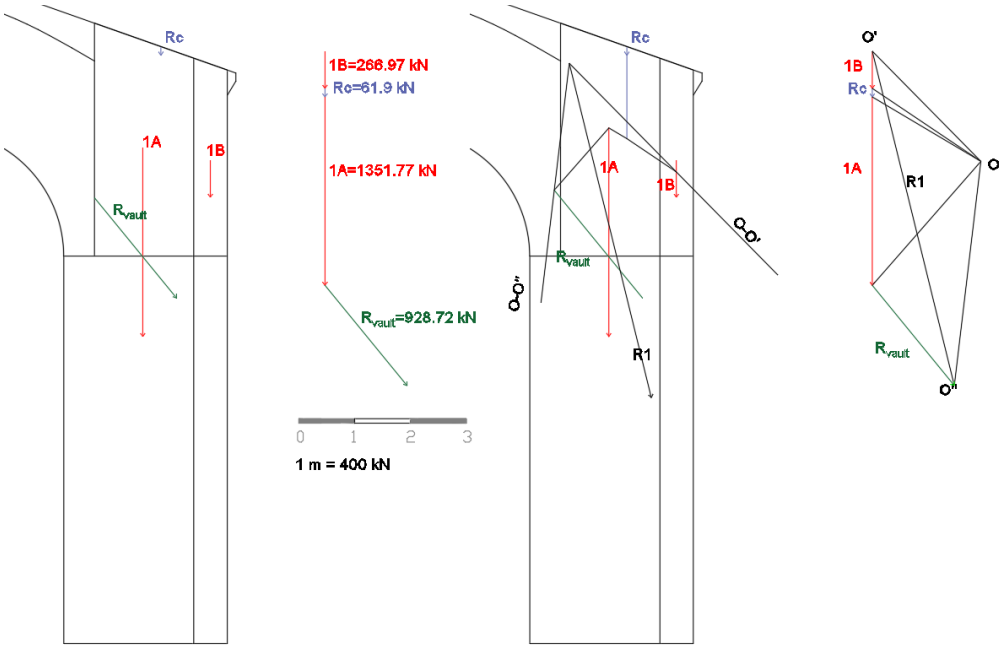

Fig. A. 80- Thrust line in the structure with deformations (5)

Then, starting from the resultant R1, all the blocks of the walls are added with the force polygon.

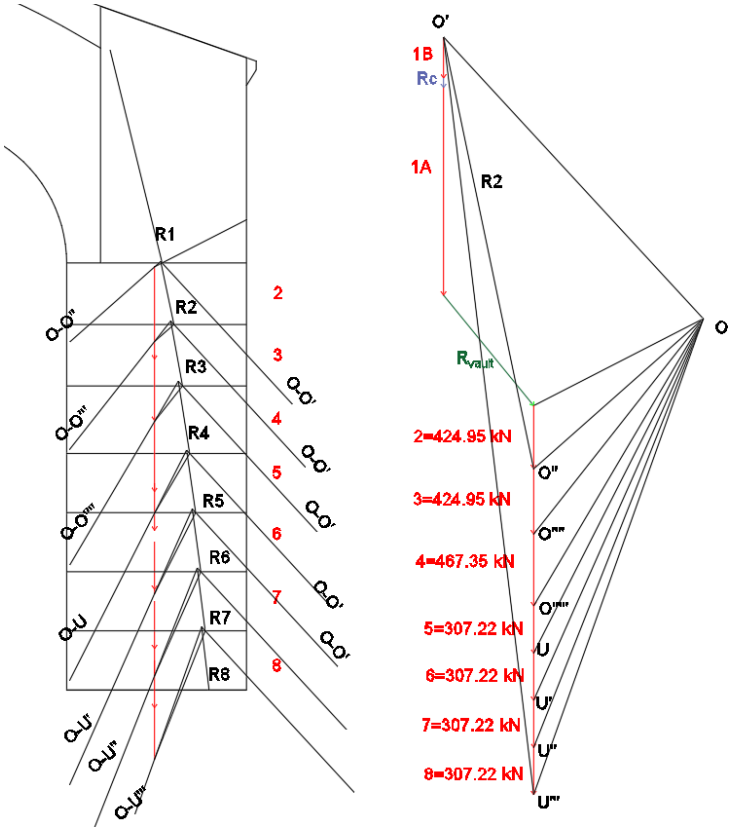

Fig. A. 81- Thrust line in the structure with deformations (6)

The procedure is repeated on the left side, starting from the resultant R1 which is obtained adding the reaction of the barrel vault, the reaction of the flying arch, the weight of the block 1 of the wall and the reactions of the roofs.

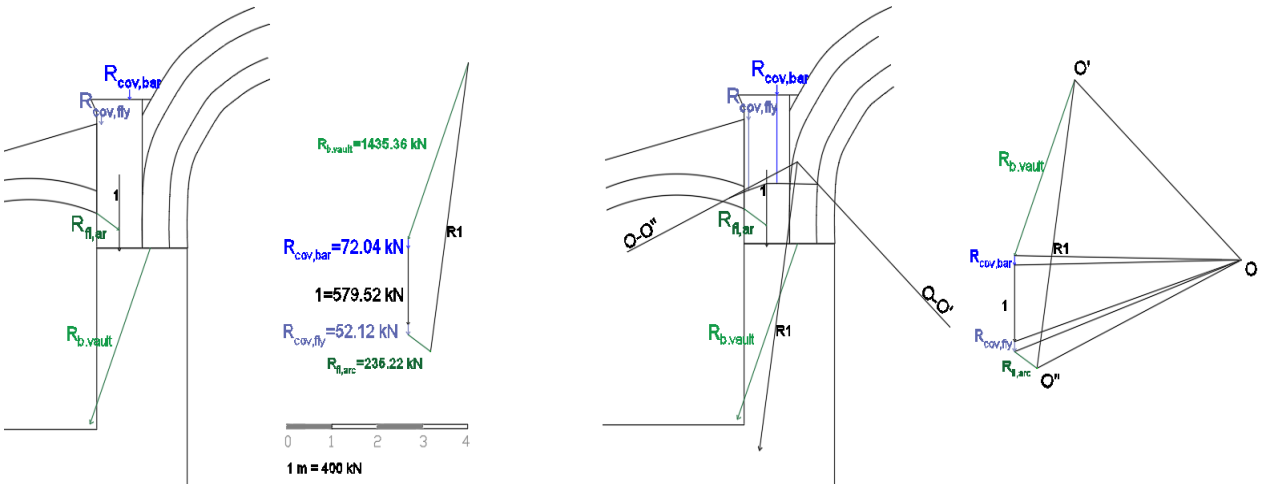

Fig. A. 82- Thrust line in the structure with deformations (7)

Here the parallelogram rule is applied between the R1 and 2, and then it's repeated. After, the reactions of the cross vault and of the longitudinal are considered.

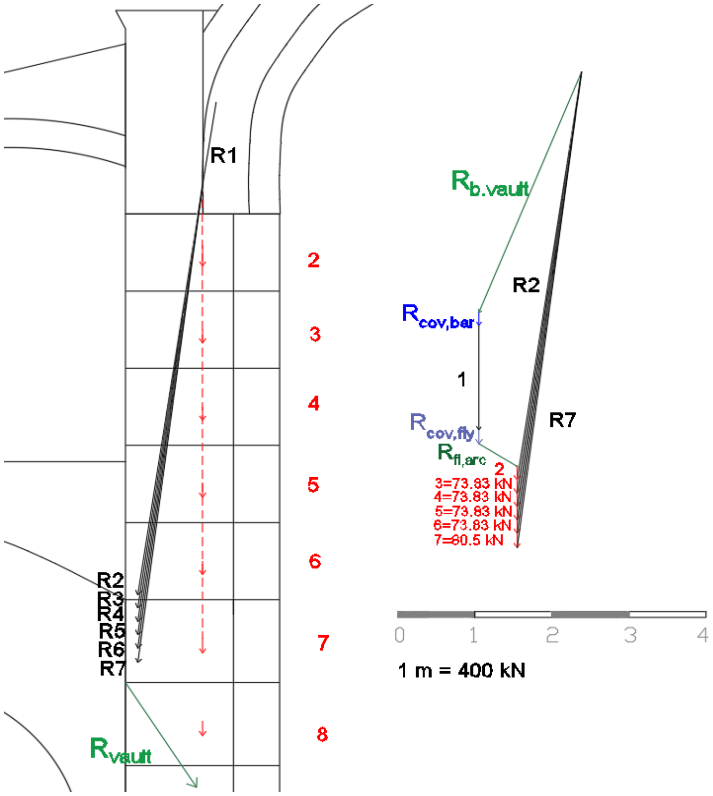

Fig. A. 83- Thrust line in the structure with deformations (8)

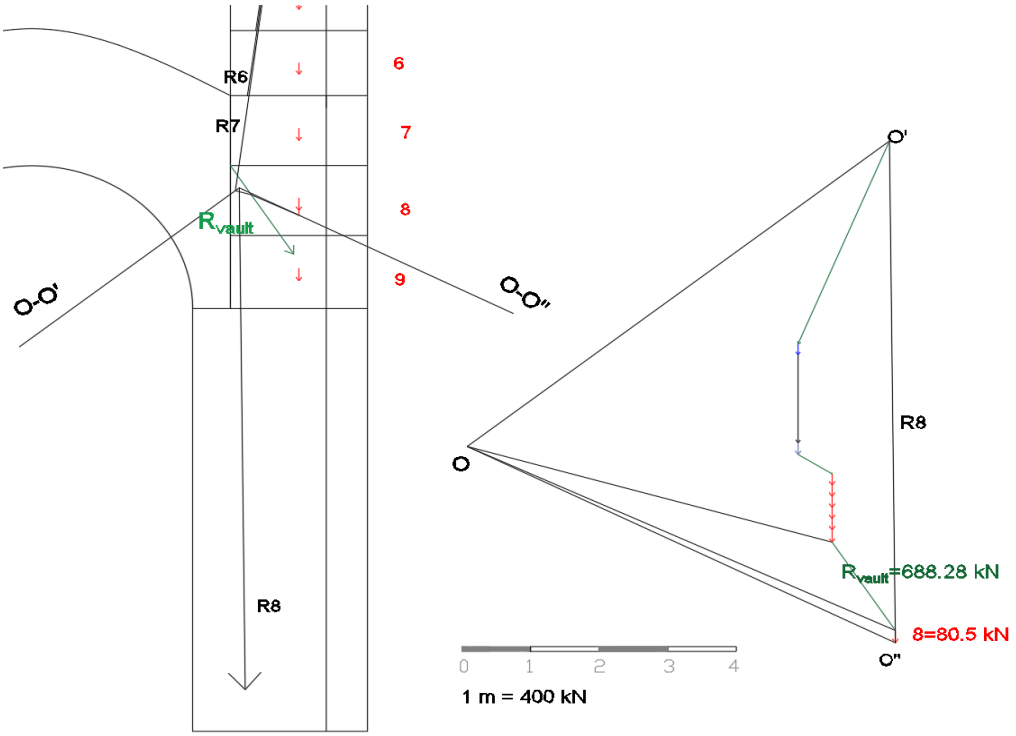

Fig. A. 84- Thrust line in the structure with deformations (9)

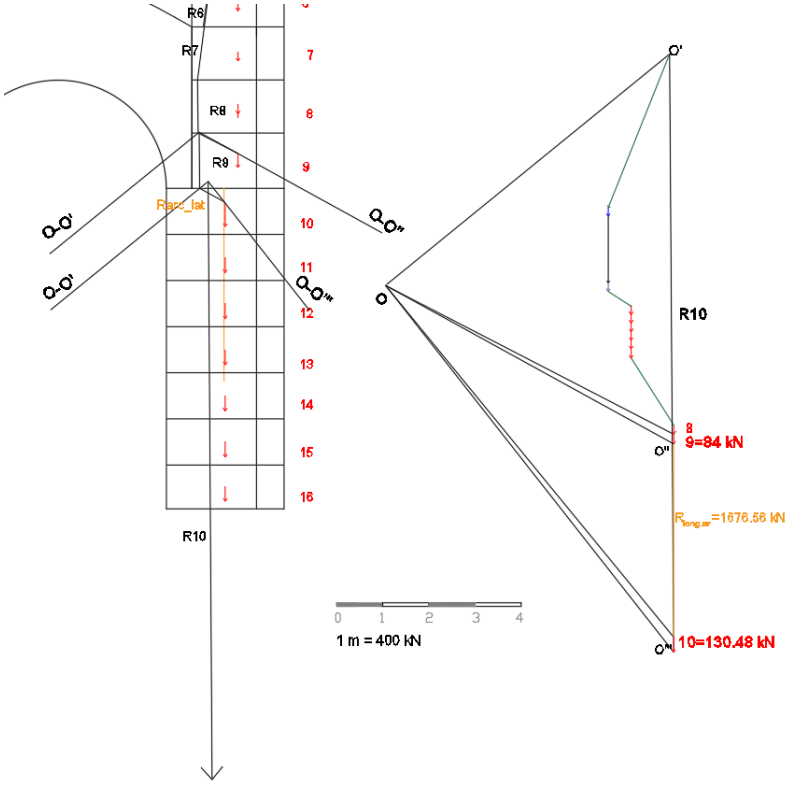

Fig. A. 85- Thrust line in the structure with deformations (10)

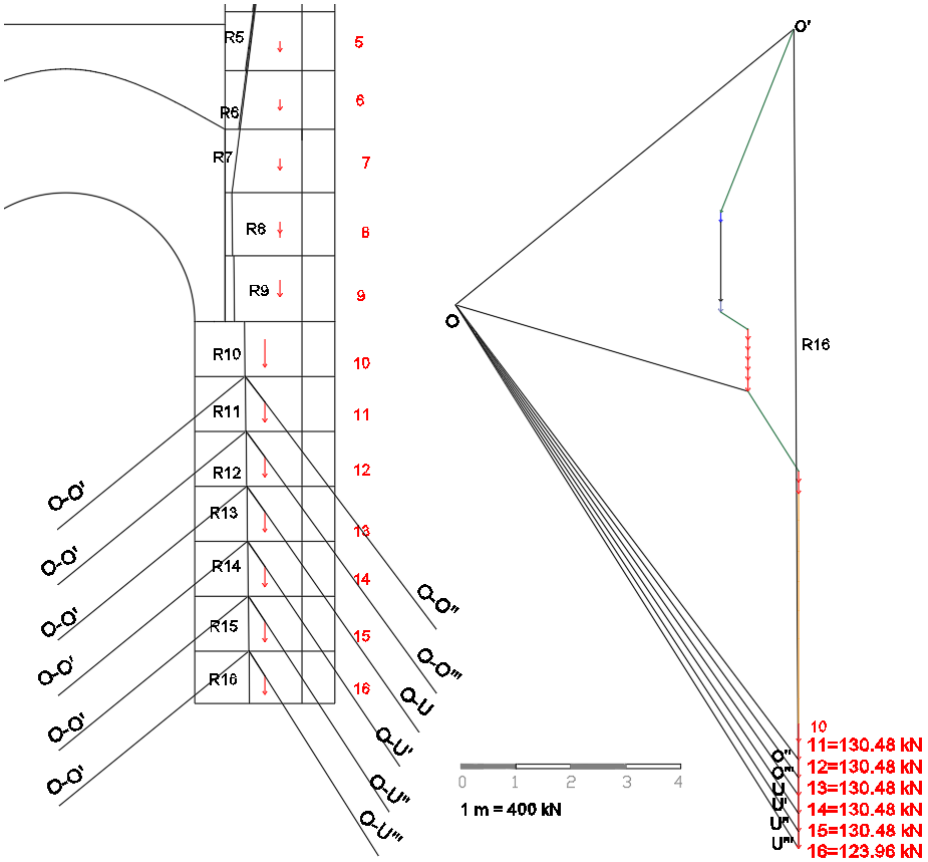

Fig. A. 86- Thrust line in the structure with deformations (11)

So, the procedure continued at the left of the flying arch.

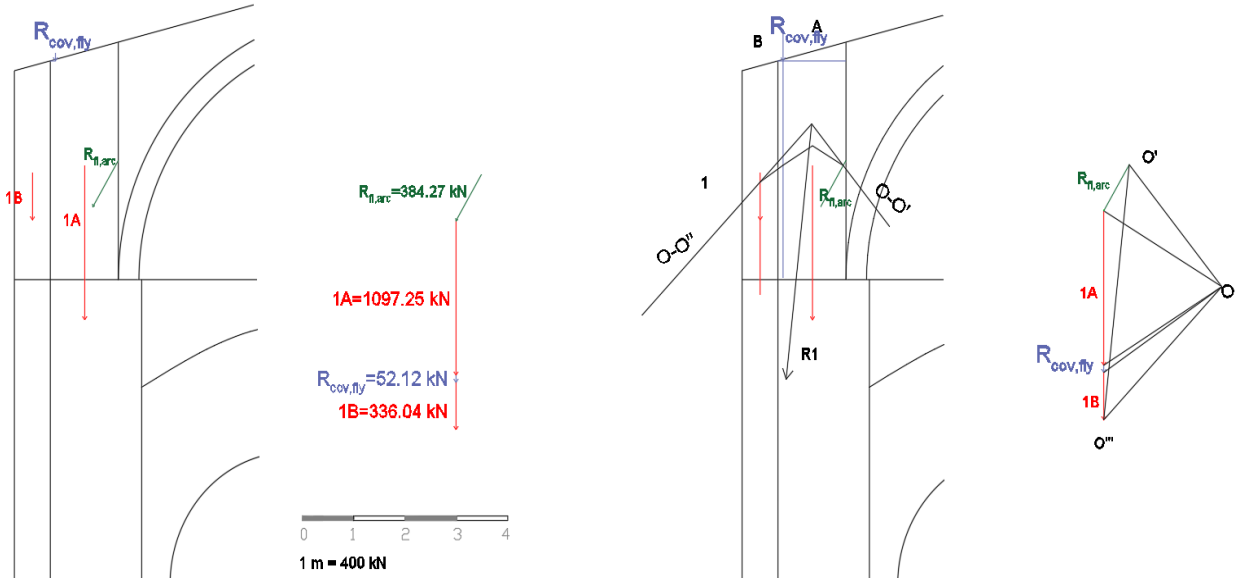

Fig. A. 87- Thrust line in the structure with deformations (12)

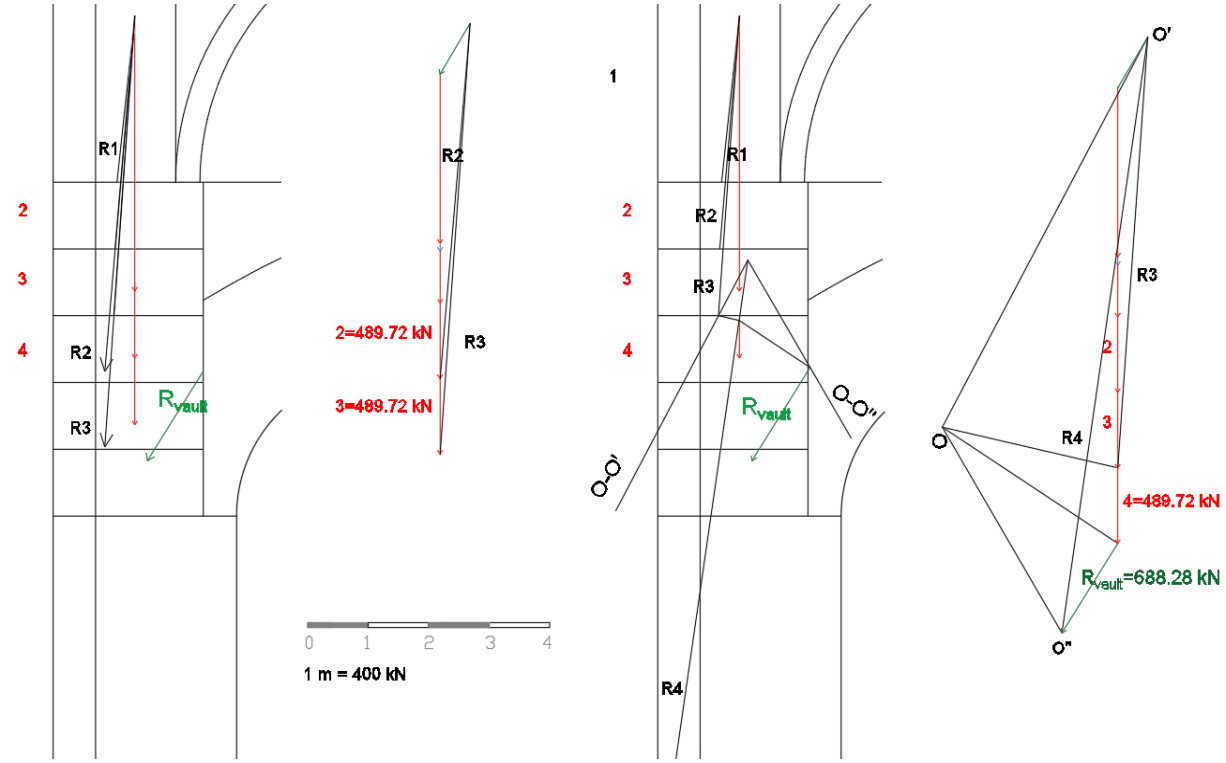

Fig. A. 88- Thrust line in the structure with deformations (13)

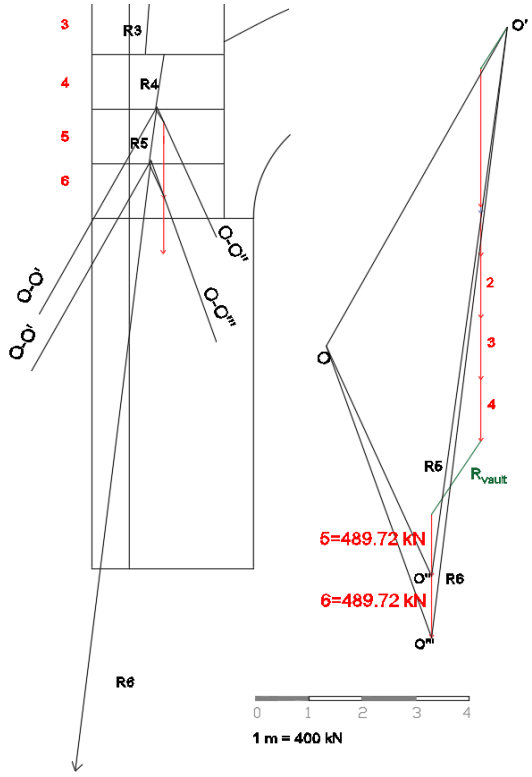

Fig. A. 89- Thrust line in the structure with deformations (14)

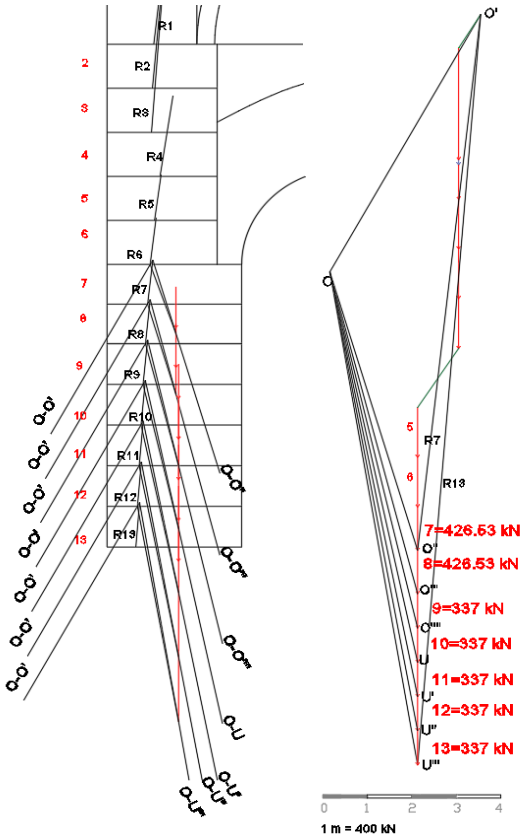

Fig. A. 90- Thrust line in the structure with deformations (15)

Finally, the thrust line in the structure with deformations can be drawn.

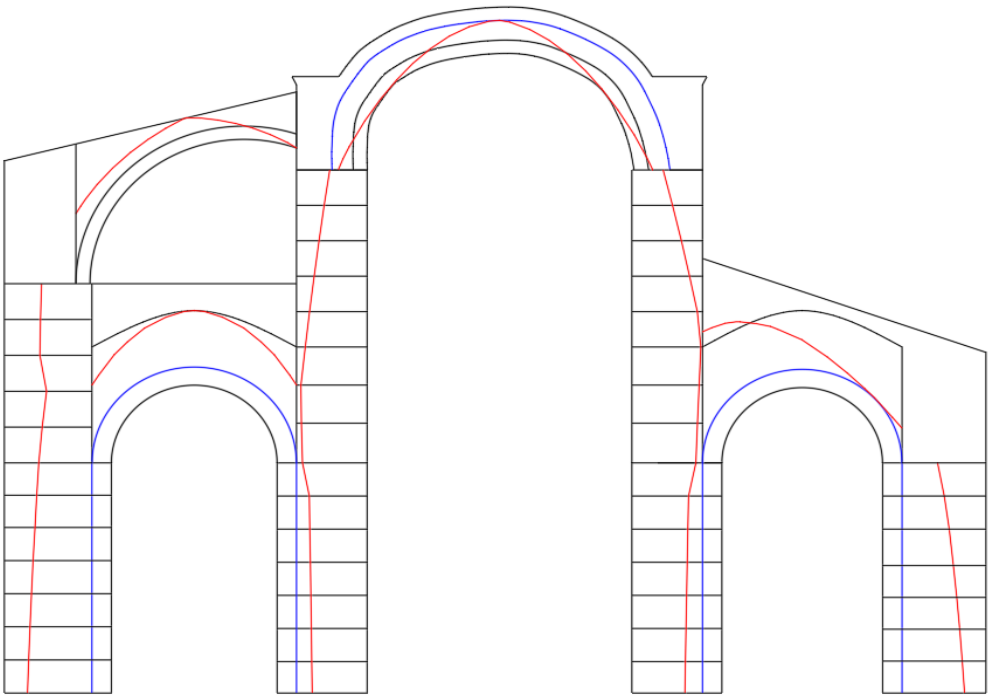

Fig. A. 91- Thrust line in the structure with deformations (16)

4) STRUCTURE WITH SEISMIC ACTION

A horizontal force is added at each weight force calculated in the previous case of the structure with deformations. As mentioned in the previous chapter, this horizontal force to be applied is proportional to the weight by the coefficient α=0.05.

There are two cases investigated, in fact the direction of the seismic action is considered to right (+) and to the left (-) separately. So, in the following pages there are all the calculation to obtain the thrust lines in the single structural part, and then the combination of them in order to obtain the thrust line in the structure both in left direction (-) and right direction (+).

BARREL VAULT

- Seismic direction (-)

A horizontal force is added to each force,, so the following new force vectors have obtained.

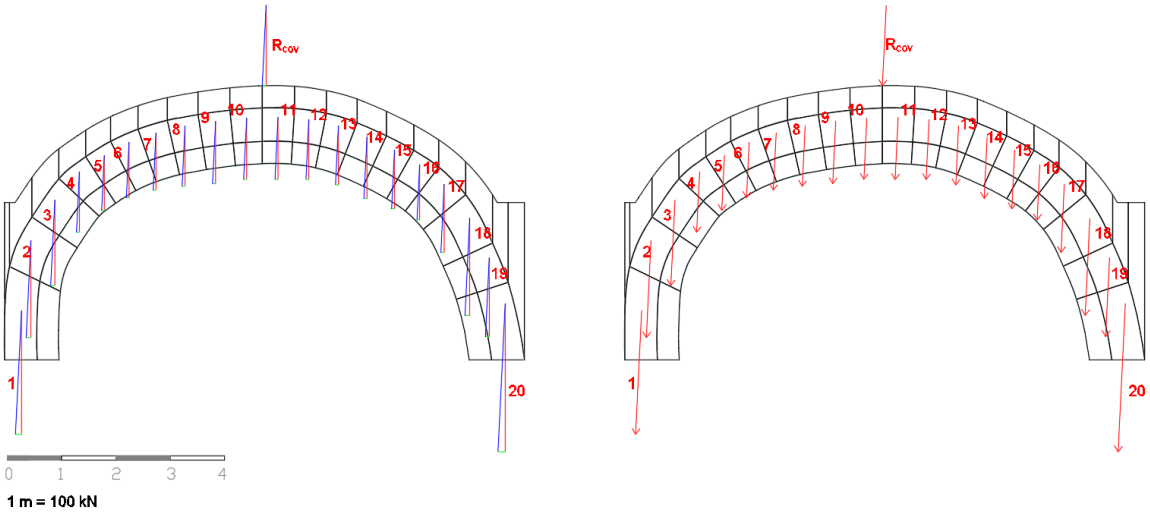

Fig. A. 92- Force vectors in the barrel vault - seismic (-)

So from the force polygon it's possible to realize the funicular polygon.

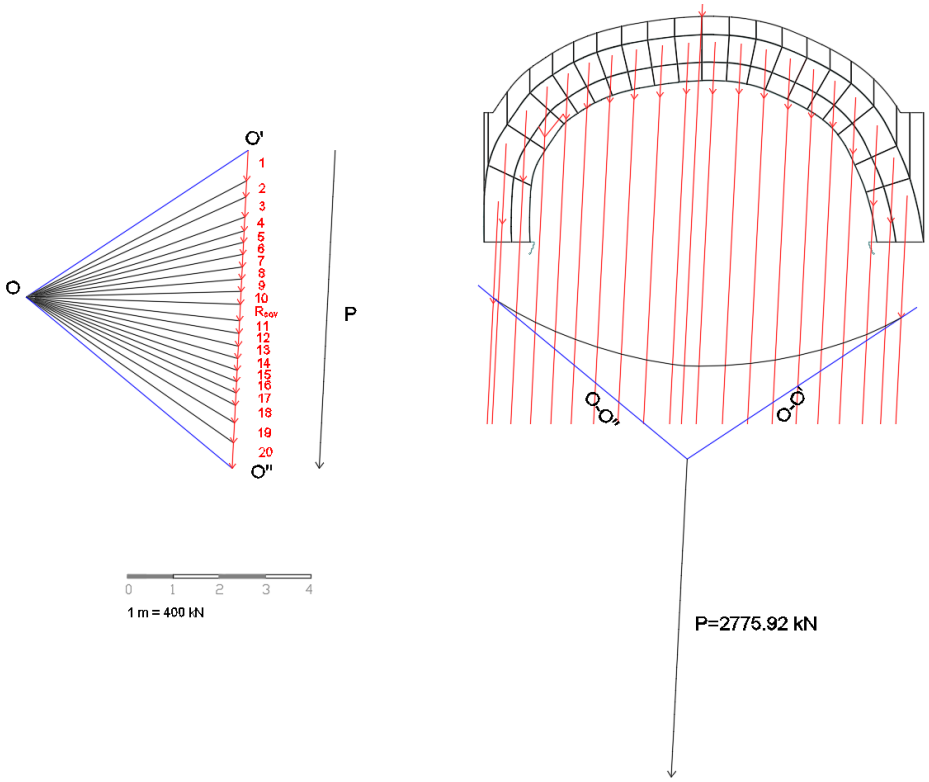

Fig. A. 93- Force polygon and funicular polygon in the barrel vault – seismic direction (-) (1)

So it's possible to find a minimum thrust line supposing the passage of the thrust line for three points (A, B, C):

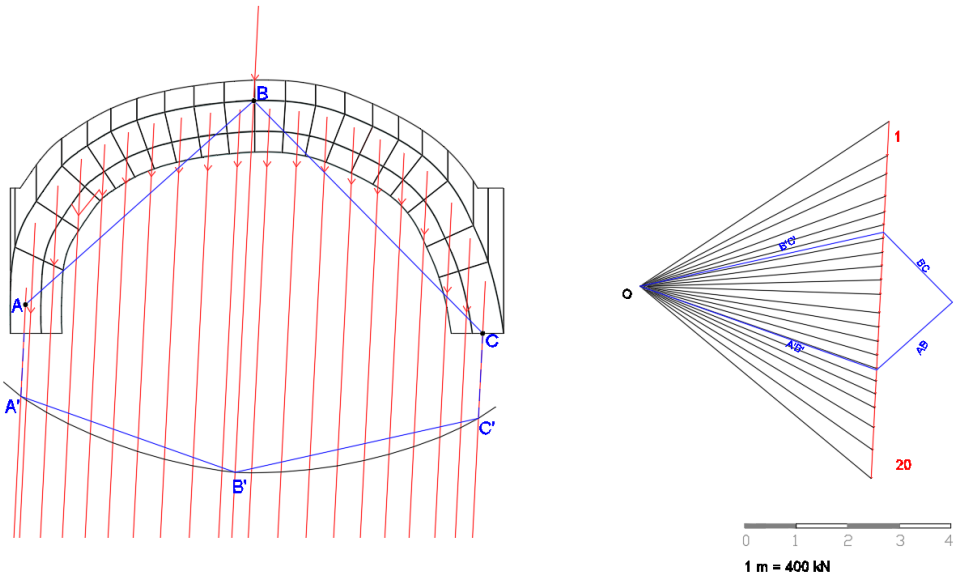

Fig. A. 94- Force polygon and funicular polygon in the barrel vault – seismic direction (-) (2)

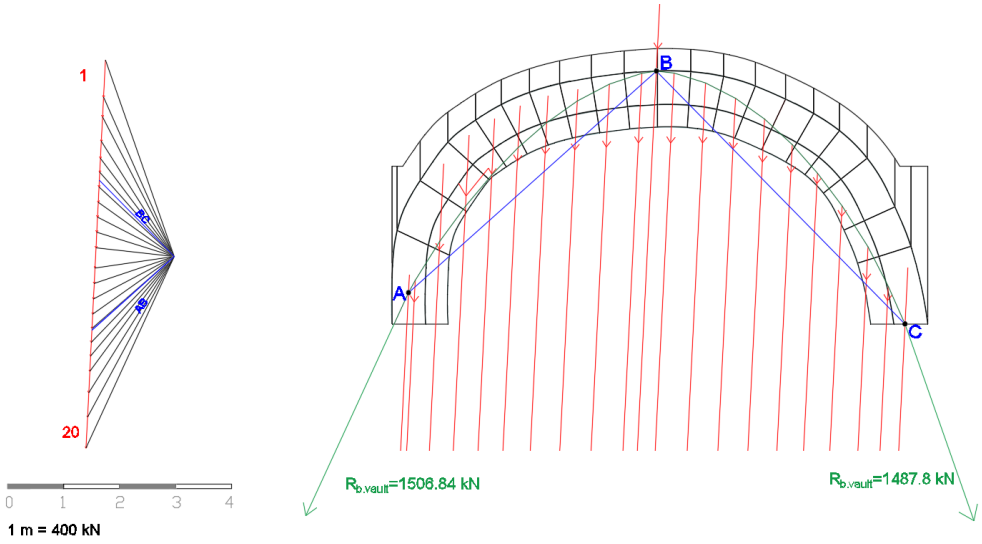

Fig. A. 95- Thrust line in the barrel vault - seismic direction (-)

- Seismic direction (+)

The previous passages are repeated for the other case with seismic direction (+).

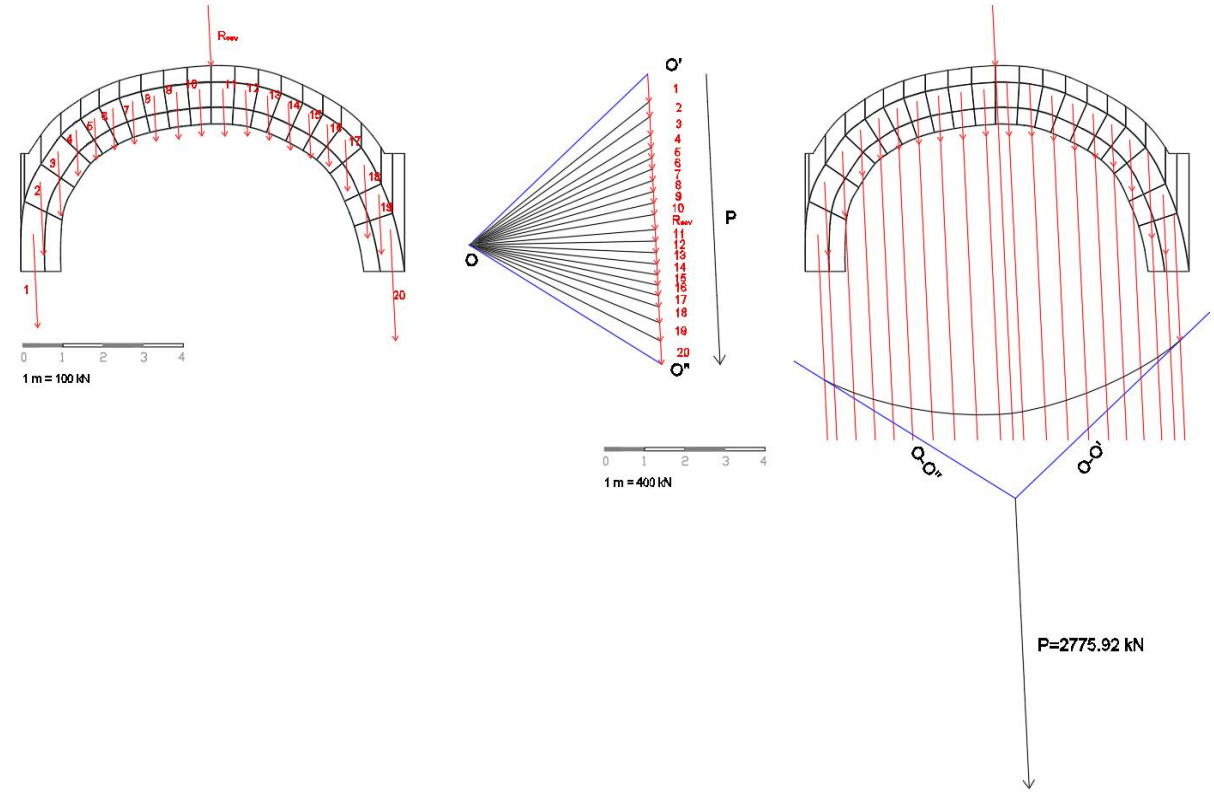

Fig. A. 96- Force vectors, force polygon and funicular polygon in the barrel vault - seismic (+)

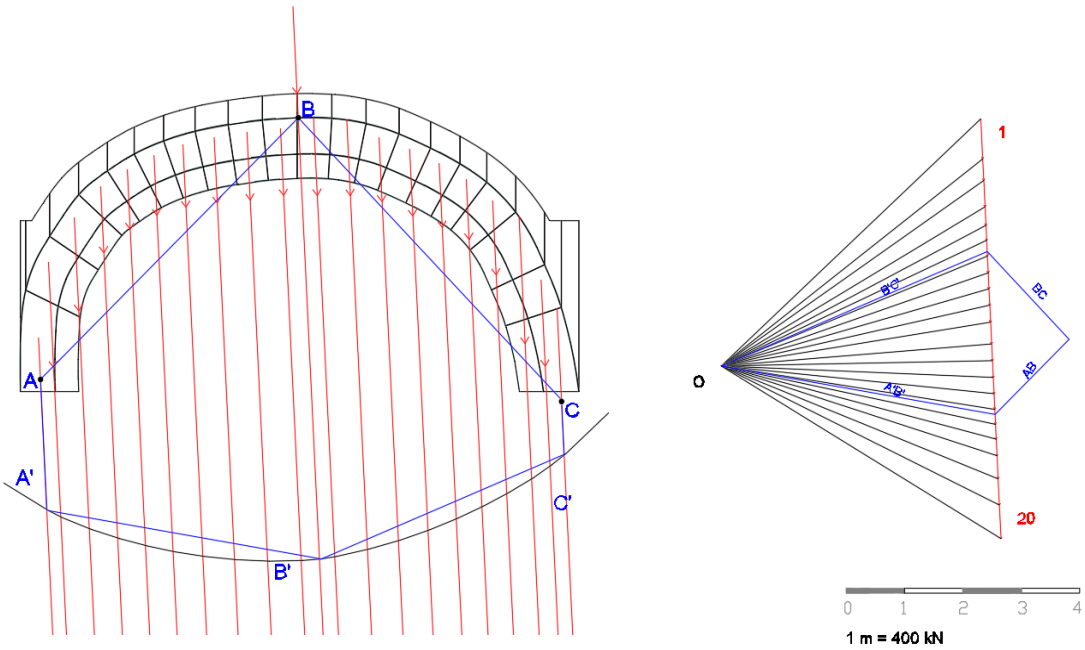

Fig. A. 97- Force polygon and funicular polygon in the barrel vault – seismic direction (+)

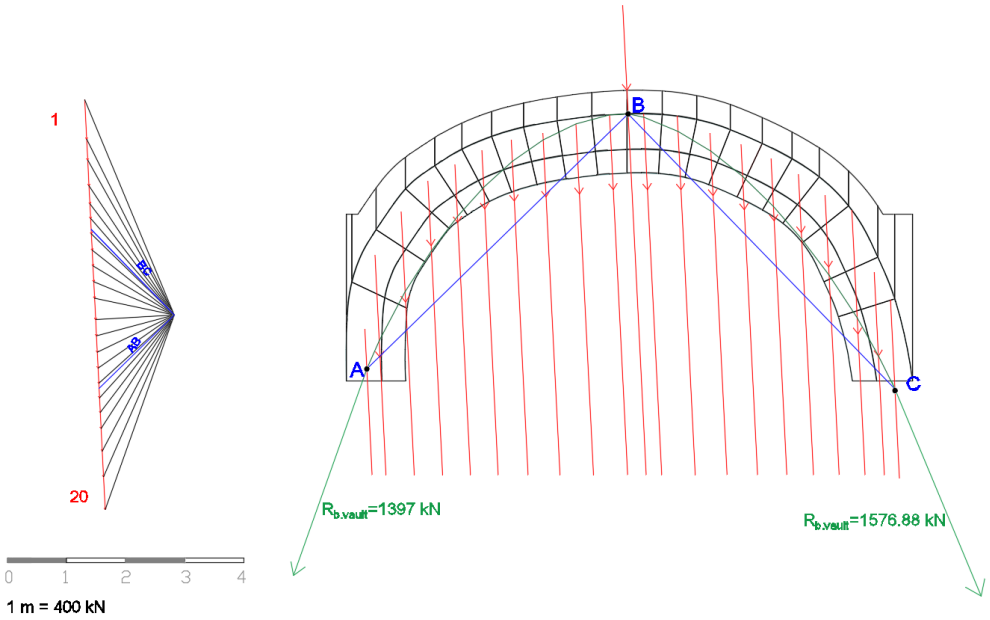

Fig. A. 98- Thrust line in the barrel vault – seismic direction (+)

CROSS VAULTS

- Seismic direction (-)

First of all, a horizontal force is added to each force. Then the force polygon and the funicular polygon have been realized.

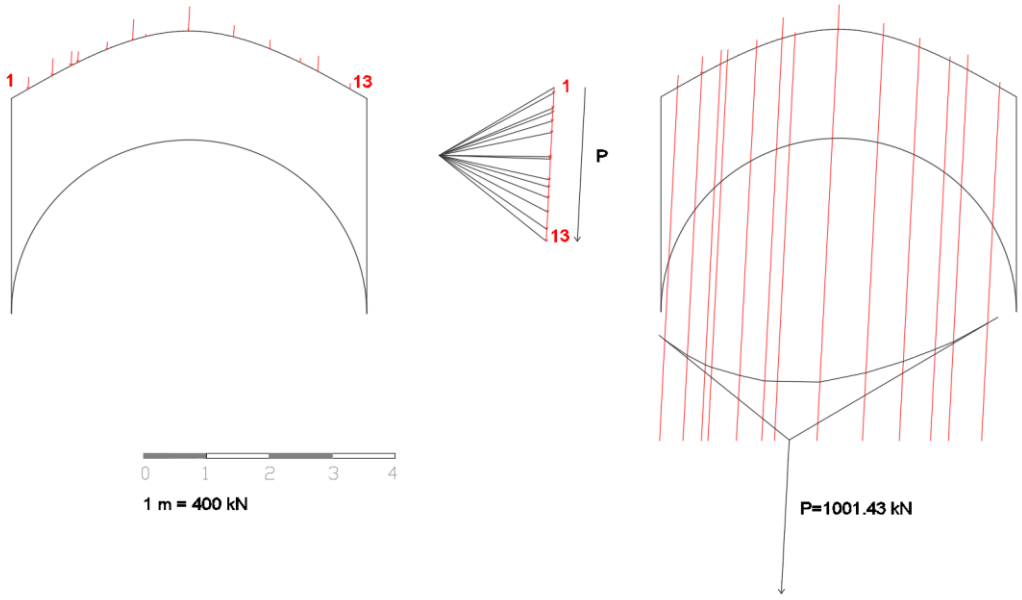

Fig. A. 99- Force polygon and funicular polygon of the cross vault (A) - seismic direction (-) (1)

So it's possible to find a thrust in the cross vault supposing the passage of the thrust line for three points (A, B, C); the choice of these points is linked to the thrust line that is generated in the structure:

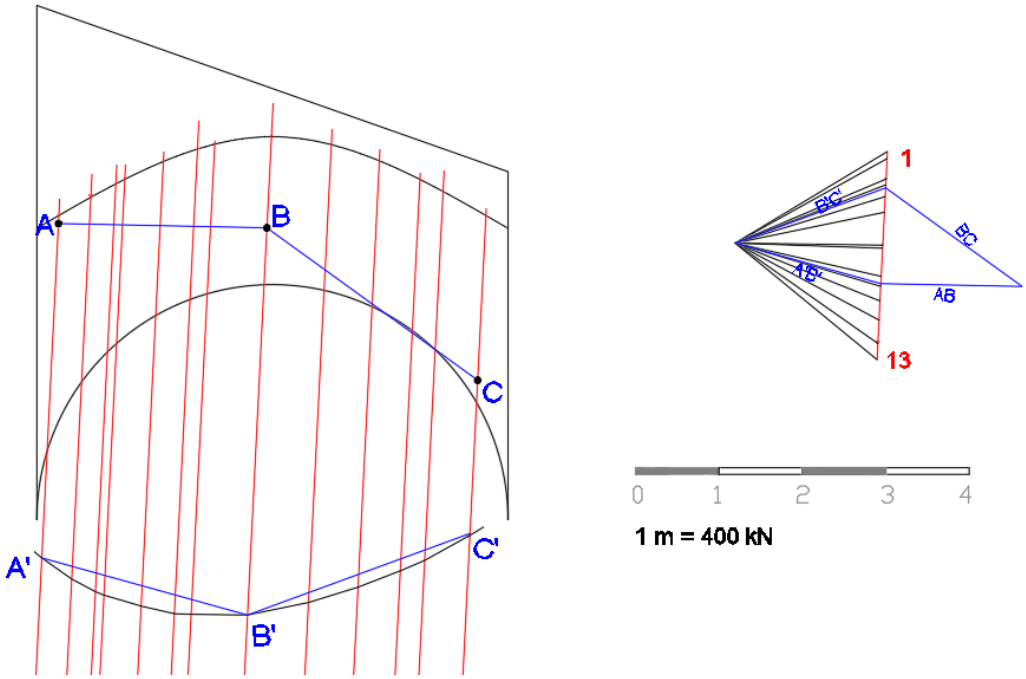

Fig. A. 100- Force polygon and funicular polygon of the cross vault (A) - seismic direction (-) (2)

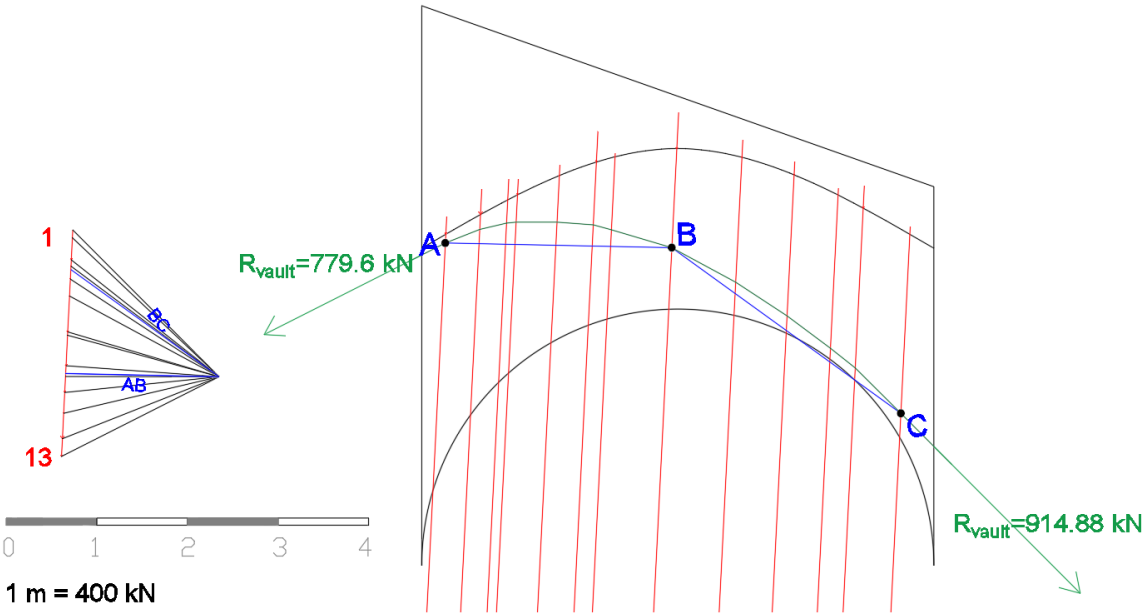

Fig. A. 1011- Thrust line of the cross vault (A) - seismic direction (-)

In the same way, the calculation is carried out for the cross vault on the left side (B).

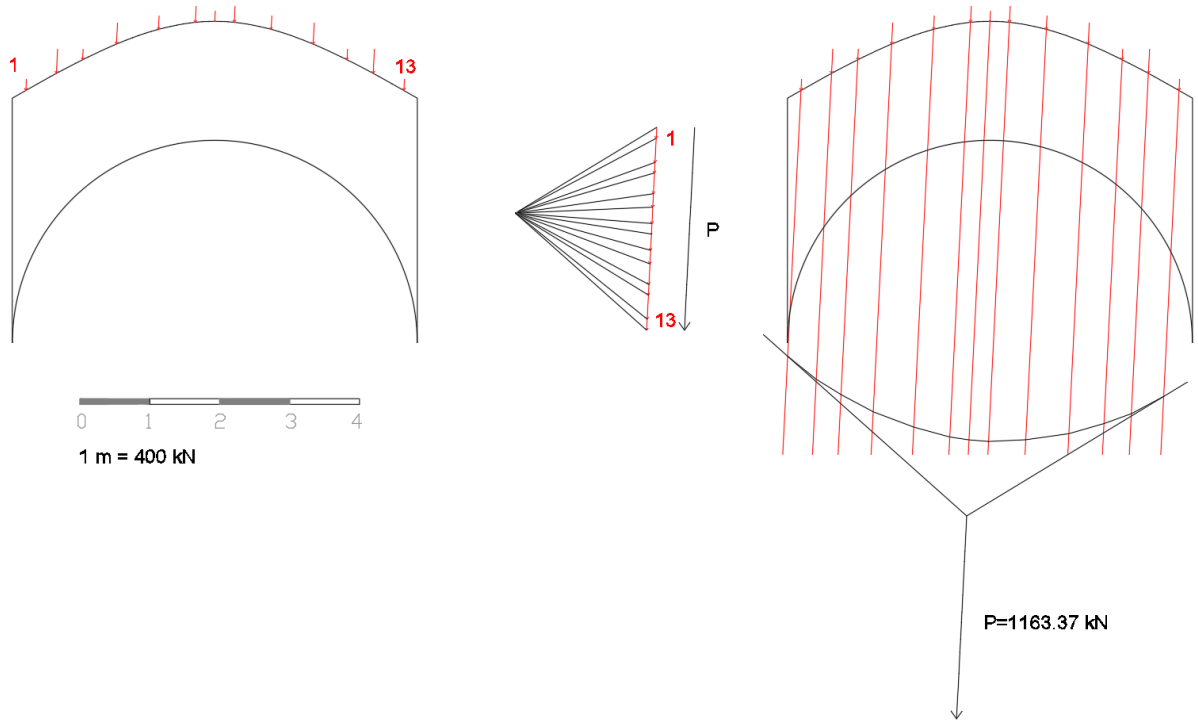

Fig. A. 102- Force polygon and funicular polygon of the cross vault (B) - seismic direction (-) (1)

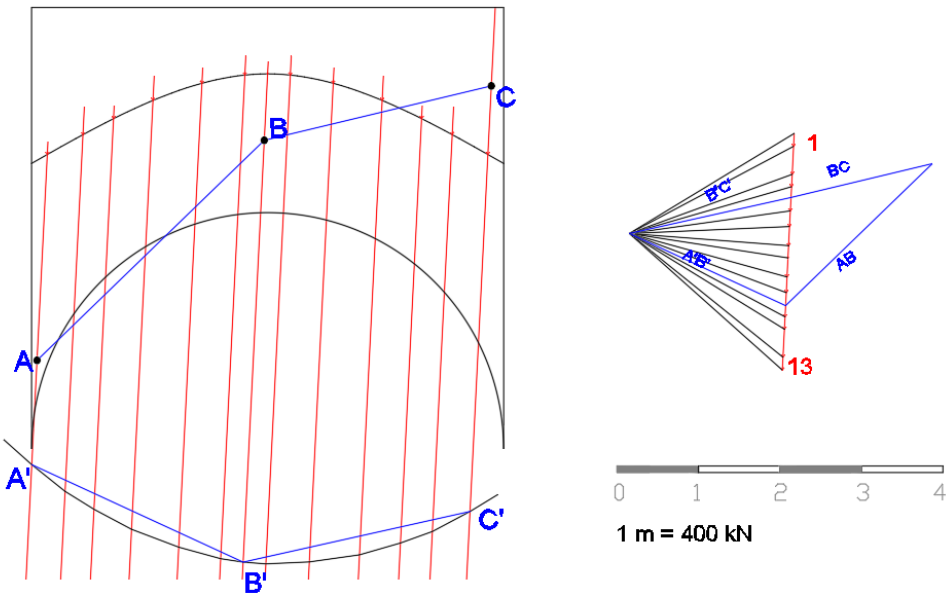

Fig. A. 103- Force polygon and funicular polygon of the cross vault (B) - seismic direction (-) (2)

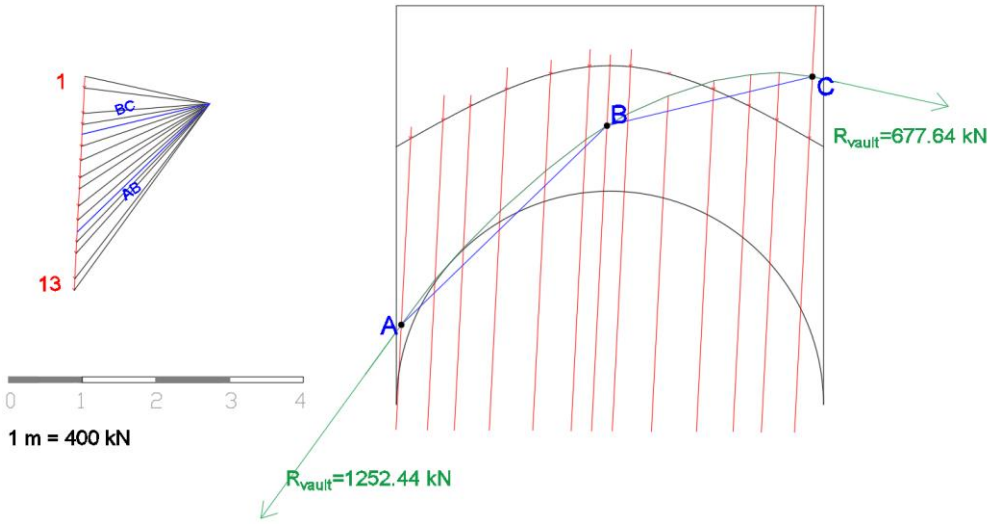

Fig. A. 104- Thrust line in the cross vault (B) - seismic direction (-)

- Seismic direction (+)

The previous passages are repeated for the other case with seismic direction (+).

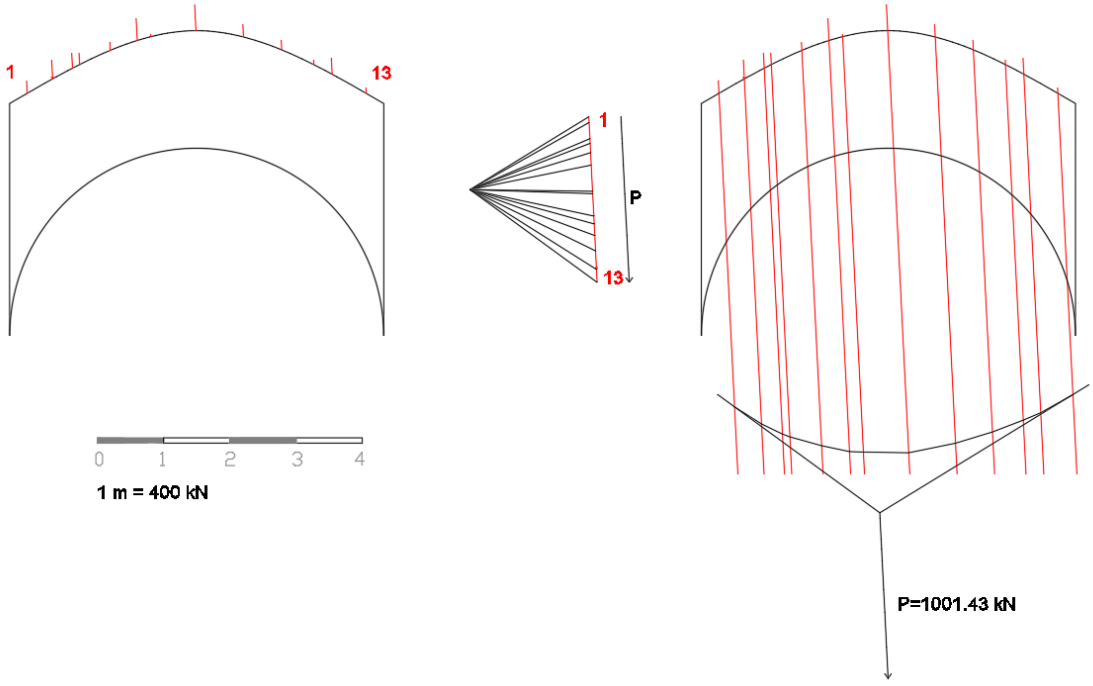

Fig. A. 105- Force polygon and funicular polygon of the cross vault (A) - seismic direction (+) (1)

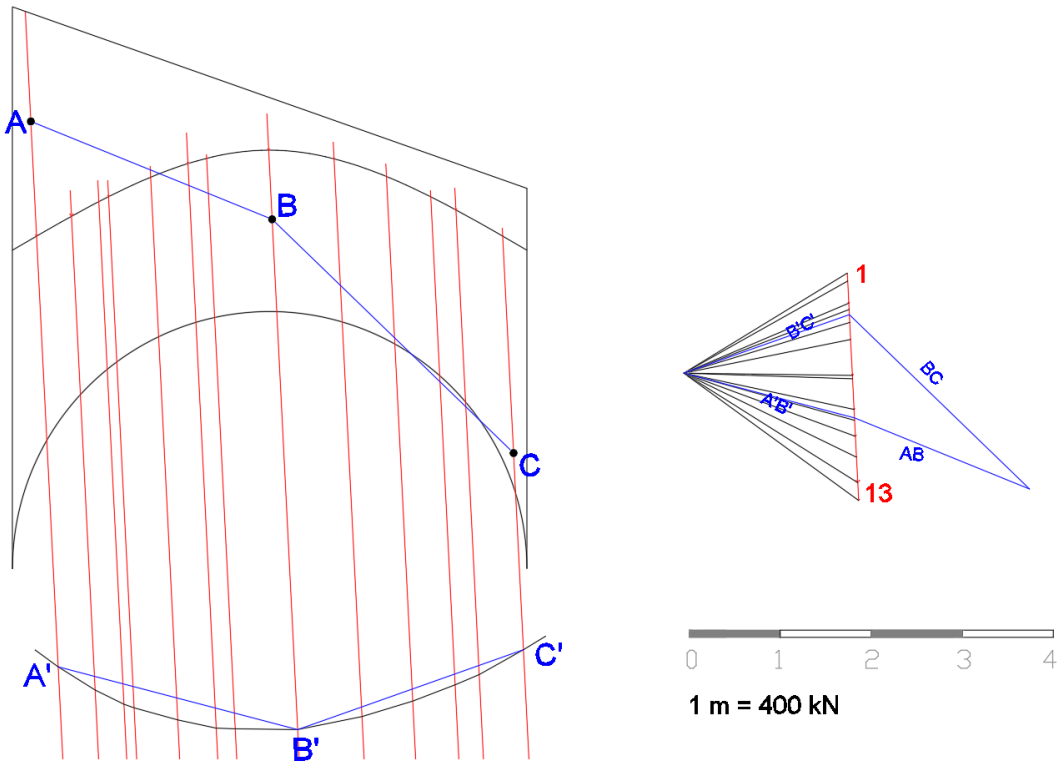

Fig. A. 106- Force polygon and funicular polygon of the cross vault (A) - seismic direction (+) (2)

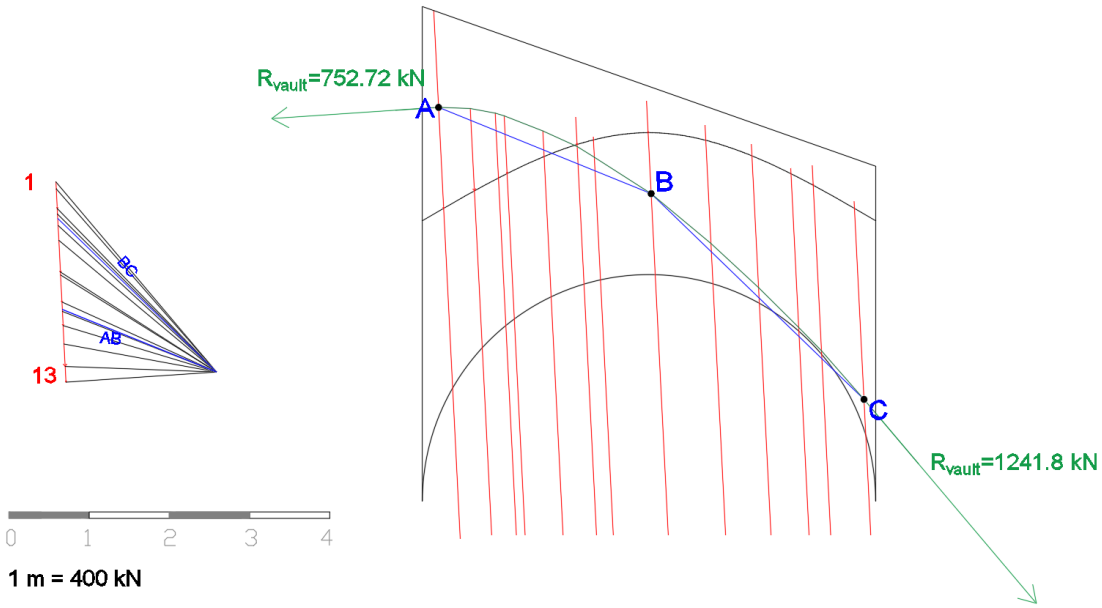

Fig. A. 107- Thrust line in the cross vault (A) - seismic direction (+)

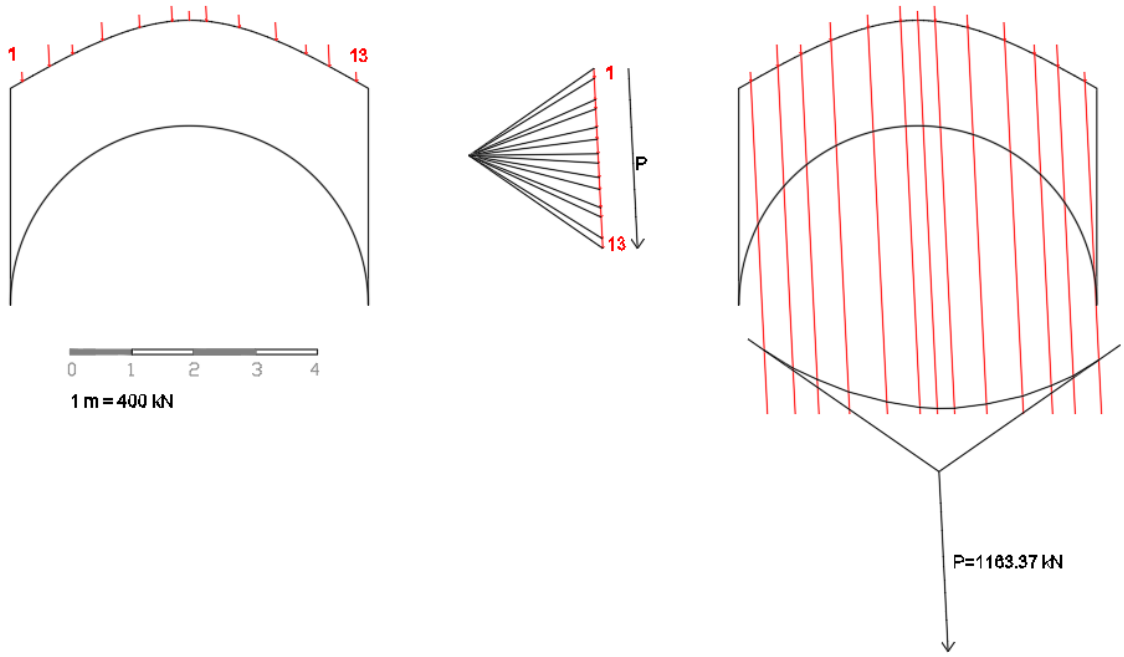

Fig. A. 108- Force polygon and funicular polygon of the cross vault (B) - seismic direction (+) (1)

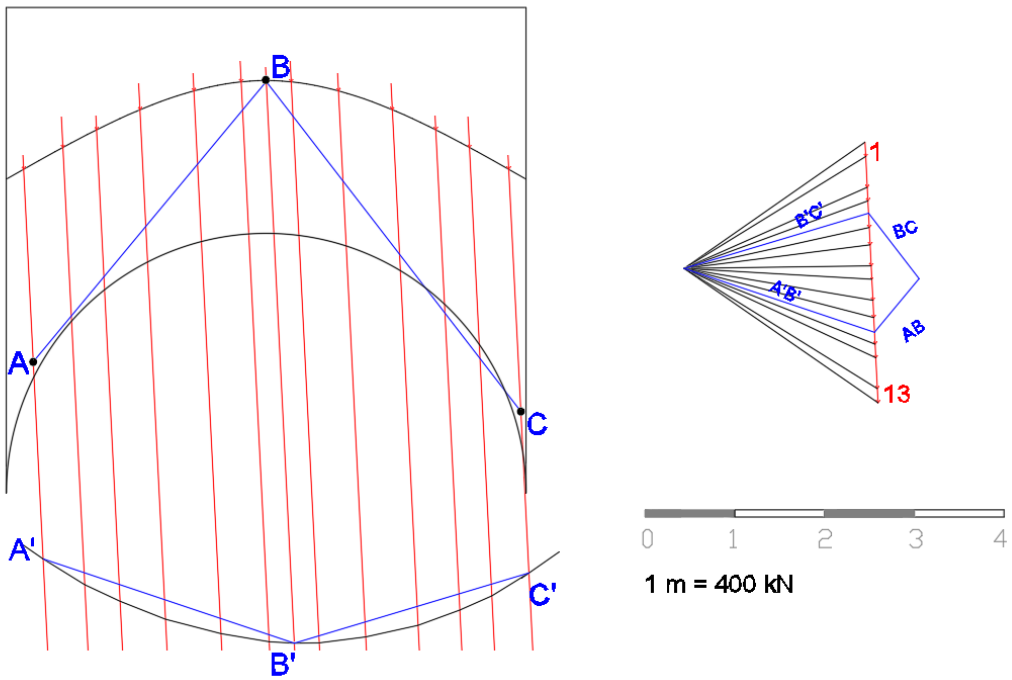

Fig. A. 109- Force polygon and funicular polygon of the cross vault (B) - seismic direction (+) (2)

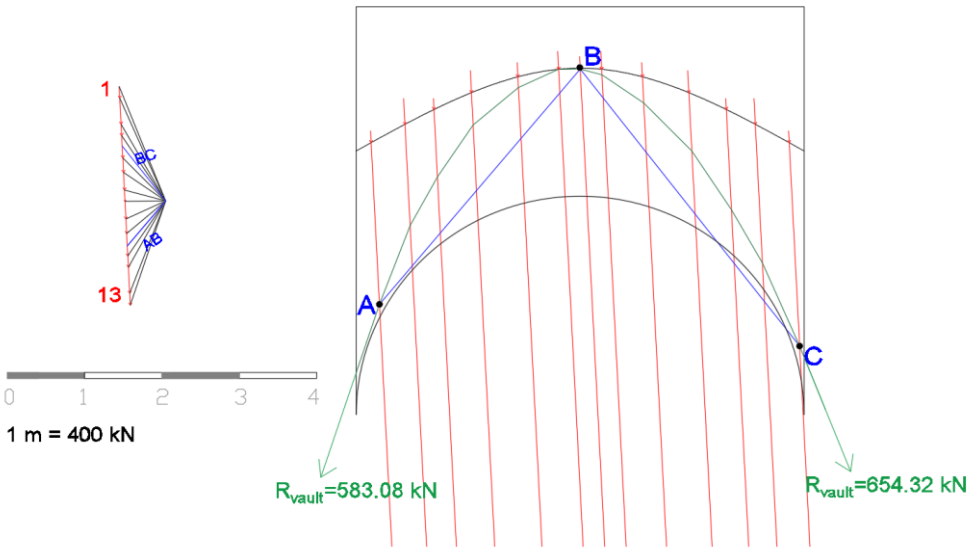

Fig. A. 110- Thrust line in the cross vaul (B) - seismic direction (+)

FLYING ARCH

- Seismic direction (-)

First of all, a horizontal force is added to each force. Then the force polygon and the funicular polygon have been realized.

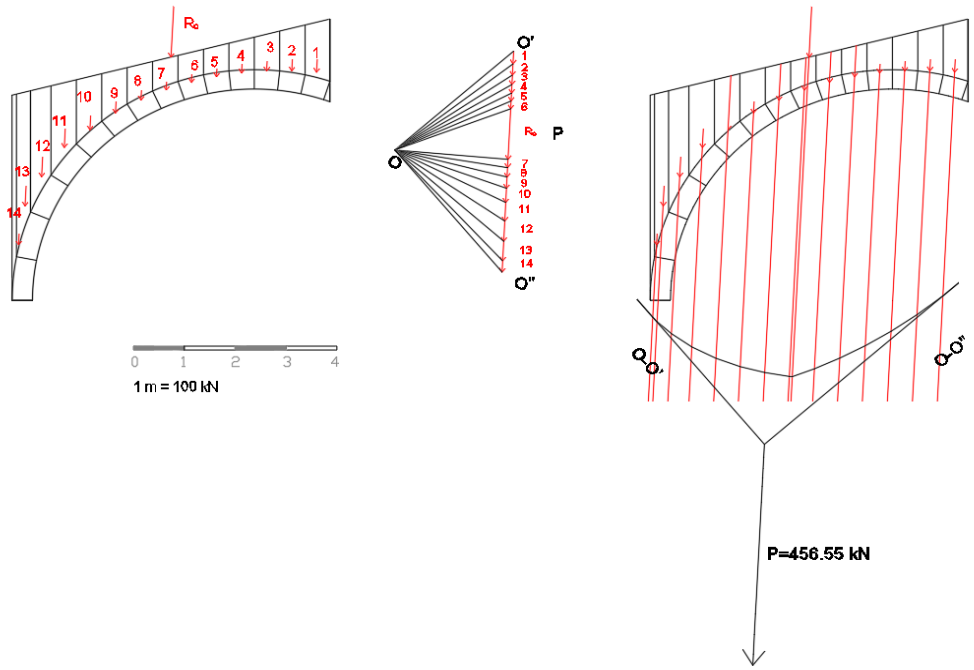

Fig. A. 111- Force vectors, force polygon and funicular polygon in the flying arch - seismic direction (-)

So it's possible to find a thrust in the cross vault supposing the passage of the thrust line for three points (A, B, C); the choice of these points is linked to the thrust line that is generated in the structure:

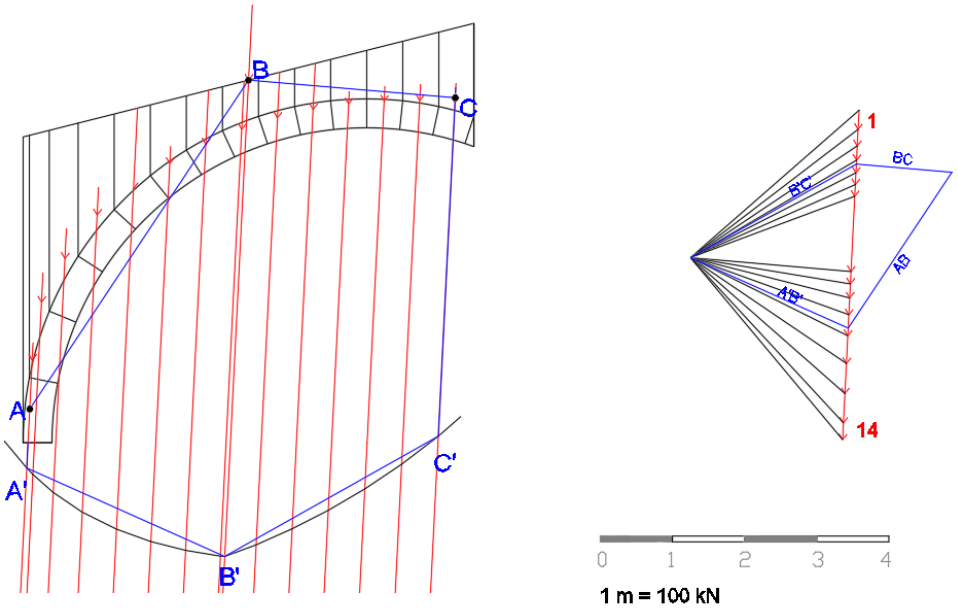

Fig. A. 112- Force polygon and funicular polygon in the flying arch - seismic direction (-)

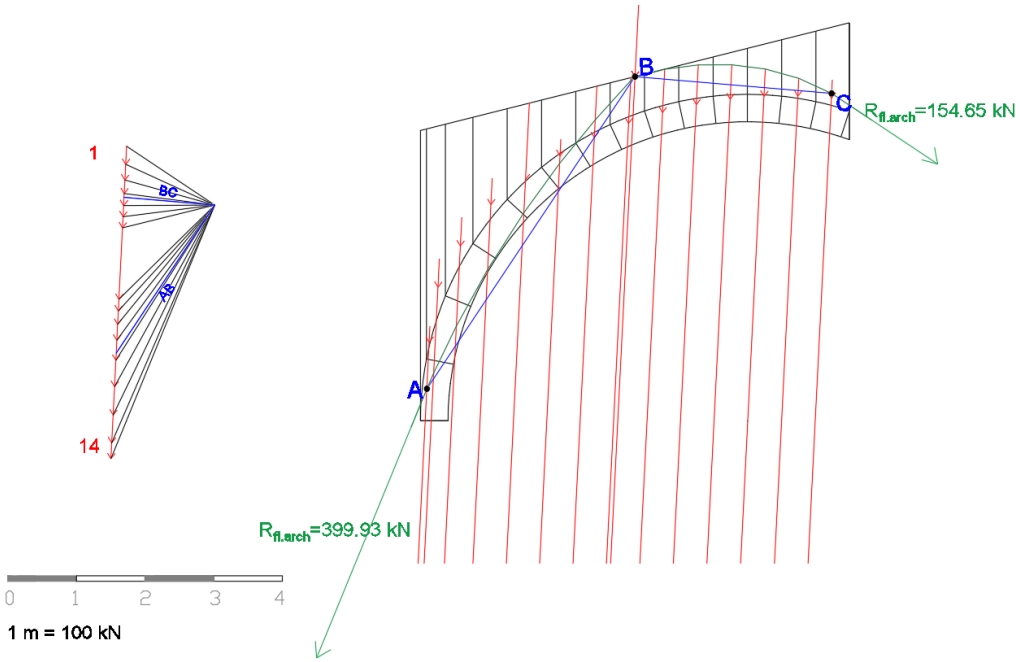

Fig. A. 113- Thrust line in the flying arch - seismic direction (-)

- Seismic direction (+)

The previous passages are repeated for the other case with seismic direction (+).

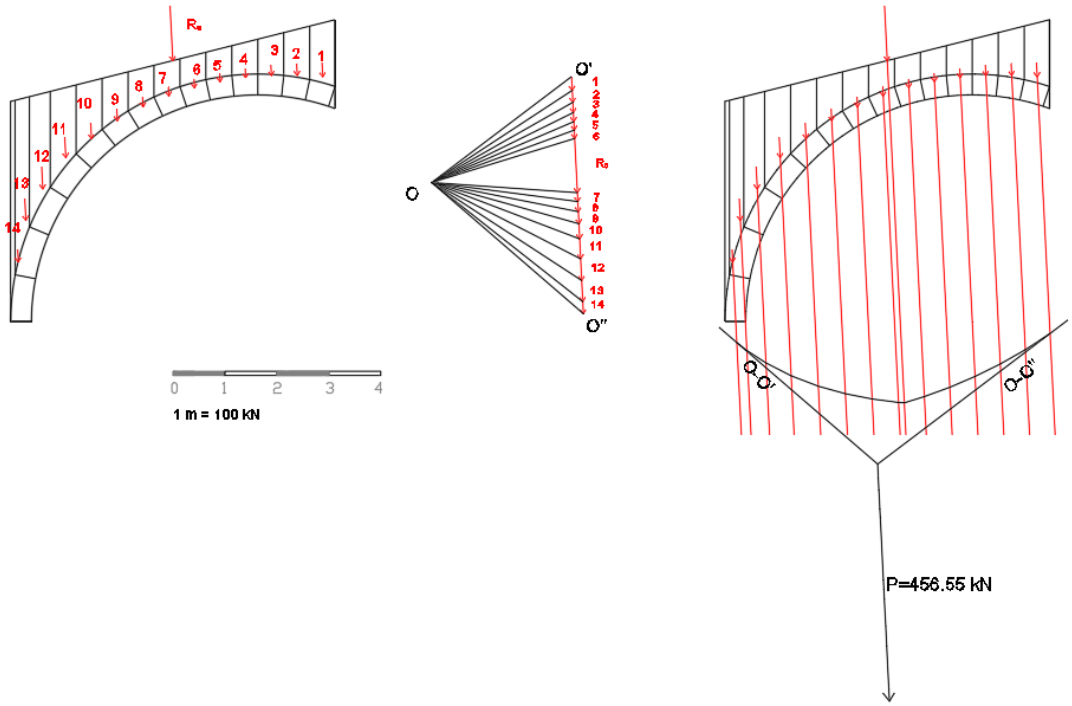

Fig. A. 114- Force vectors, force polygon and funicular polygon in the flying arch - seismic direction (+)

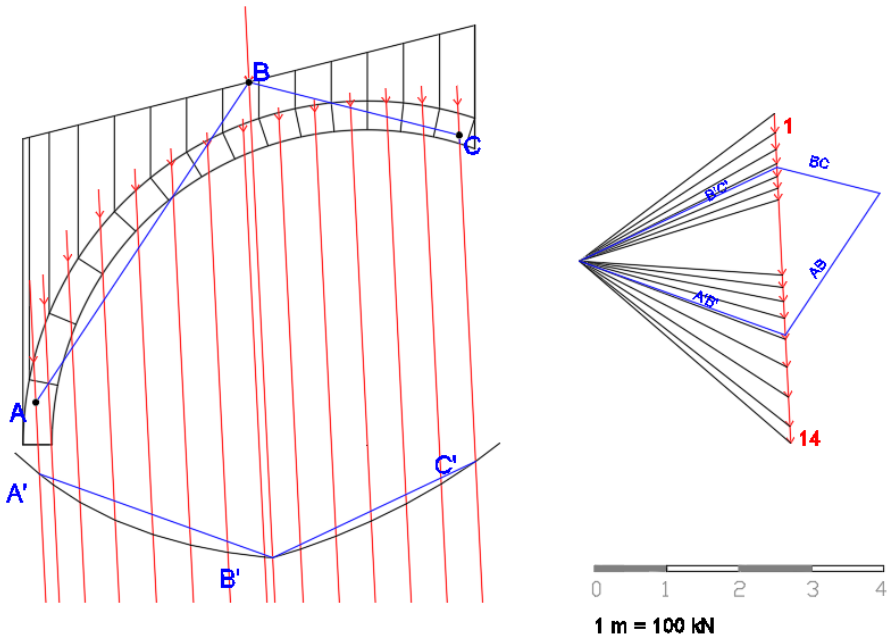

Fig. A. 115- Force polygon and funicular polygon in the flying arch - seismic direction (+)

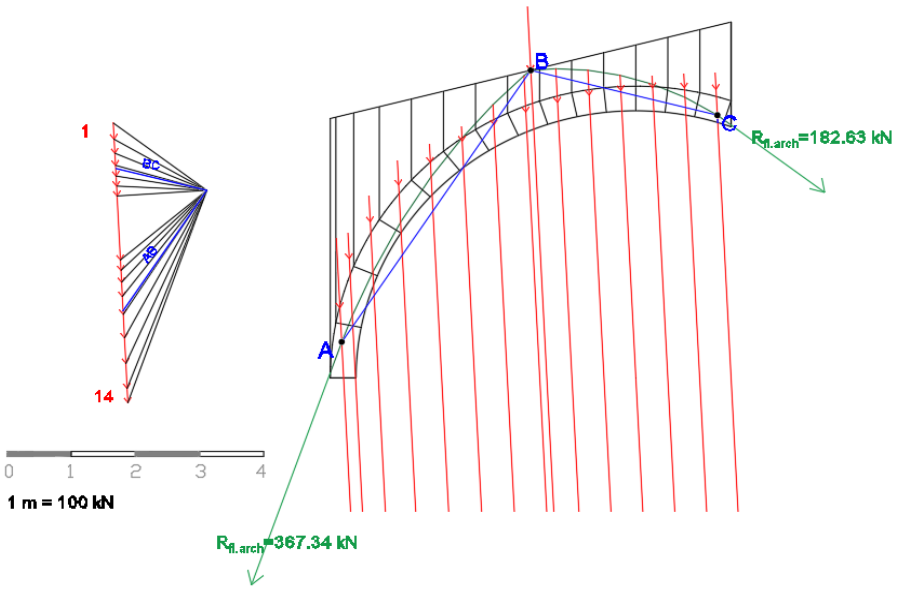

Fig. A. 116- Thrust line in the flying arch - seismic direction (+)

THRUST LINE OF THE STRUCTURE

- Seismic direction (-)

In the following figure, with the force polygon the resultant R1 is found. This is obtained from the sum of the reaction of the barrel vault, the weight of the block 1 and the reaction of the roof.

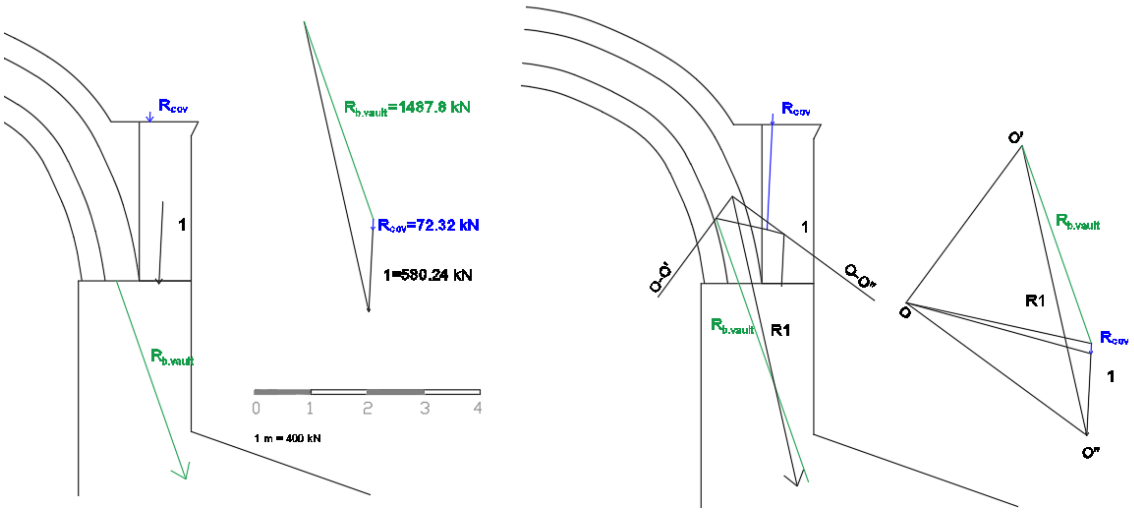

Fig. A. 117-Thrust line in the structure - seismic direction (-) (1)

Here is the application of the parallelogram rule with the block of the pillars, the sum of the resultant with the reaction of the cross vault and then the sum with the reaction of longitudinal arch; finally, the final part of the pillar.

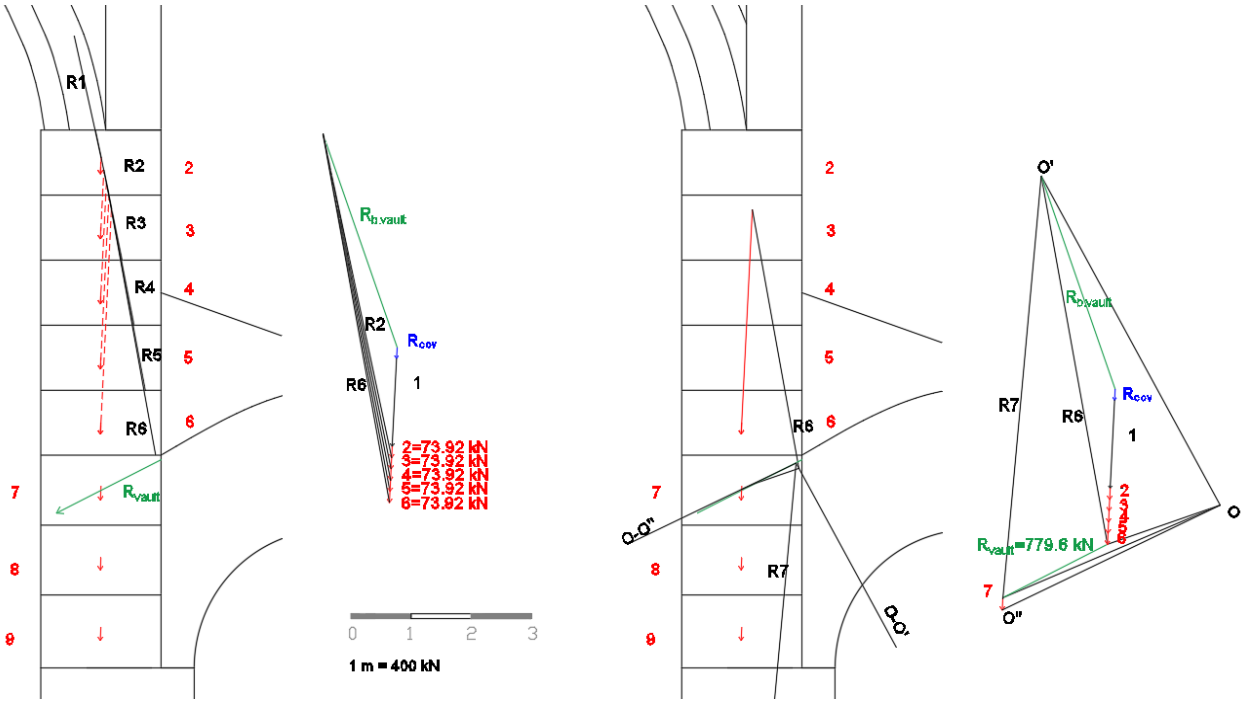

Fig. A. 118- Thrust line in the structure - seismic direction (-) (2)

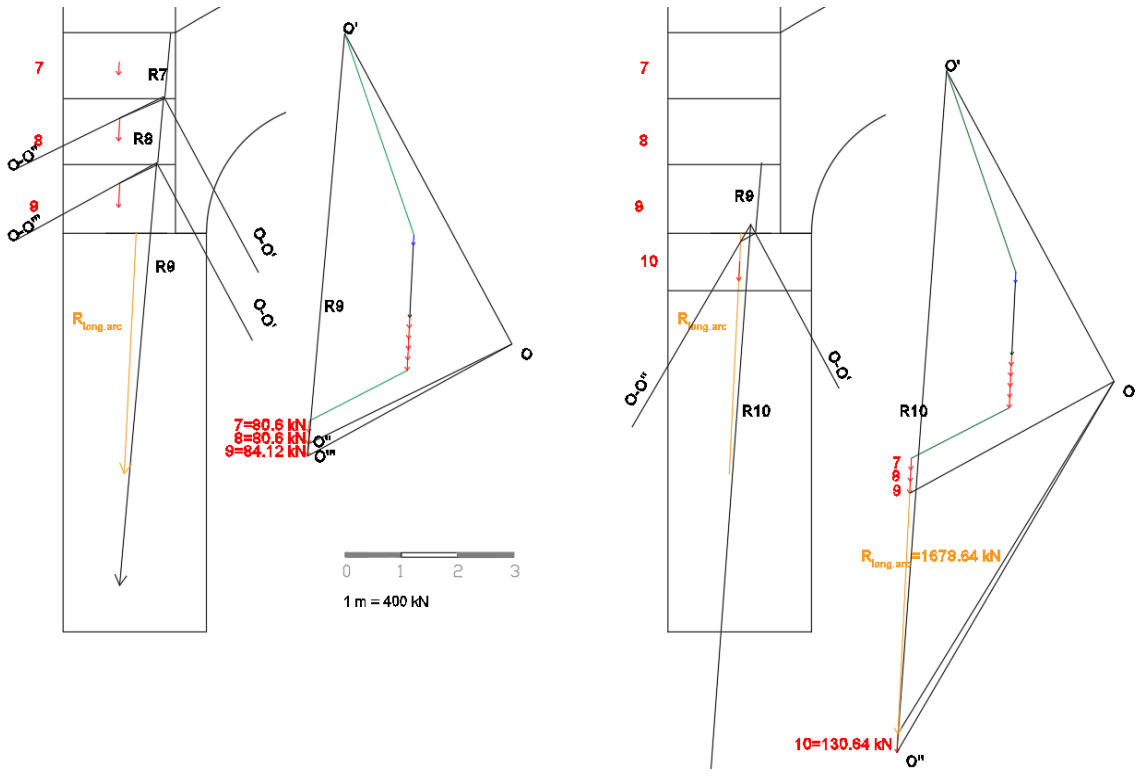

Fig. A. 119- Thrust line in the structure - seismic direction (-) (3)

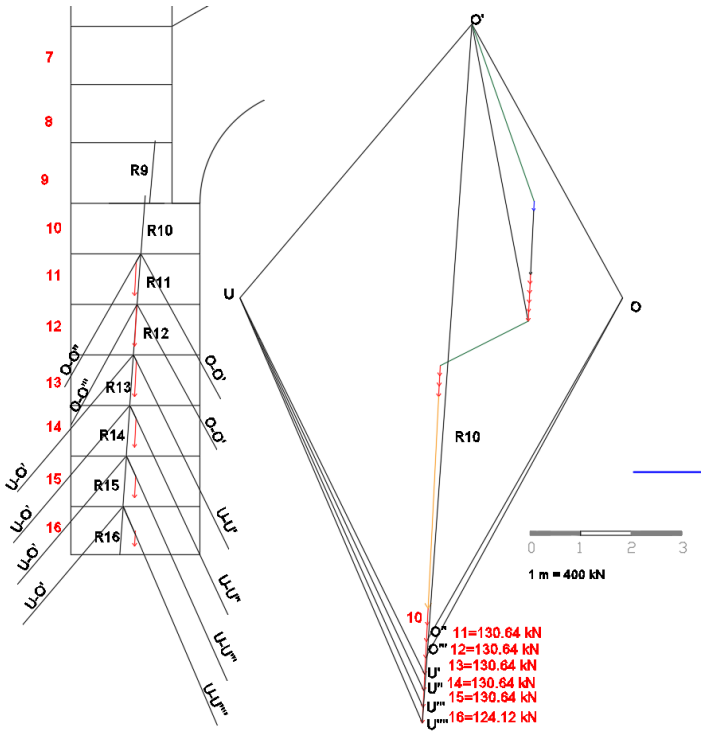

Fig. A. 120- Thrust line in the structure - seismic direction (-) (4)

Here the right side is analyzed, starting from the resultant R1 summing the reaction of the cross vault, the blocks of the wall (1A and 1B) and the reaction of the roof with force polygon. Then, the resultant is summing with the weight force of the wall.

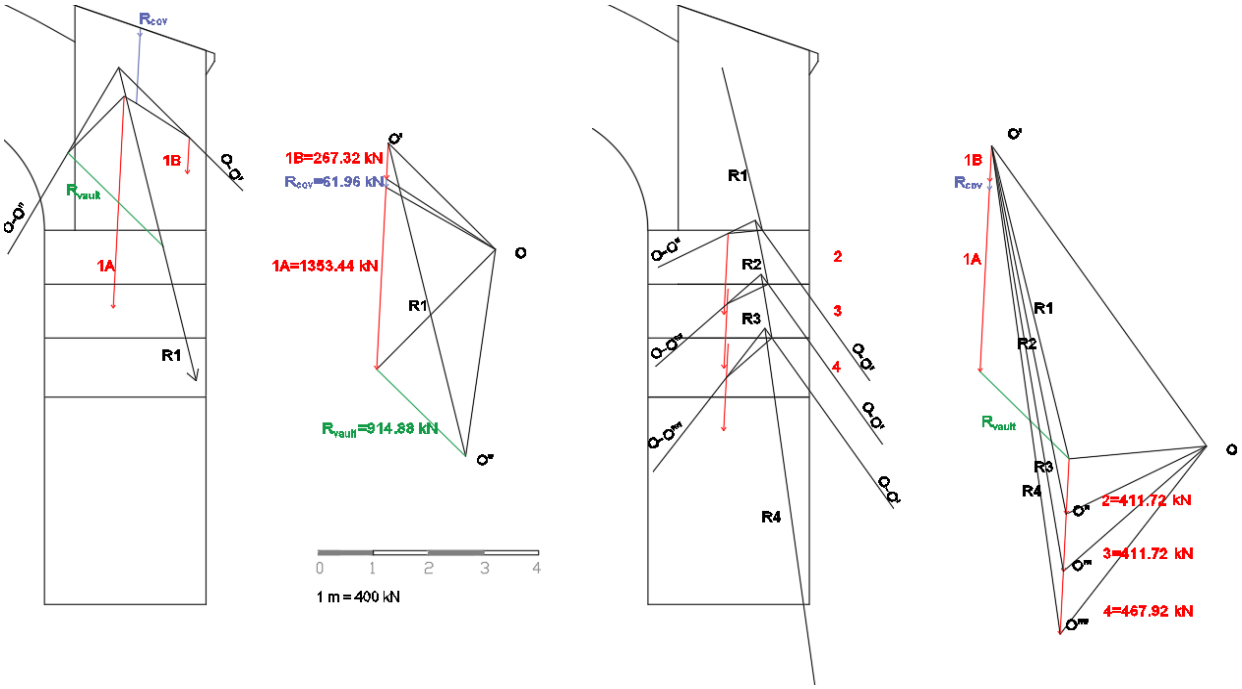

Fig. A. 121- Thrust line in the structure - seismic direction (-) (5)

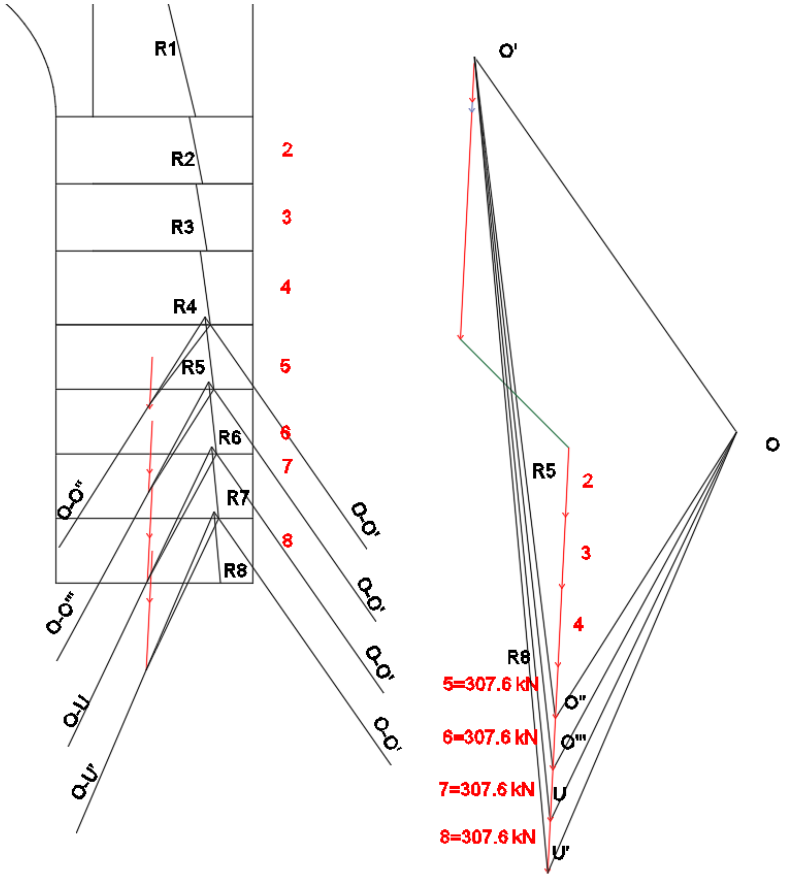

Fig. A. 122- Thrust line in the structure - seismic direction (-) (6)

The procedure is repeated on the left side, starting from the resultant R1 which is obtained adding the reaction of the barrel vault, the reaction of the flying arch, the weight of the block 1 of the wall and the reactions of the roofs.

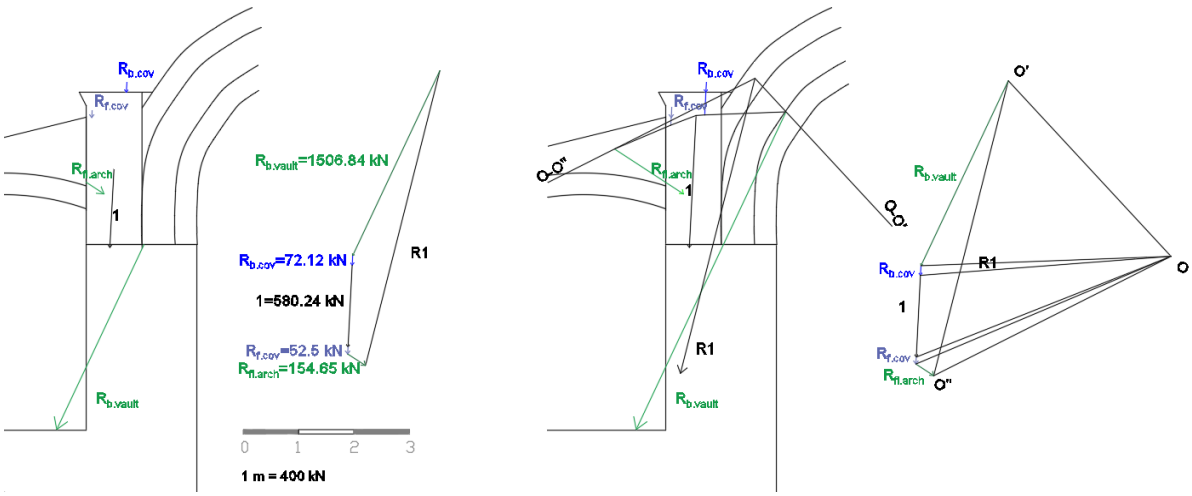

Fig. A. 123- Thrust line in the structure - seismic direction (-) (7)

Here the parallelogram rule is applied between the R1 and 2, and then it's repeated. After, the reactions of the cross vault and of the longitudinal are considered.

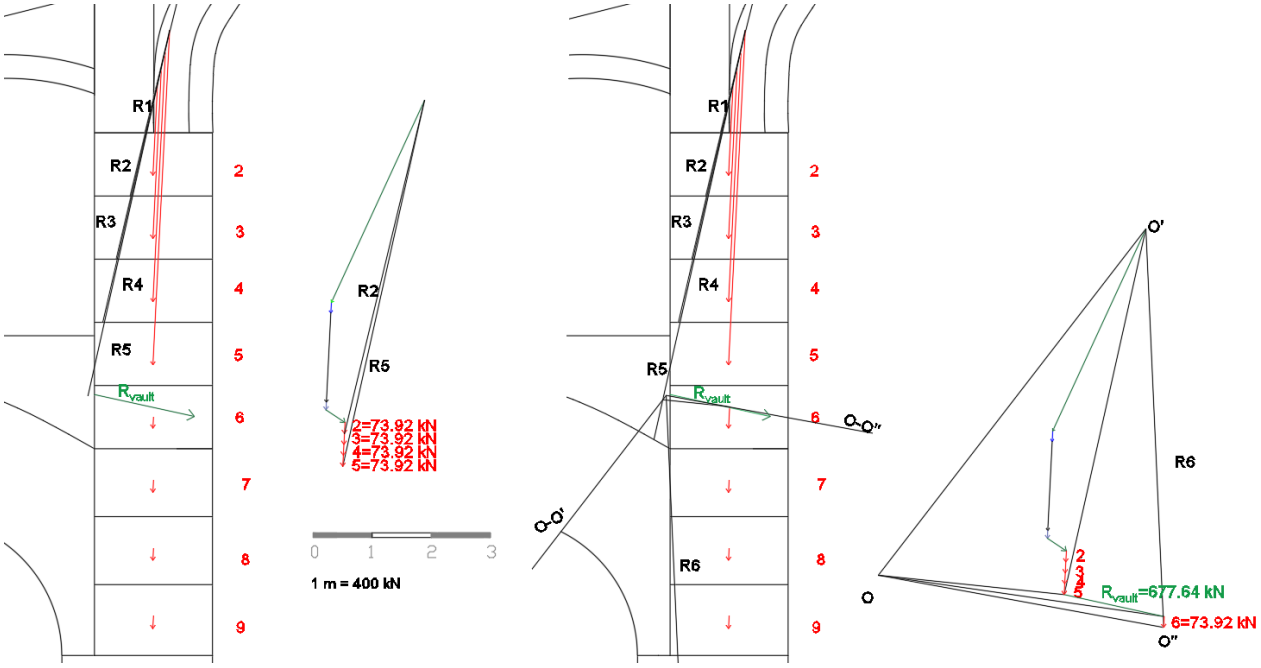

Fig. A. 124- Thrust line in the structure - seismic direction (-) (8)

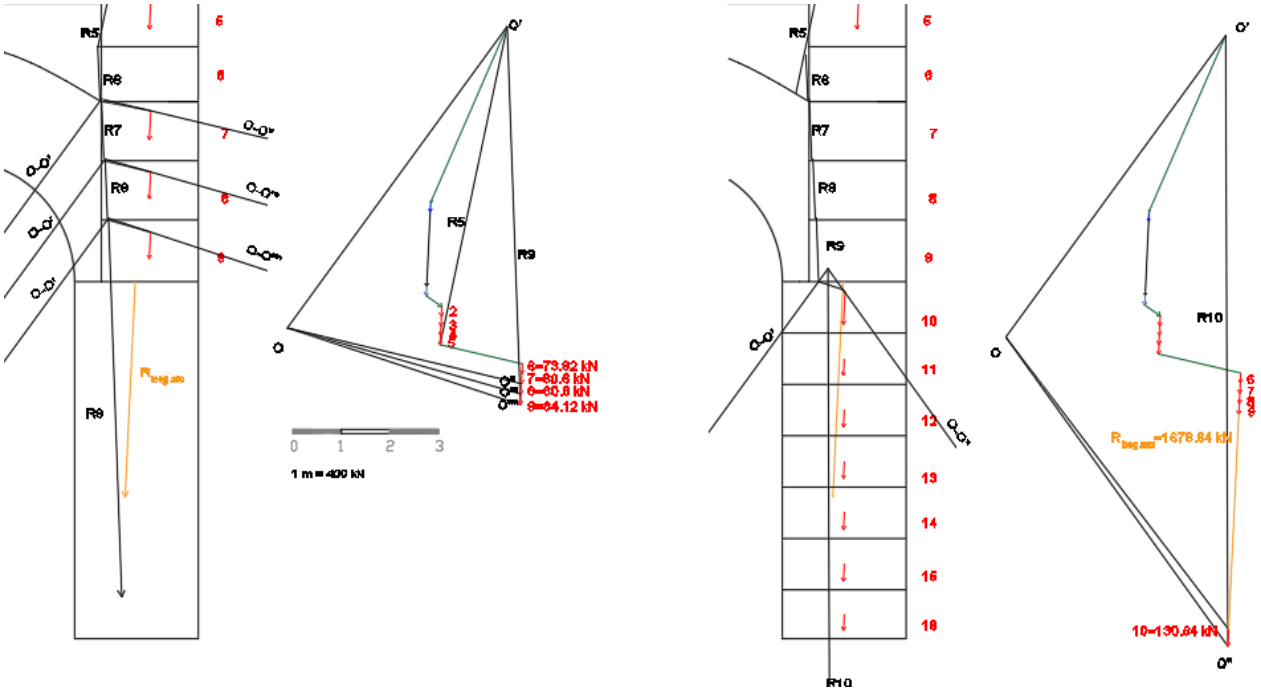

Fig. A. 125- Thrust line in the structure - seismic direction (-) (9)

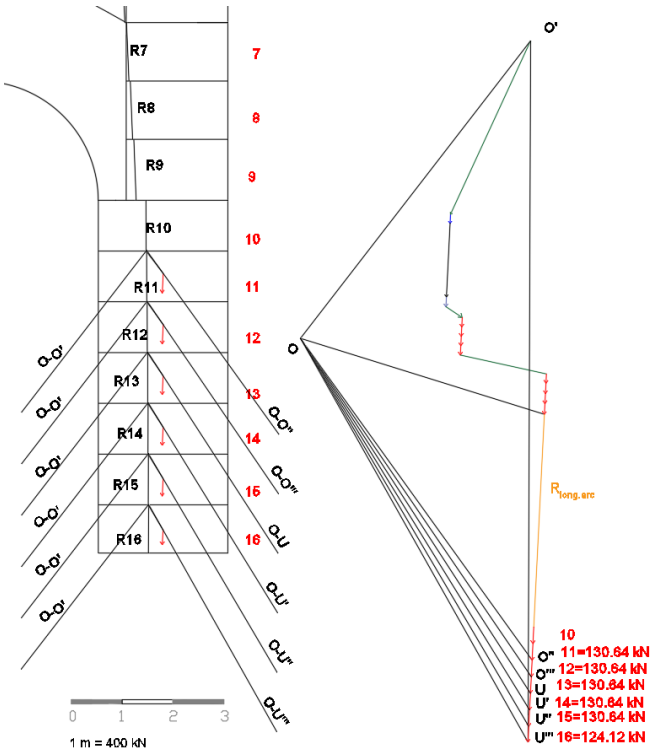

Fig. A. 126- Thrust line in the structure - seismic direction (-) (10)

So, the procedure continued at the left of the flying arch, starting from the resultant R1 which is obtained adding the reaction of the flying arch, the weights of the wall (1A and 1B) and the reaction of the roof.

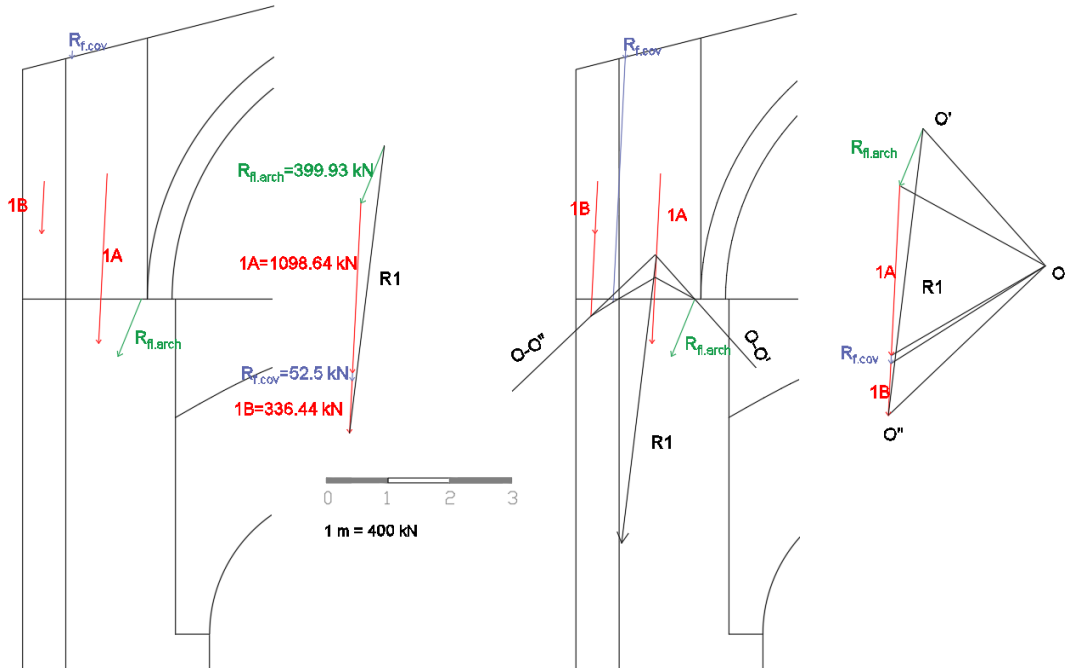

Fig. A. 127- Thrust line in the structure - seismic direction (-) (11)

Then, the parallelogram rule is applied until the block 5. So, a new resultant is calculated with the force polygon. Finally, it's over with the final part of the pillar.

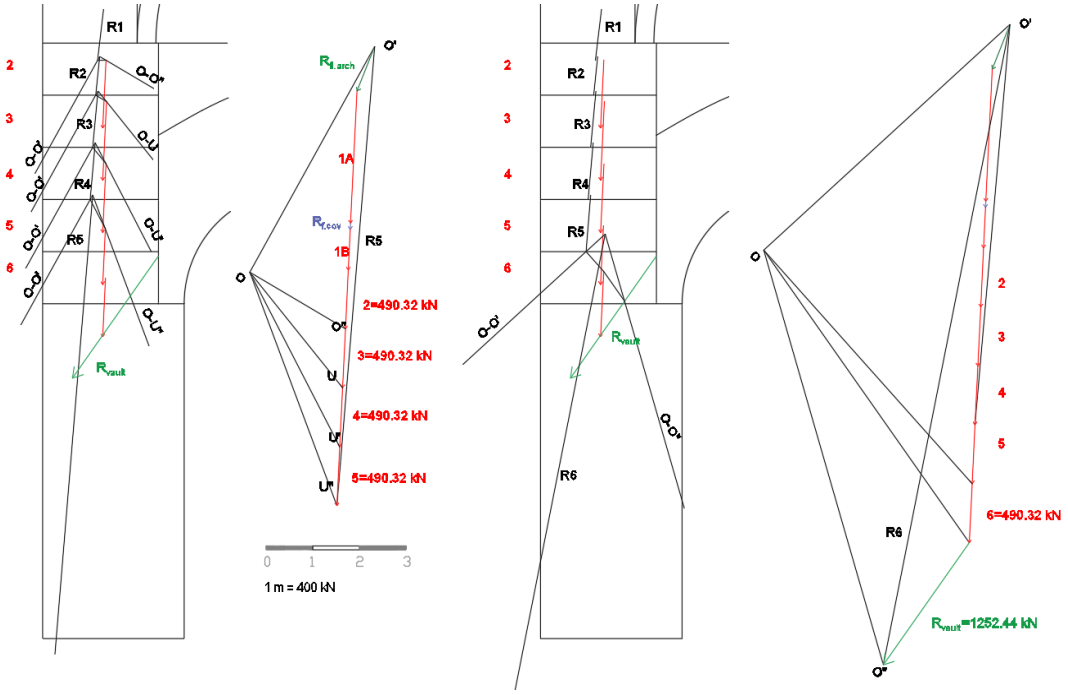

Fig. A. 128- Thrust line in the structure - seismic direction (-) (12)

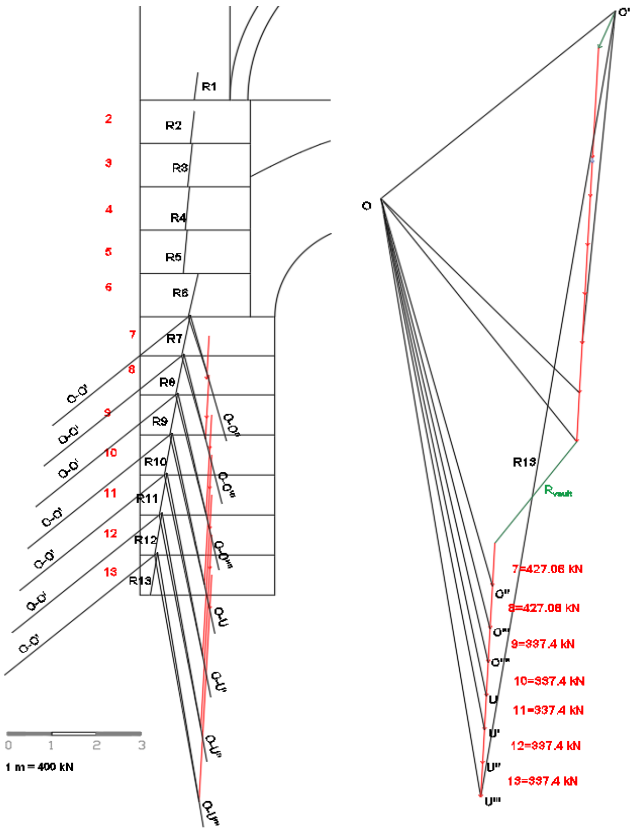

Fig. A. 129- Thrust line in the structure - seismic direction (-) (13)

Finally, the thrust line in the structure considering the seismic action in the left direction (-) can be drawn.

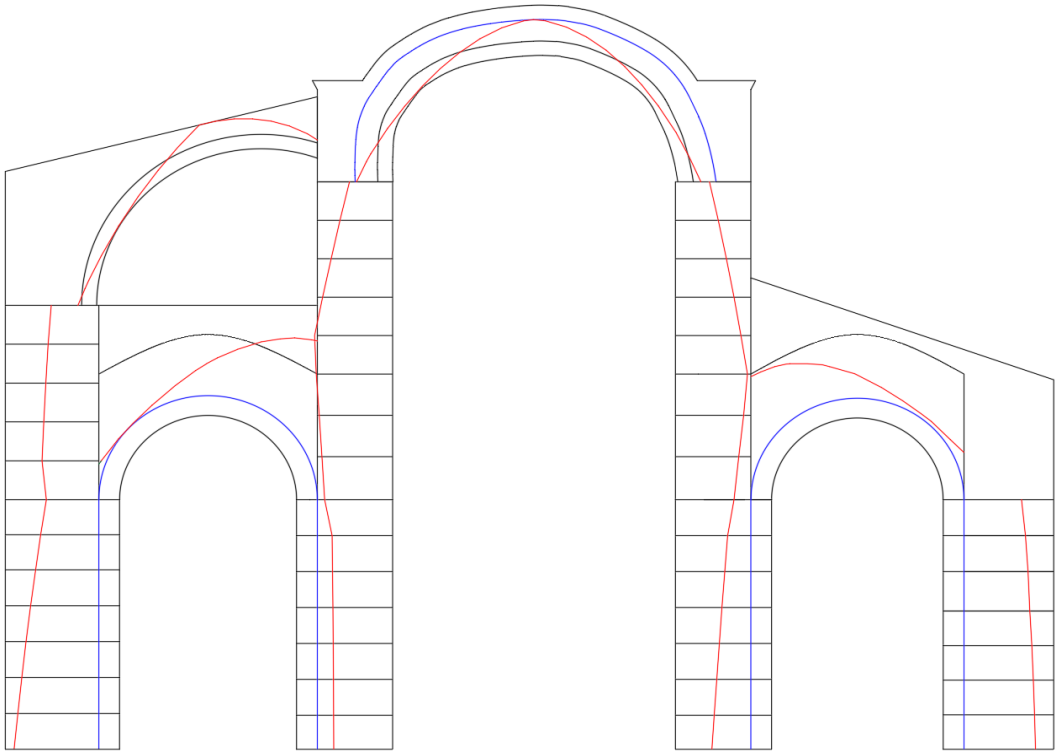

Fig. A. 130- Thrust line in the structure - seismic direction (-) (14)

- Seismic direction (+)

The previous passages are repeated for the other case with seismic direction (+).

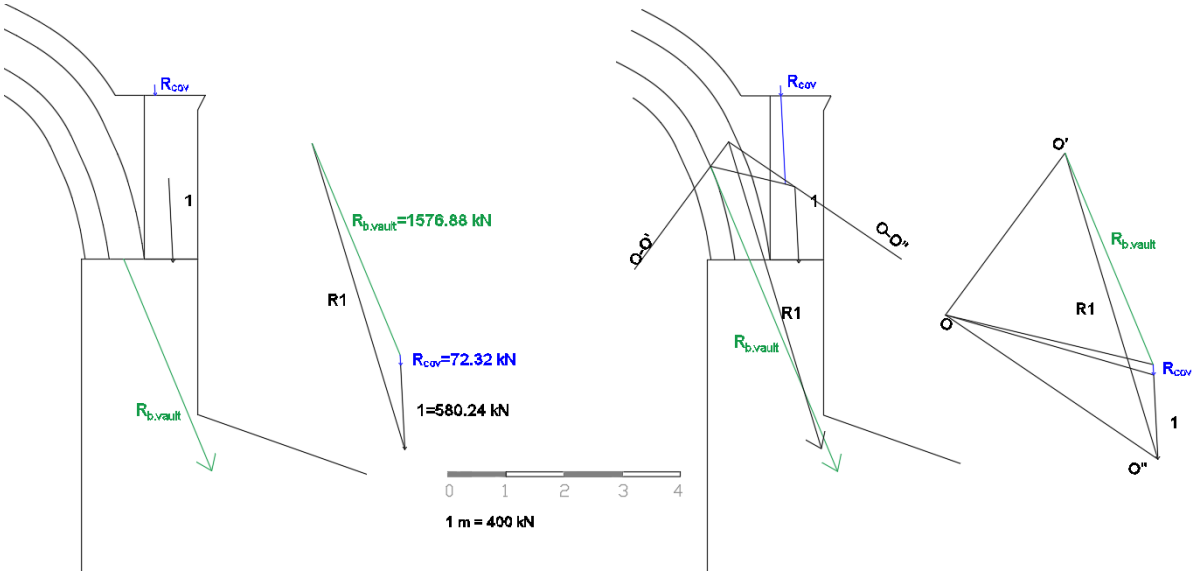

Fig. A. 131- Thrust line in the structure - seismic direction (+) (1)

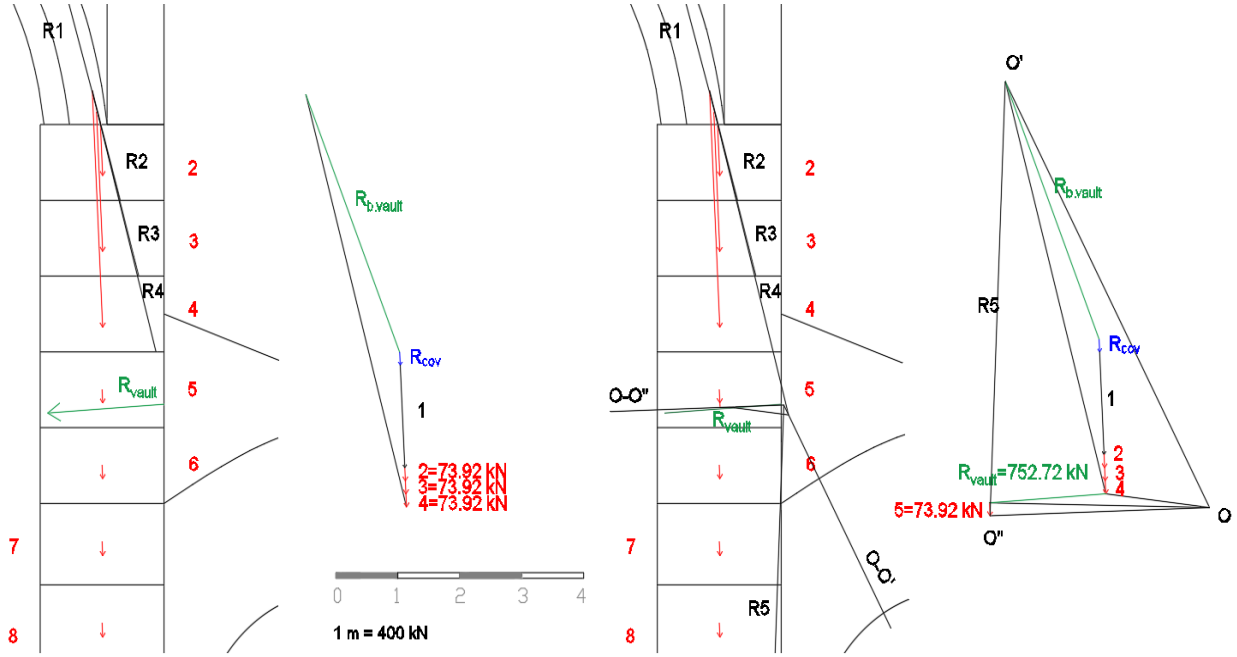

Fig. A. 132- Thrust line in the structure - seismic direction (+) (2)

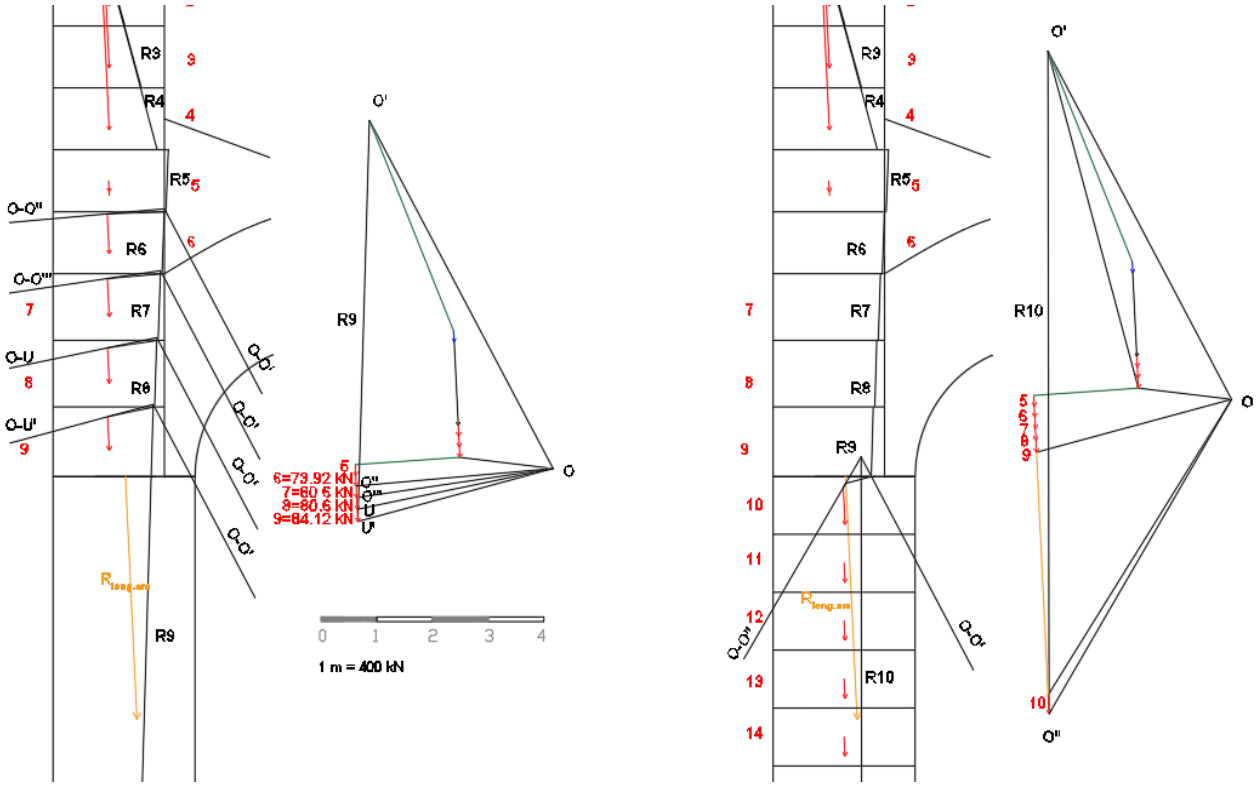

Fig. A. 133- Thrust line in the structure - seismic direction (+) (3)

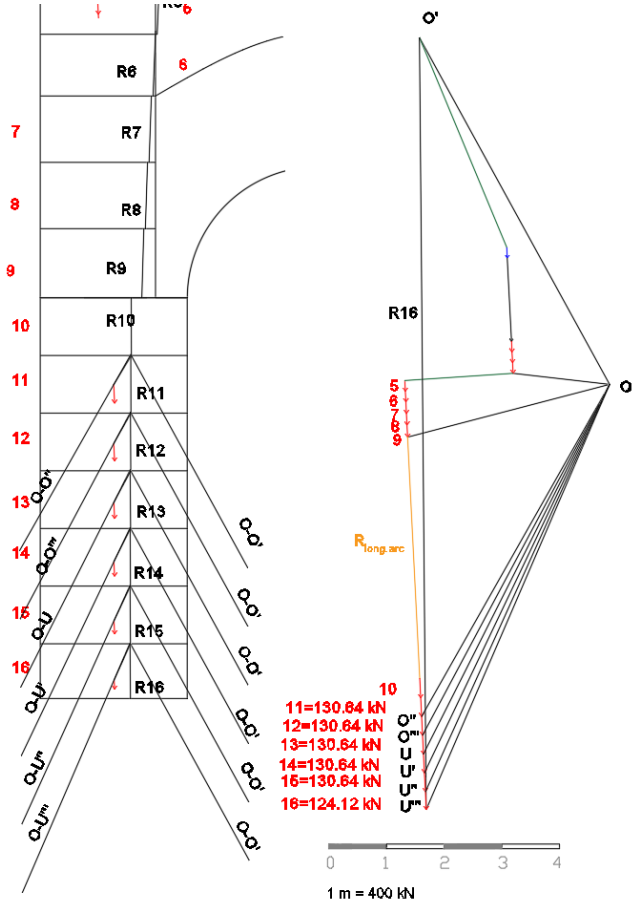

Fig. A. 134- Thrust line in the structure - seismic direction (+) (4)

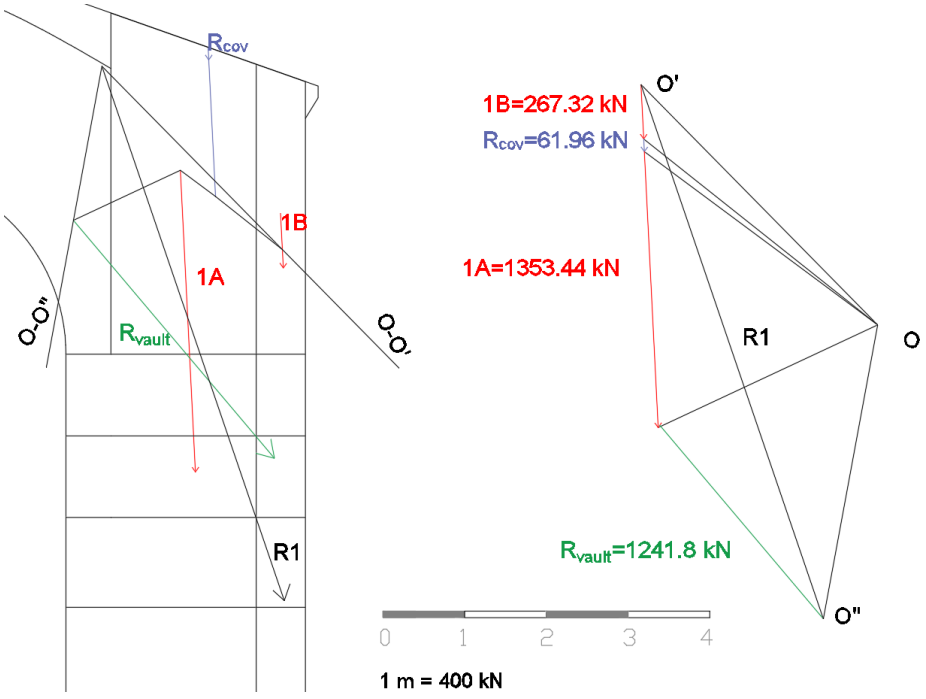

Fig. A. 135- Thrust line in the structure - seismic direction (+) (5)

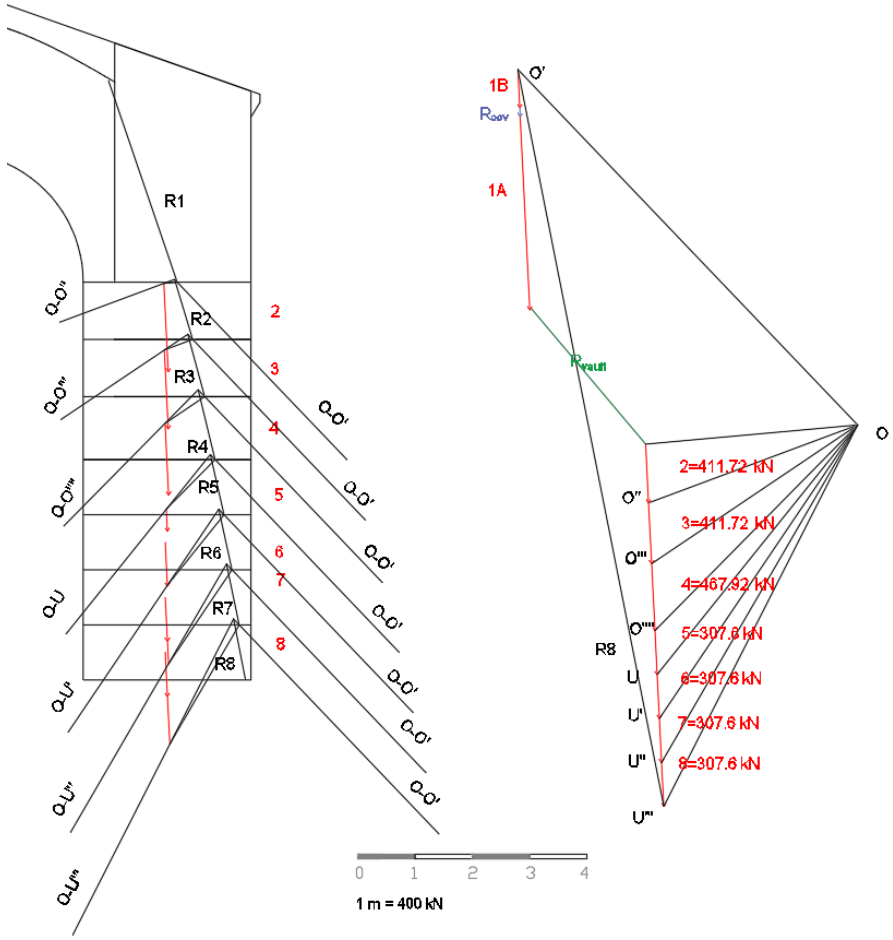

Fig. A. 136- Thrust line in the structure - seismic direction (+) (6)

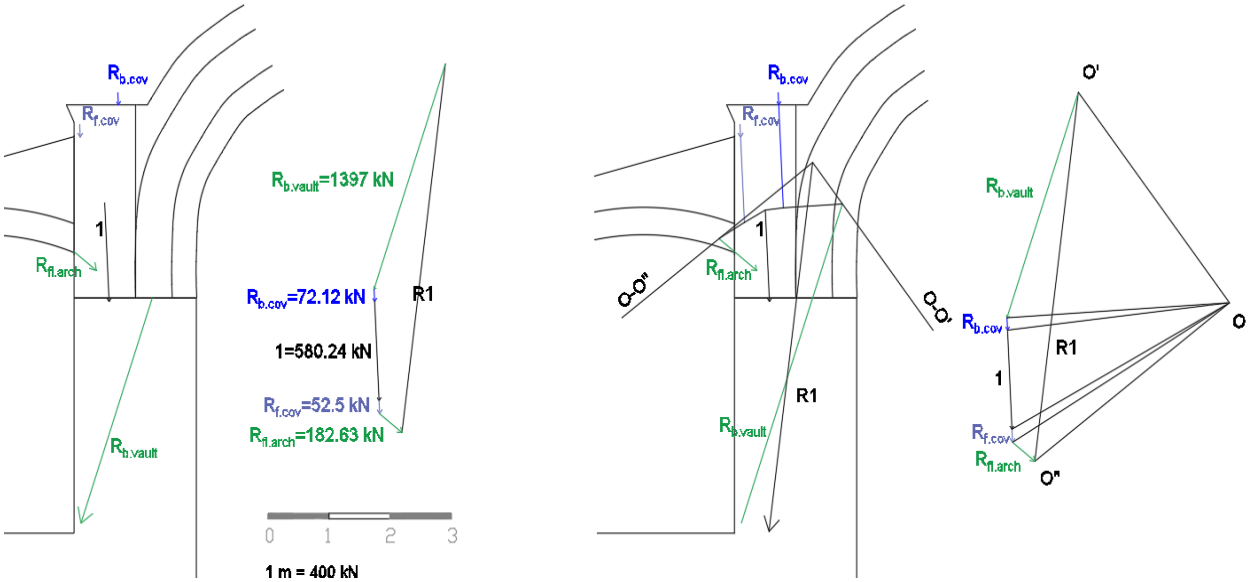

Fig. A. 137- Thrust line in the structure - seismic direction (+) (7)

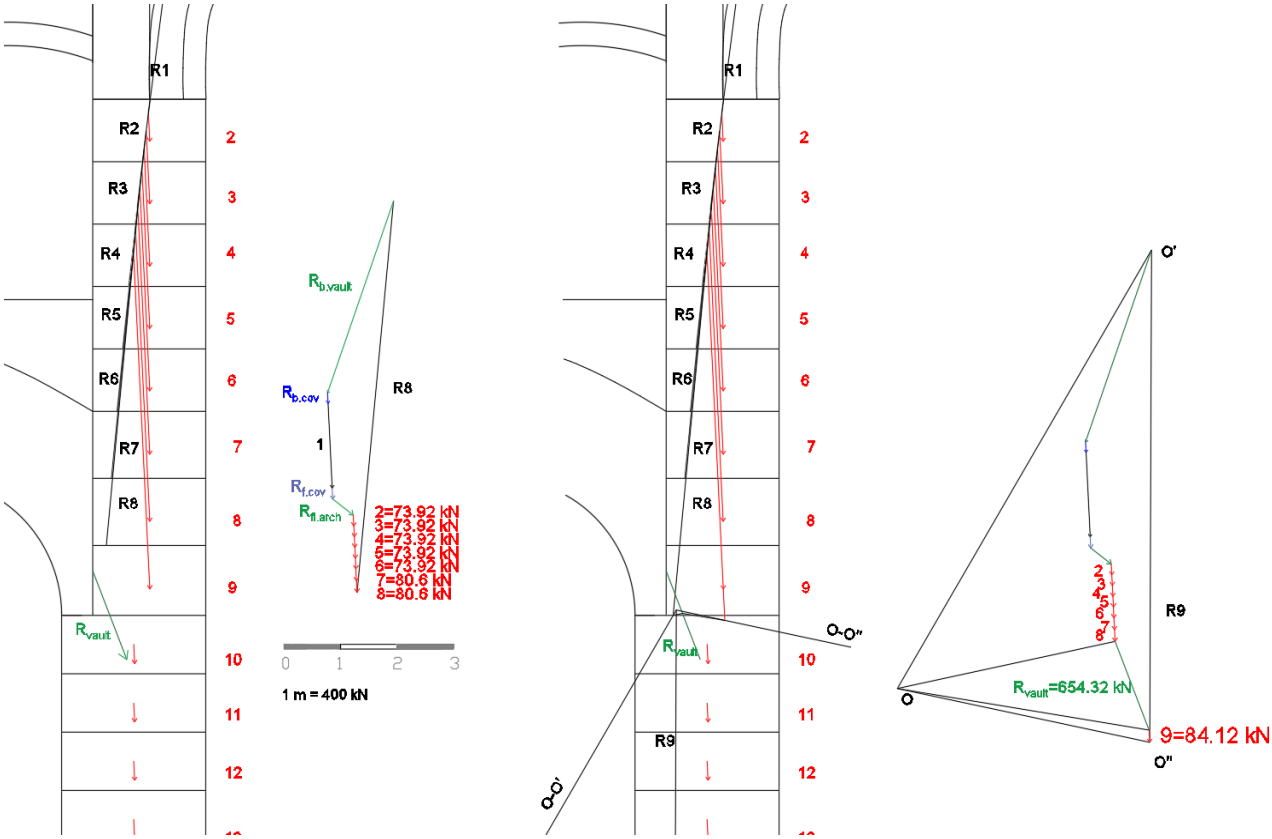

Fig. A. 138- Thrust line in the structure - seismic direction (+) (8)

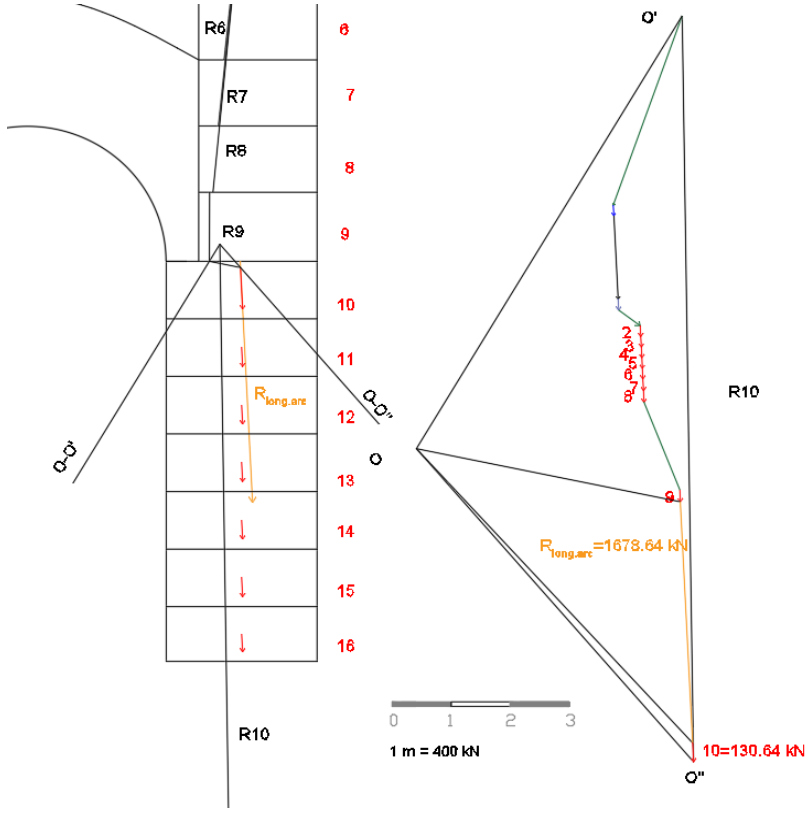

Fig. A. 139- Thrust line in the structure - seismic direction (+) (9)

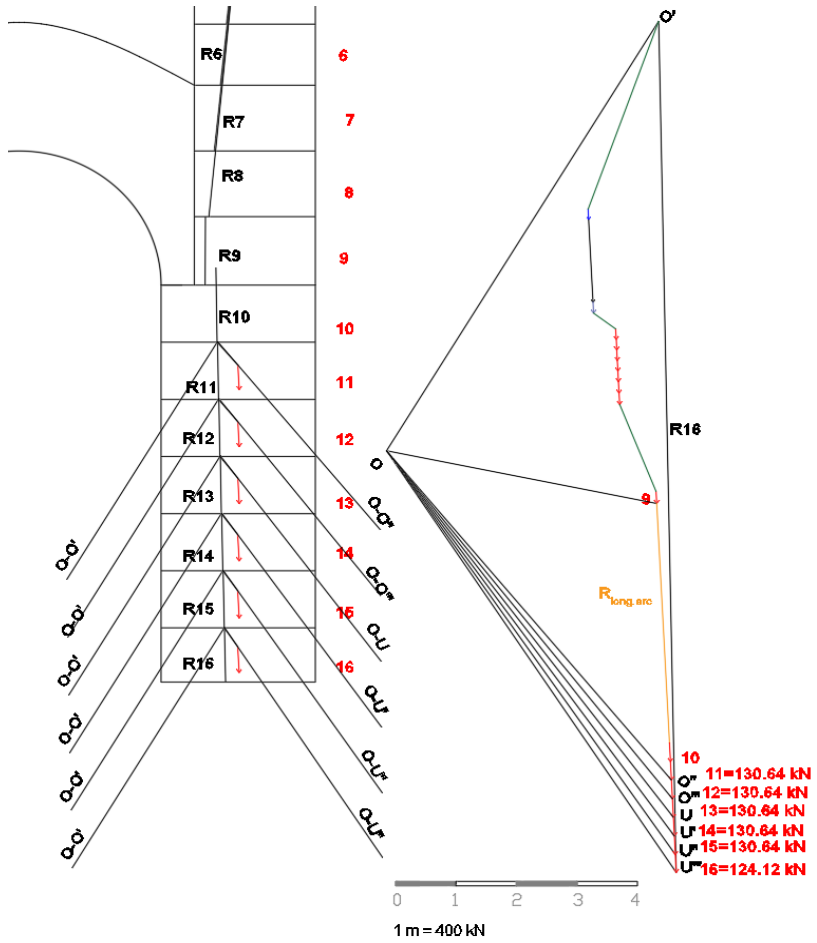

Fig. A. 140- Thrust line in the structure - seismic direction (+) (10)

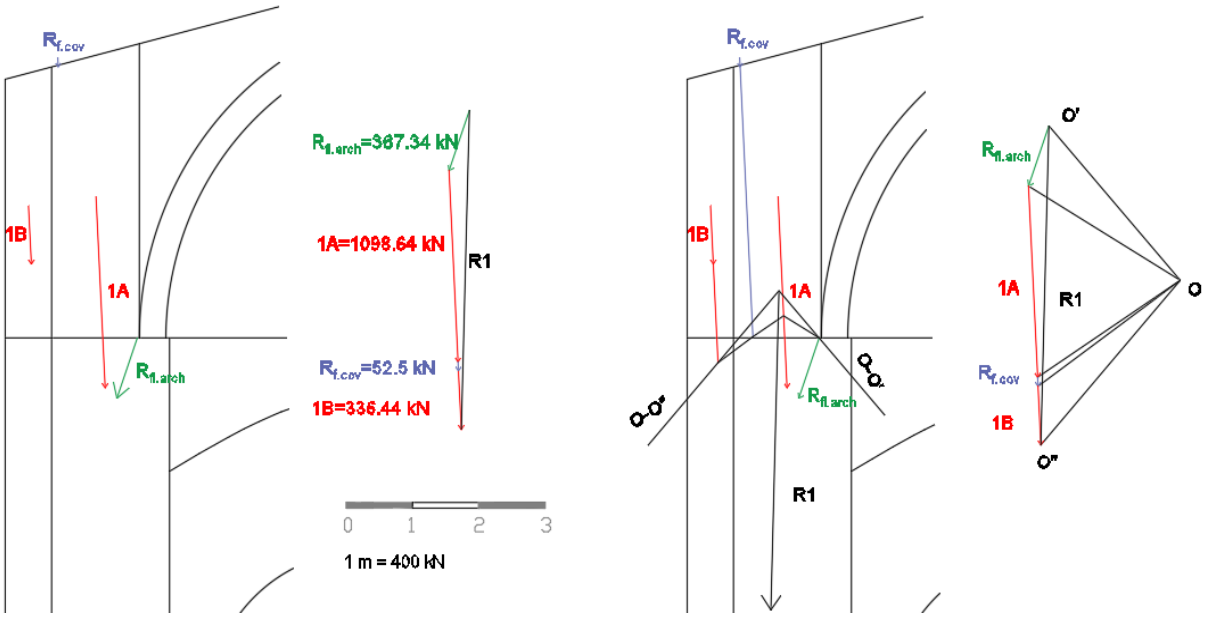

Fig. A. 141- Thrust line in the structure - seismic direction (+) (11)

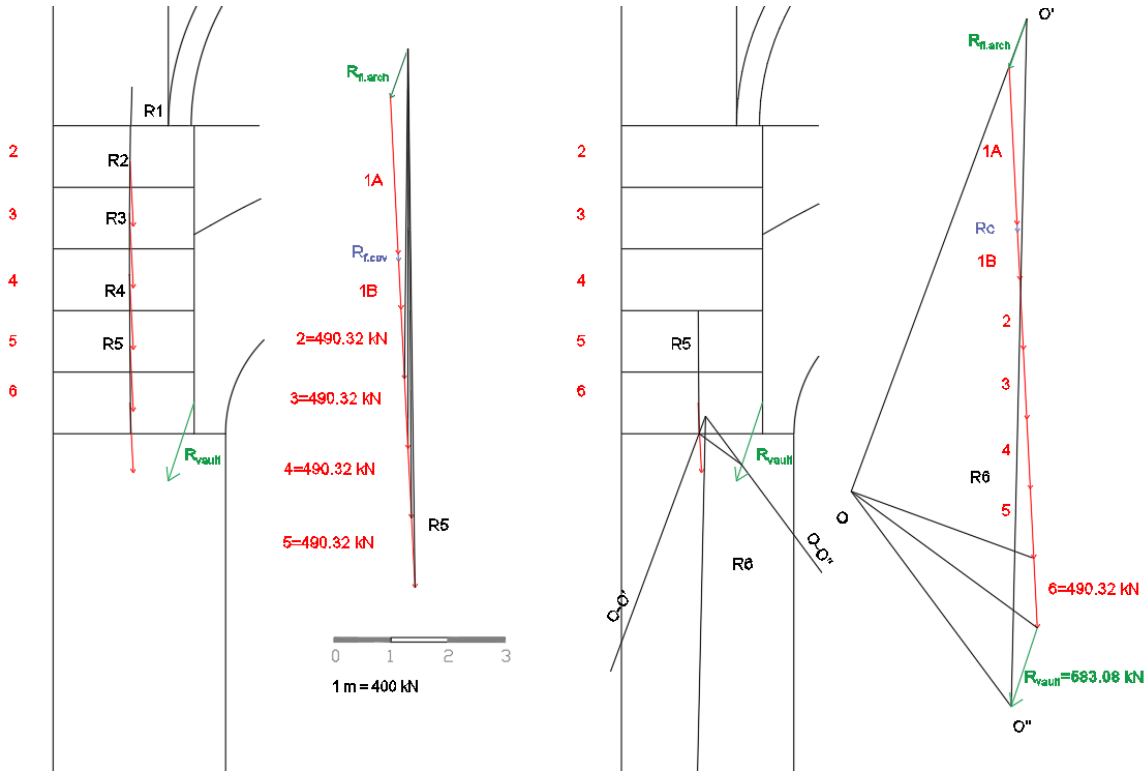

Fig. A. 142- Thrust line in the structure - seismic direction (+) (12)

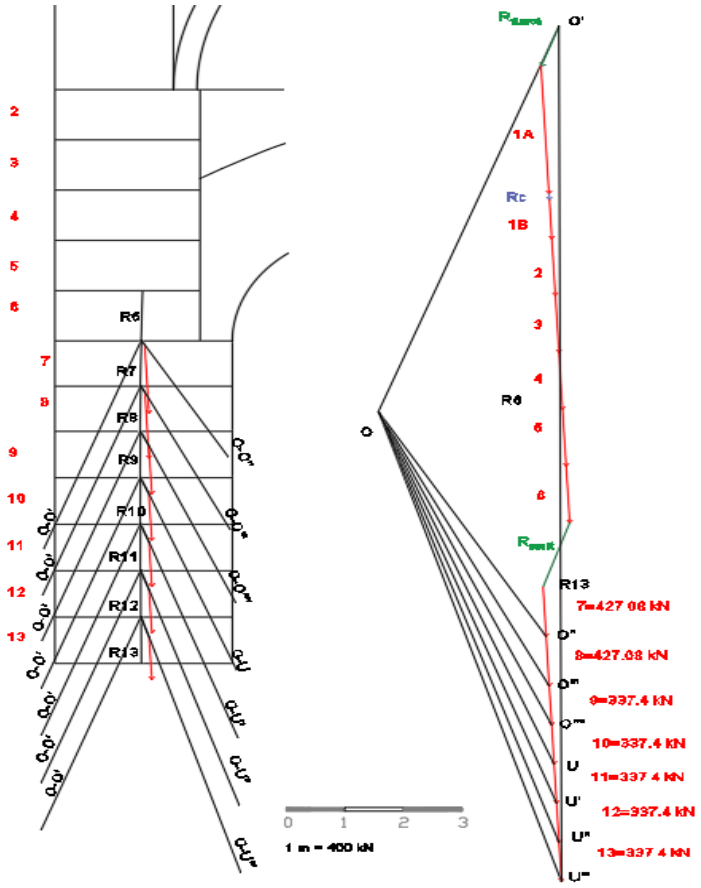

Fig. A. 143- Thrust line in the structure - seismic direction (+) (13)

Finally, the thrust line in the structure considering the seismic action in the right direction (+) can be drawn.

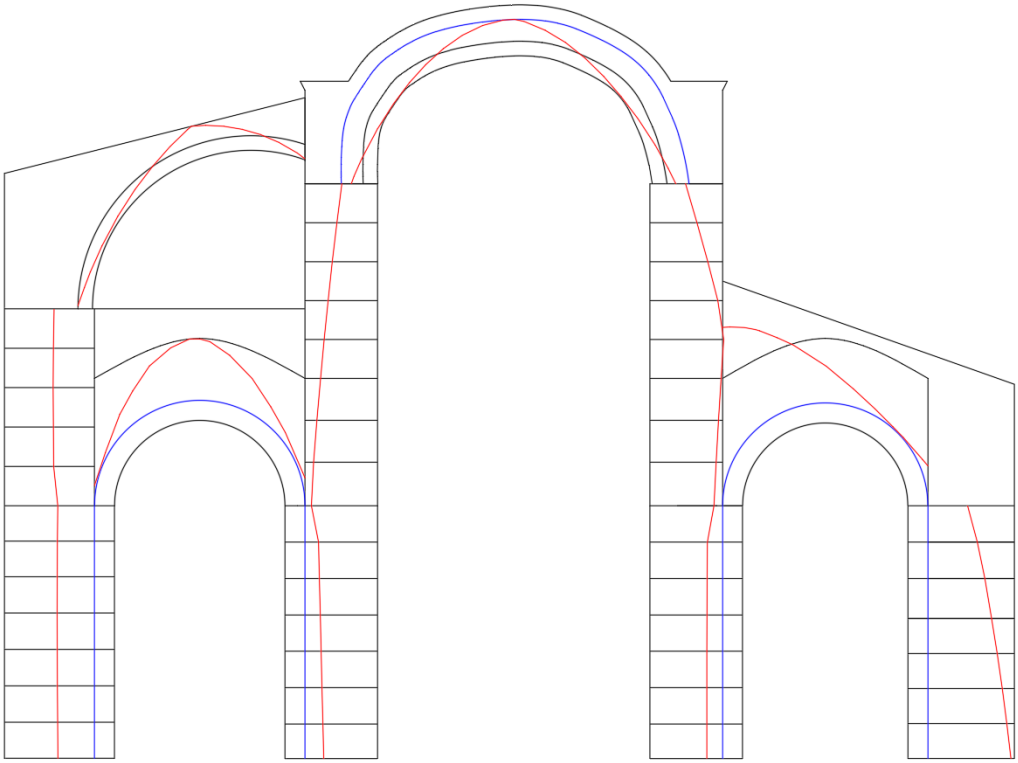

Fig. A. 144- Thrust line in the structure - seismic direction (+) (14)